

Gas-melt interactions in the C-H-O-S-(Cl)-silicate system

Roberto Moretti

Seconda Università di Napoli

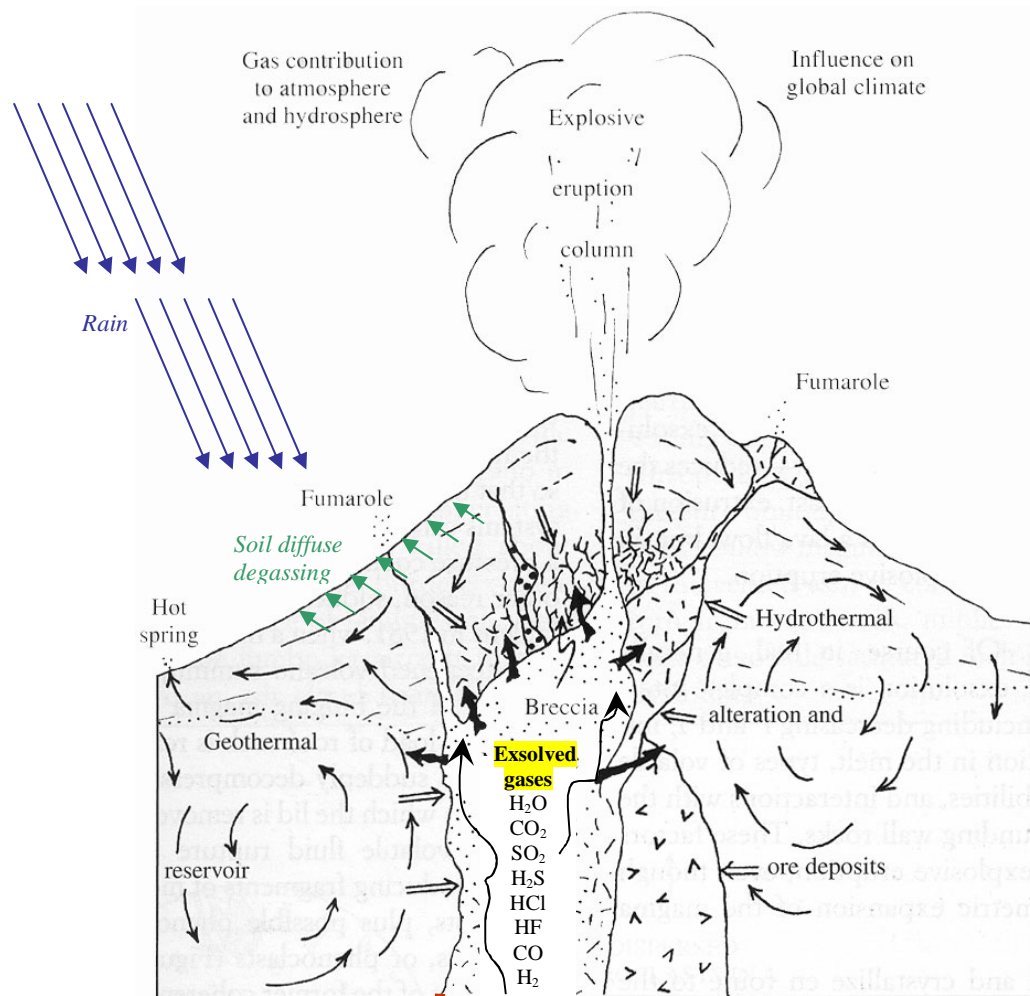
Dip. Ingegneria Civile, Design, Edilizia, Ambiente
Via Roma 29 - 81031 Aversa (I)

INGV - Osservatorio Vesuviano

Via Diocleziano 328 - 80124 Napoli (I)



Andy Warhol, 1985



**H₂O, CO₂, S, Cl, F
dissolved in magma**

Major goals for volcanology:

- global evolution and degassing of magma bodies
- modeling and simulation of volcanic processes

Major goals for Civil Protection:

- impact of volcanic eruptions, volcanic and diffuse degassing
- pollution by volcanic gases

Major goals for industrial applications:

- glass, ceramics, steel, cement, metallurgy, ...

Major goals for ore deposits and exploration geochemistry...

Volatile components in magmas

Analysis of volcanic gases

Direct sampling

Air borne IR-measurements

Satellite linked spectroscopic measurements

Analysis of volcanic glasses

Extraction methods, spectroscopy, electron and ion microprobe

The most abundant volatile components

H₂O

CO₂

SO₂

HCl

Mount St. Augustine: Alaska (7/79)

97% H₂O

2% CO₂

0.2% SO₂

0.4% HCl

Pinatubo Philippines (6/91)

89% H₂O

7% CO₂

3% SO₂

1% HCl

Merapi Indonesia (79)

90% H₂O

7% CO₂

2% SO₂

1% HCl



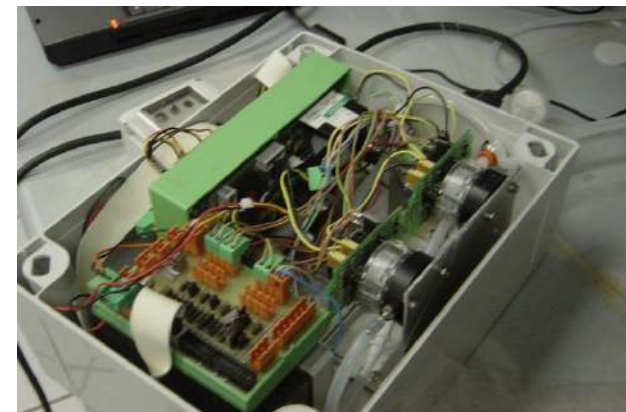
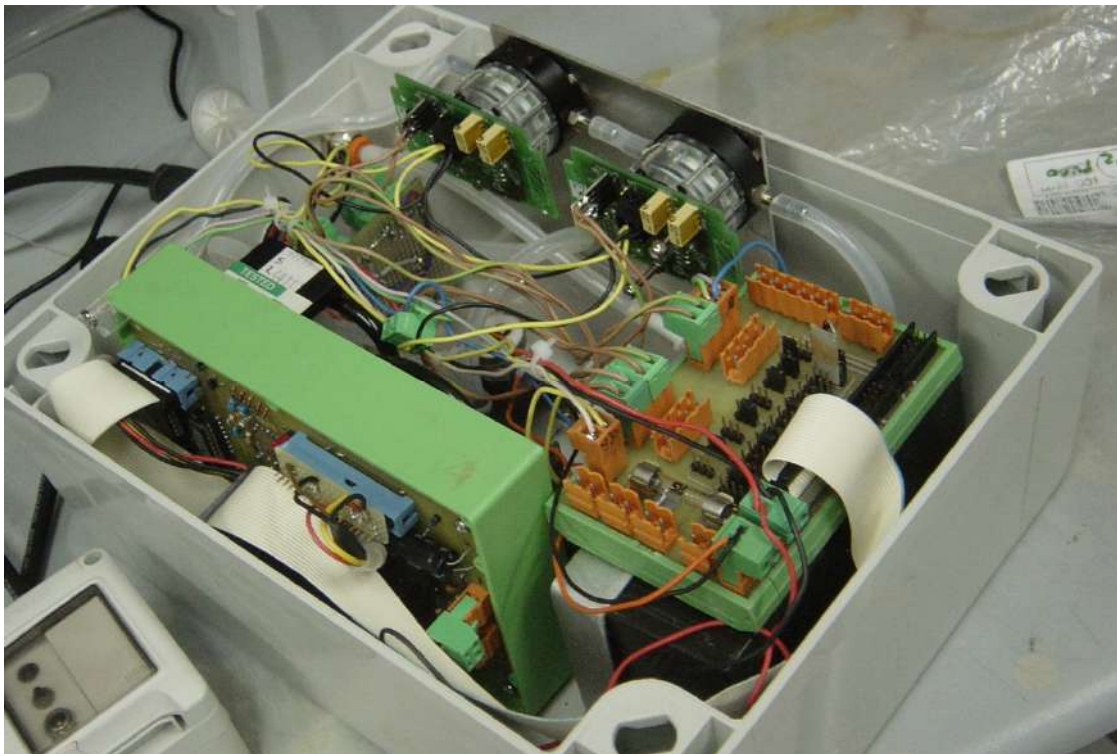
FTIR measurements of the emissions from the 2750 m. a.s.l. cone during the 2002 eruption of Mount Etna (Courtesy of Mike Burton, INGV Catania).

CO₂/SO₂

method

CO₂ : IR spectrometry SO₂ (HCl, H₂S): electrochemical sensor

***Acquisition frequency: 1s; low power consumption;
High concentration = high accuracy
Future perspective: real time continuous monitoring***

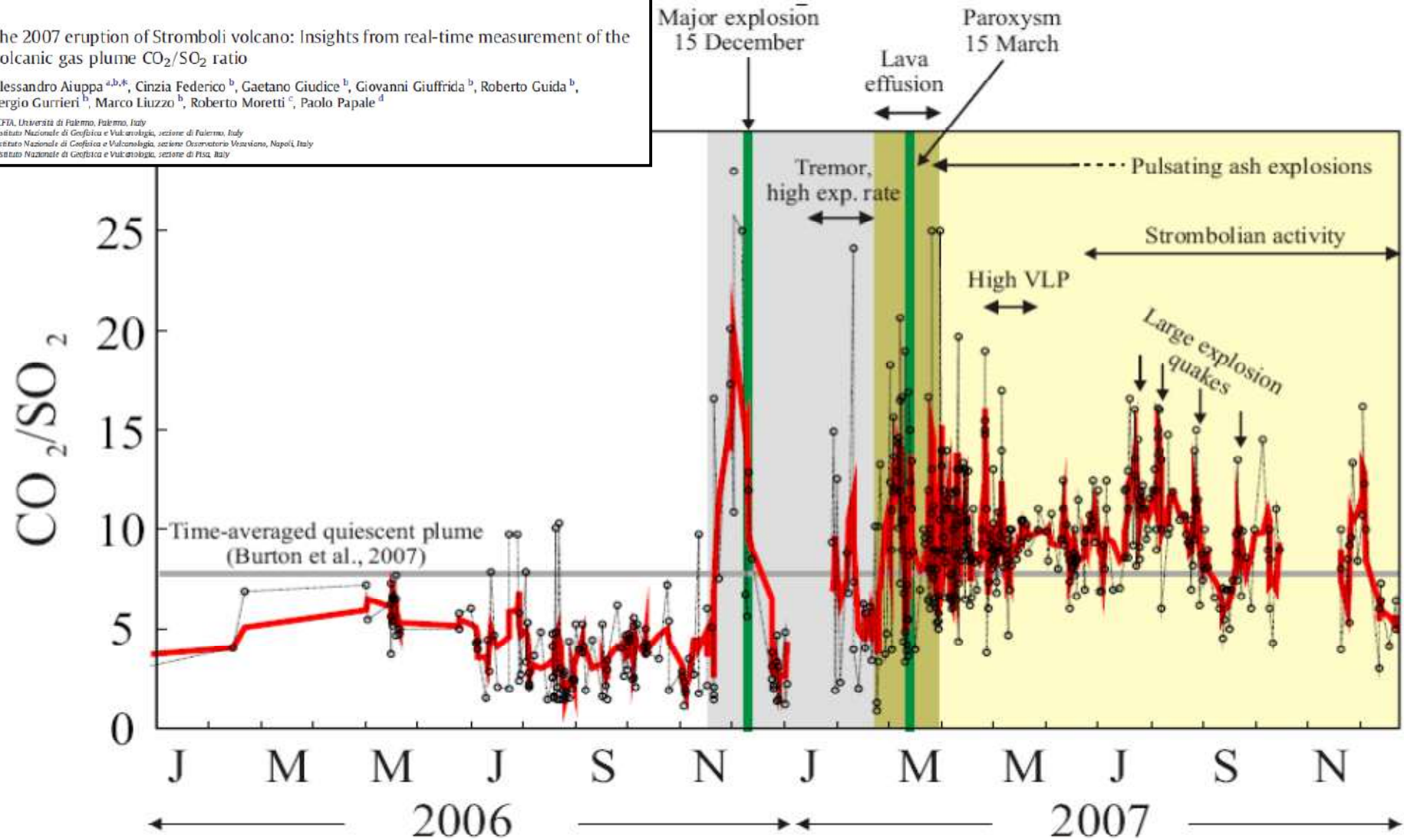




The 2007 eruption of Stromboli volcano: Insights from real-time measurement of the volcanic gas plume CO₂/SO₂ ratio

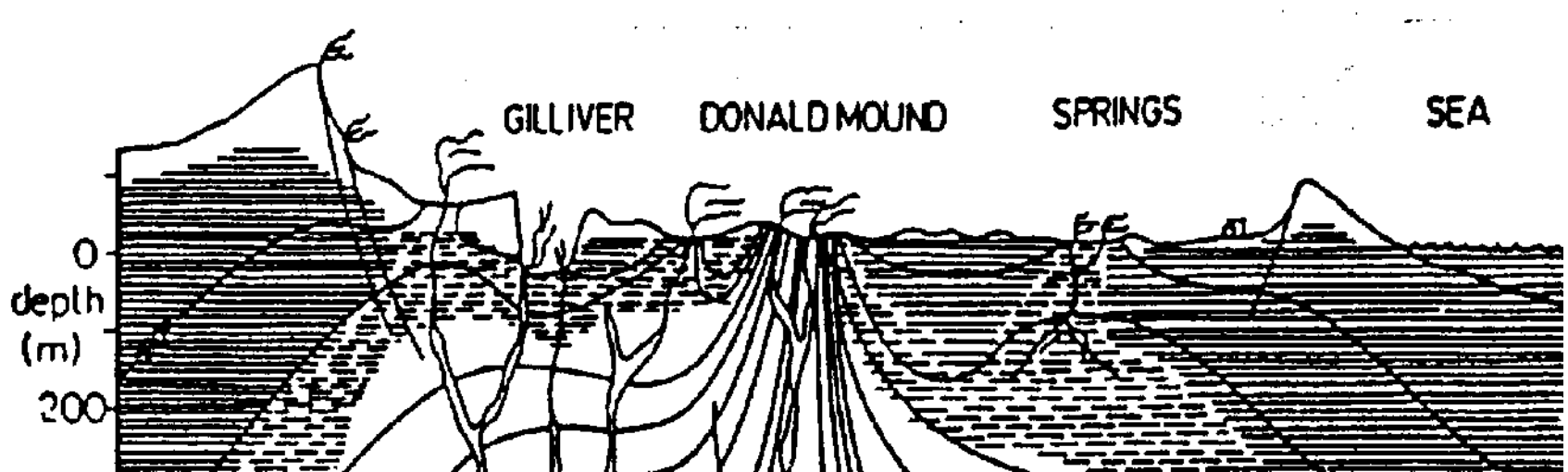
Alessandro Aiuppa ^{a,b,*}, Cinzia Federico ^b, Gaetano Giudice ^b, Giovanni Ciuffrida ^b, Roberto Guida ^b, Sergio Gurrieri ^b, Marco Liuzzo ^b, Roberto Moretti ^c, Paolo Papale ^d

^a CITA, Università di Palermo, Palermo, Italy
^b Istituto Nazionale di Geofisica e Vulcanologia, sezione di Palermo, Italy
^c Istituto Nazionale di Geofisica e Vulcanologia, sezione Osservatorio Vesuviano, Napoli, Italy
^d Istituto Nazionale di Geofisica e Vulcanologia, sezione di Pisa, Italy

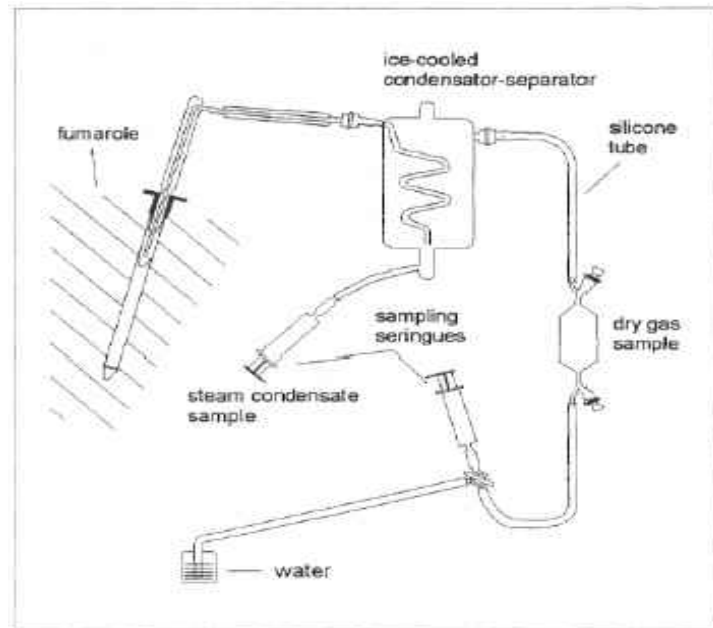
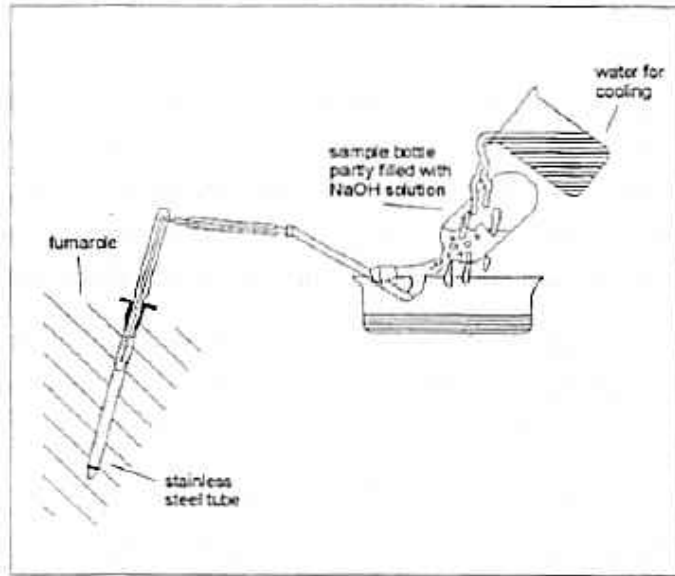


Aiuppa et al. (2009)

• ***hydrothermal liquids*** hosted in the hydrothermal systems, which are frequently interposed between the magma batch stationing at depth and the surface.



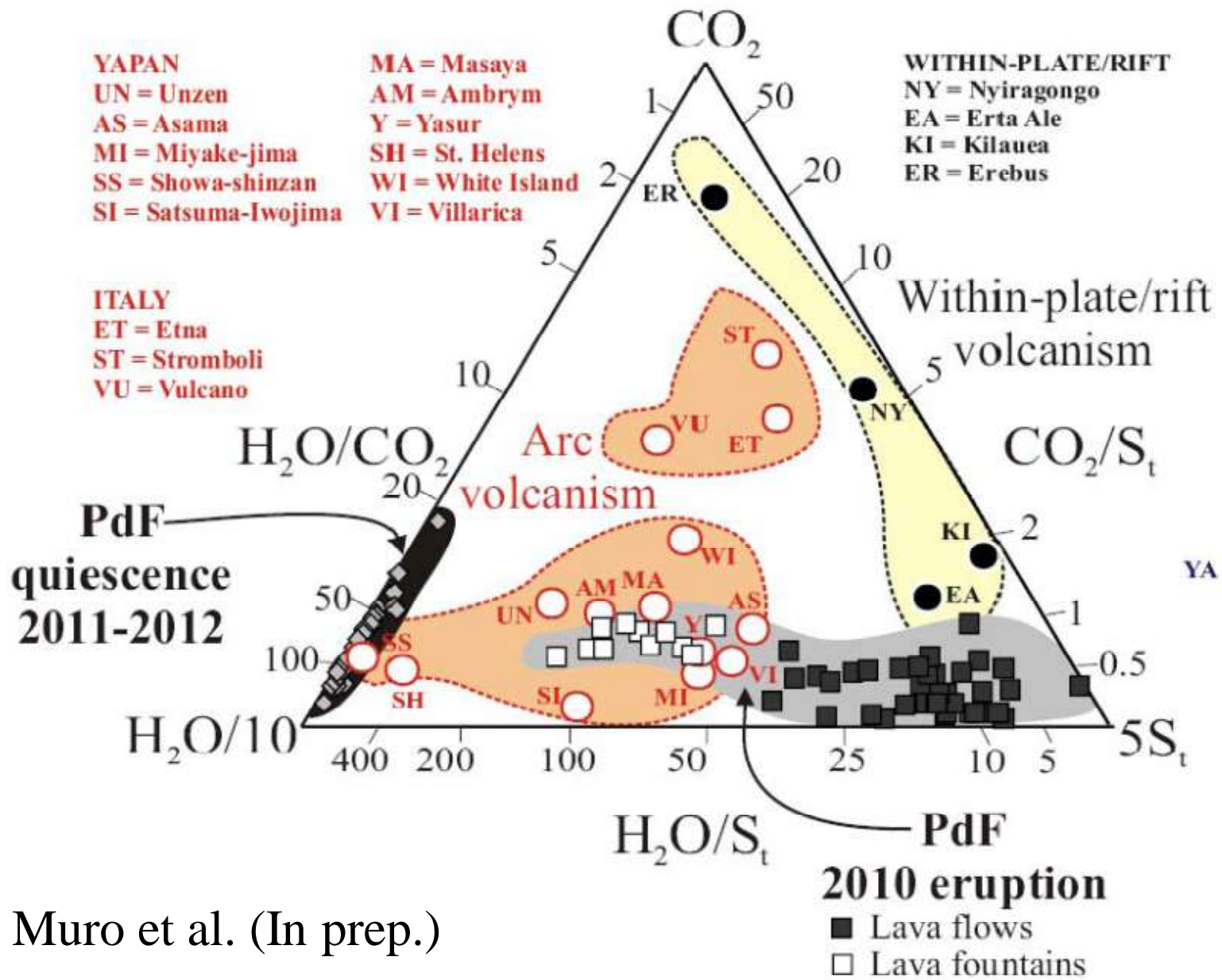
Conceptual geochemical model of White Island [Giggenbach, 1987]



Average chemical composition of Bocca Grande fumarole during 1998-2000 (the data are expressed in mmol/mol)

T °C	161
H ₂ O	843600
CO ₂	154100
H ₂ S	1360
N ₂	475
H ₂	364
CH ₄	23.2
He	1.27
CO	0.51
Ar	0.49
O ₂	0.24

The absence of typical magmatic gases (i.e. SO₂, HCl, HF) and the relatively high contents of CH₄ suggest that Solfatara fluids were stored in an hydrothermal environment before discharging.



Di Muro et al. (In prep.)

Measuring Initial Magmatic Volatiles

What is the challenge in accurately measuring/estimating amount of volatiles in magmas?

- When gas samples taken at surface, they can become contaminated with atmosphere or other secondary sources (meteoric waters etc...)
- If magma saturated and bubbles formed, lost some of its volatile supply prior to eruption

We can use “Phase Equilibria” or...

Glasses and Melt Inclusions

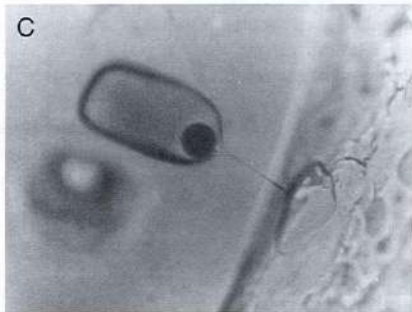
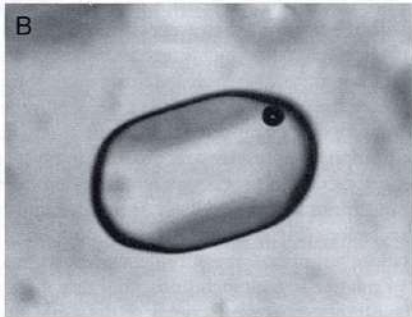
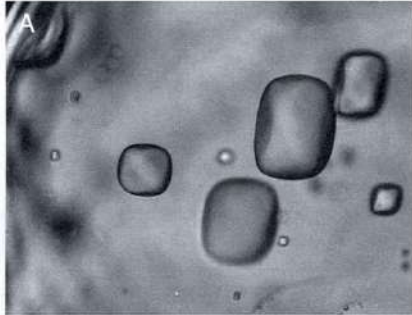
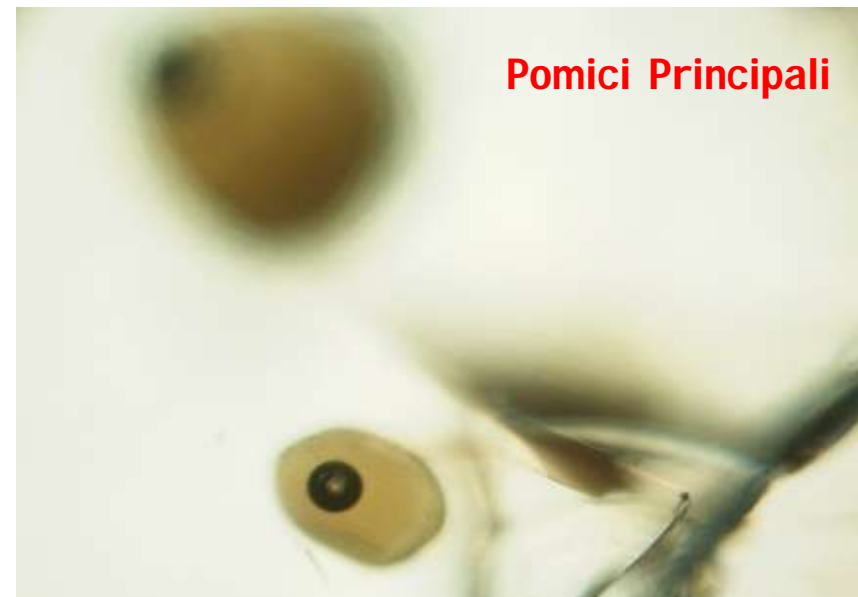
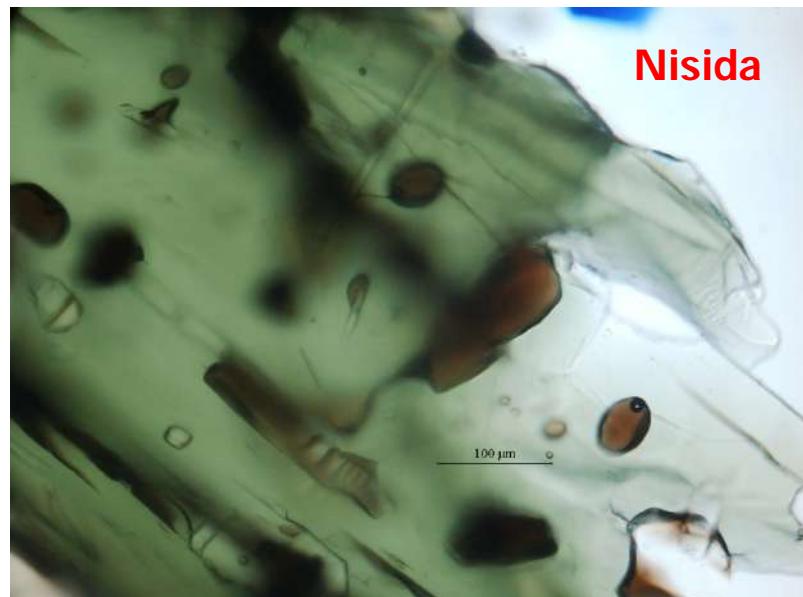
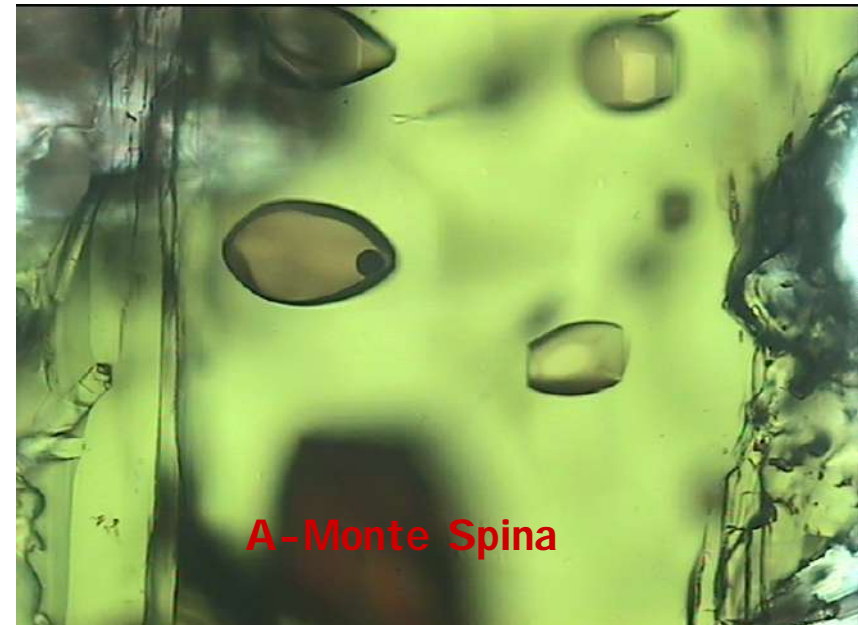


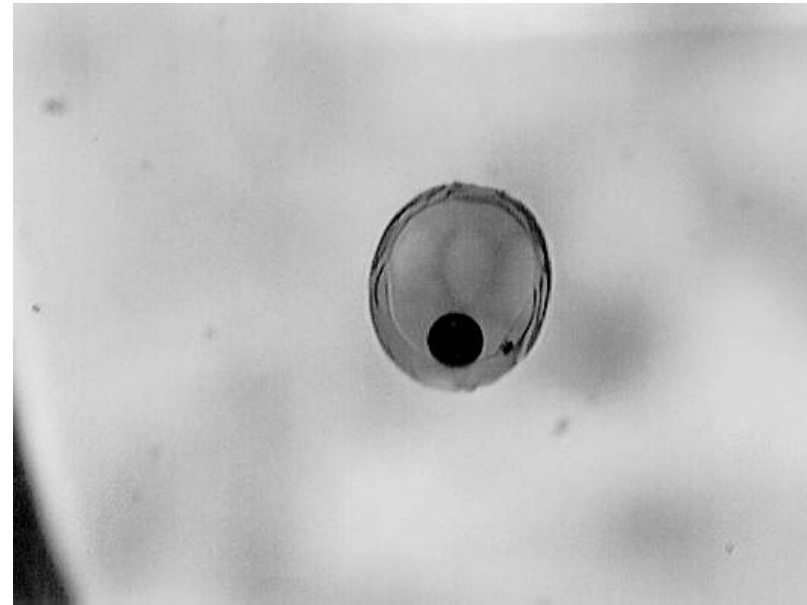
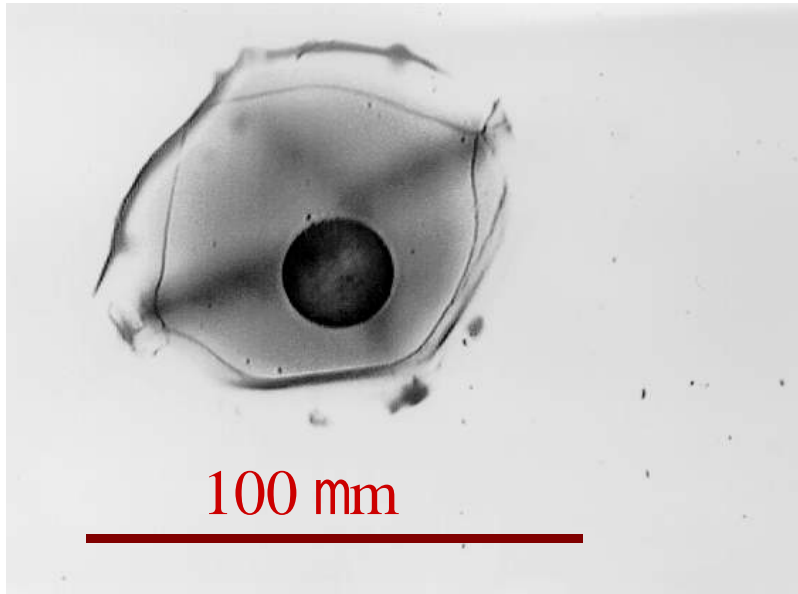
FIGURE 8 Glass (melt) inclusions in crystals from volcanic rocks. (A) A fragment of an ~3-mm quartz phenocryst from the rhyolitic Bishop Tuff containing inclusions of glass up to about 100 μm in diameter. (B) Close-up of a melt inclusion containing a small bubble. The inclusion is about 80 μm long and is

- Can measure abundances in submarine glasses because little to no degassing invoked; magma cools on contact with seawater
- Melt inclusions, which are blobs of melt (glass) surrounded by crystal.
- Interpretation is that these blobs of melt do not lose volatiles because “armored” by solid crystal.

Campi Flegrei Melt/glass inclusions

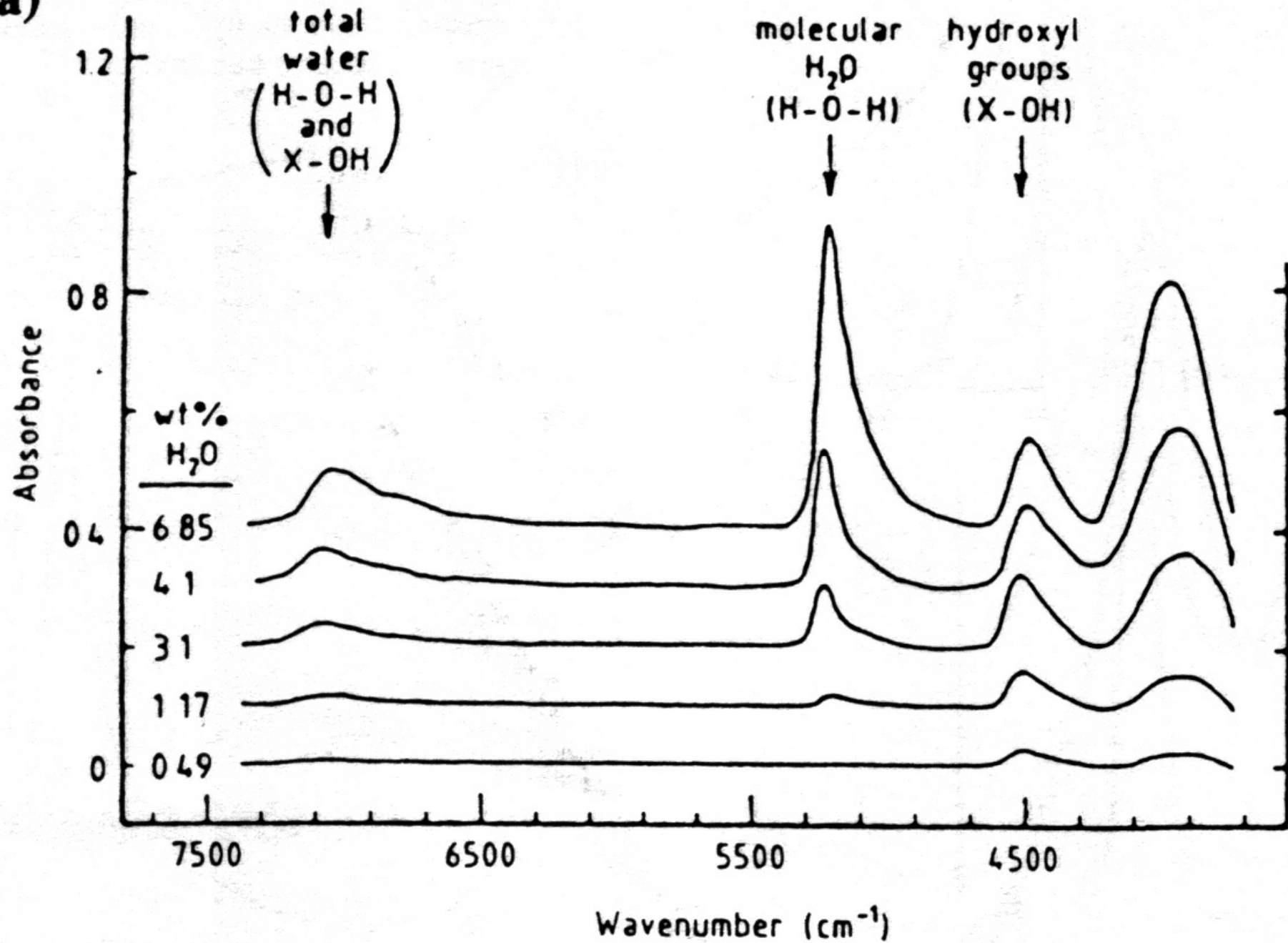


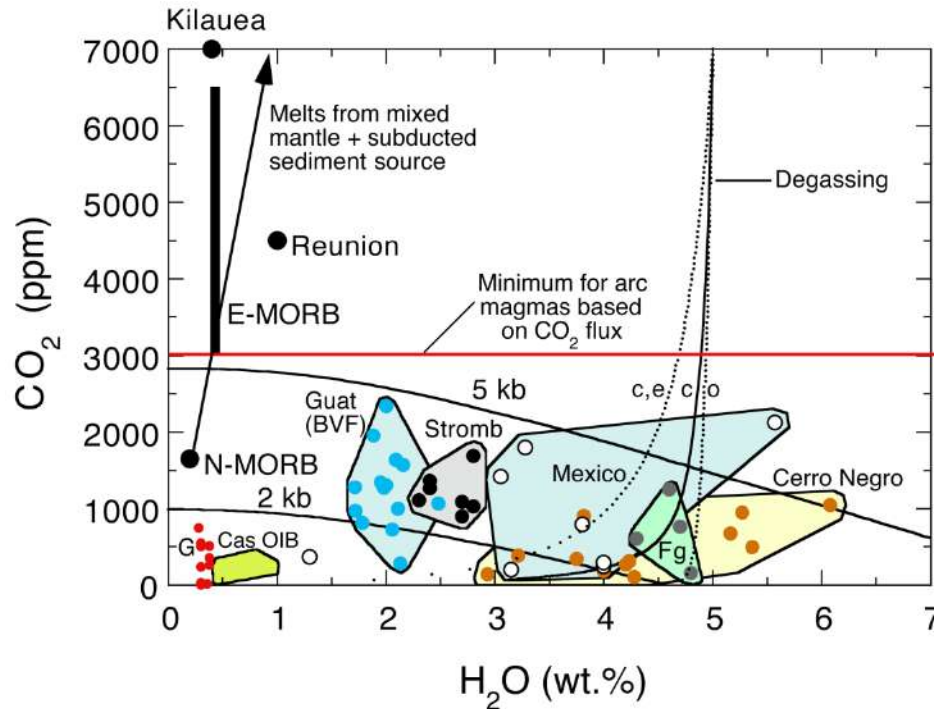
Stromboli MIs



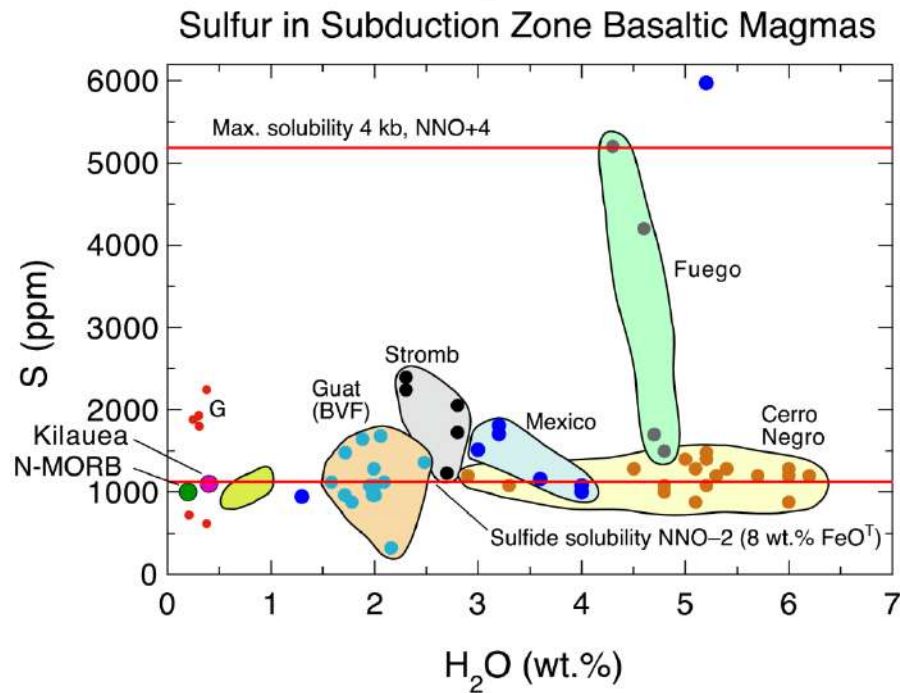
Etna MIs

(a)

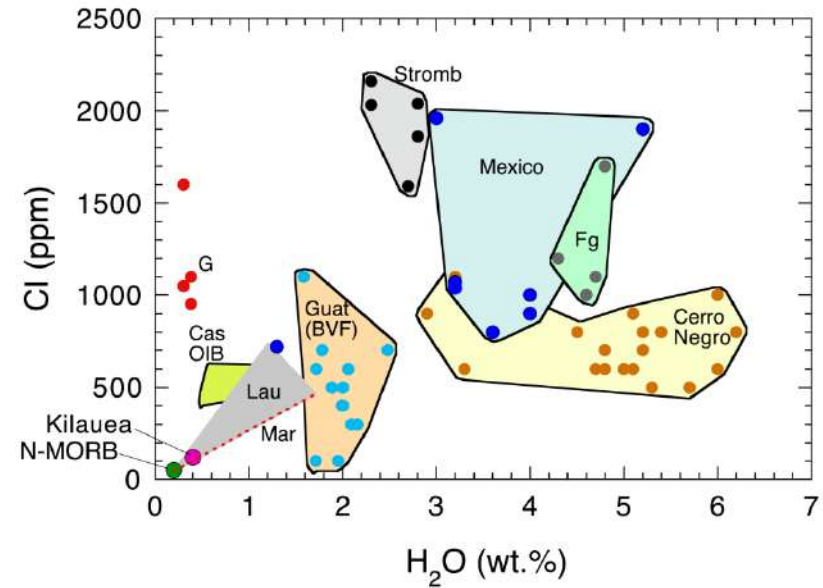




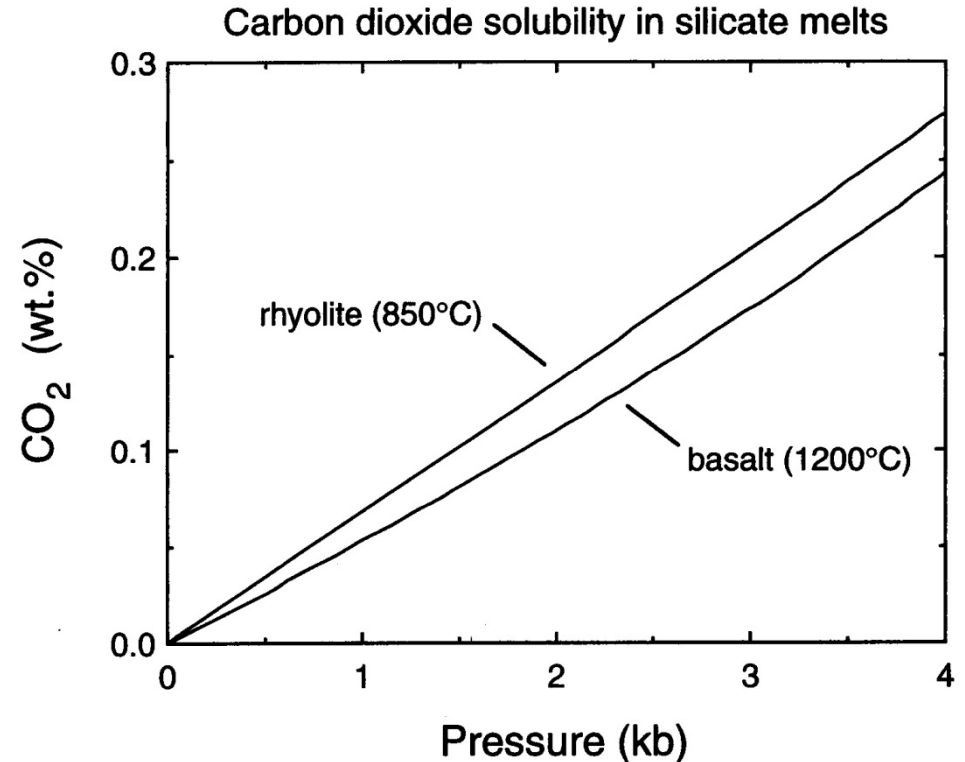
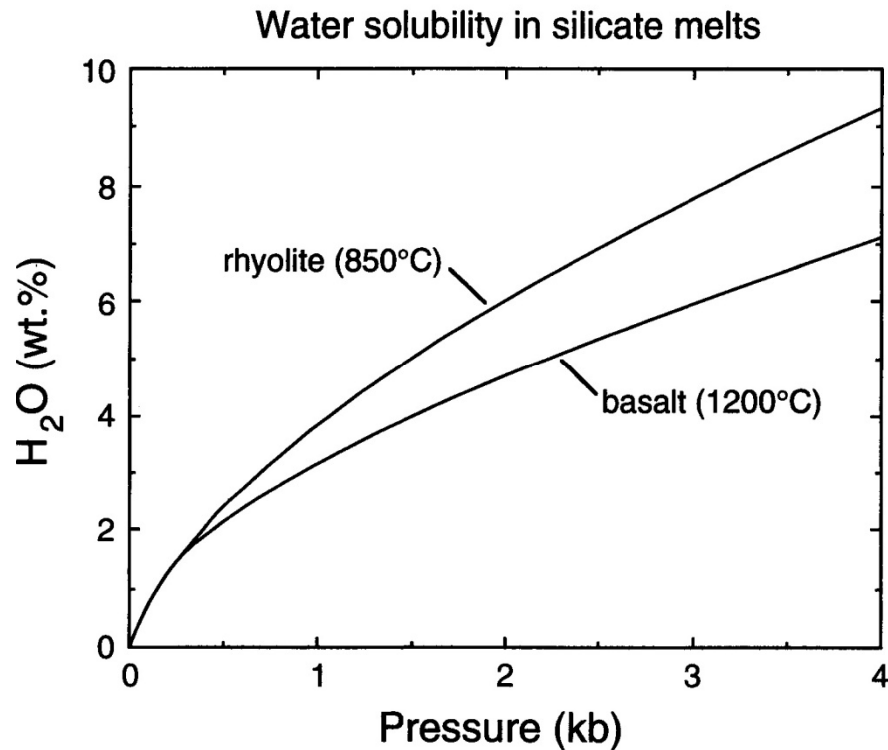
Basaltic magmas (Wallace, 2005)



Chlorine in Subduction Zone Basaltic Magmas

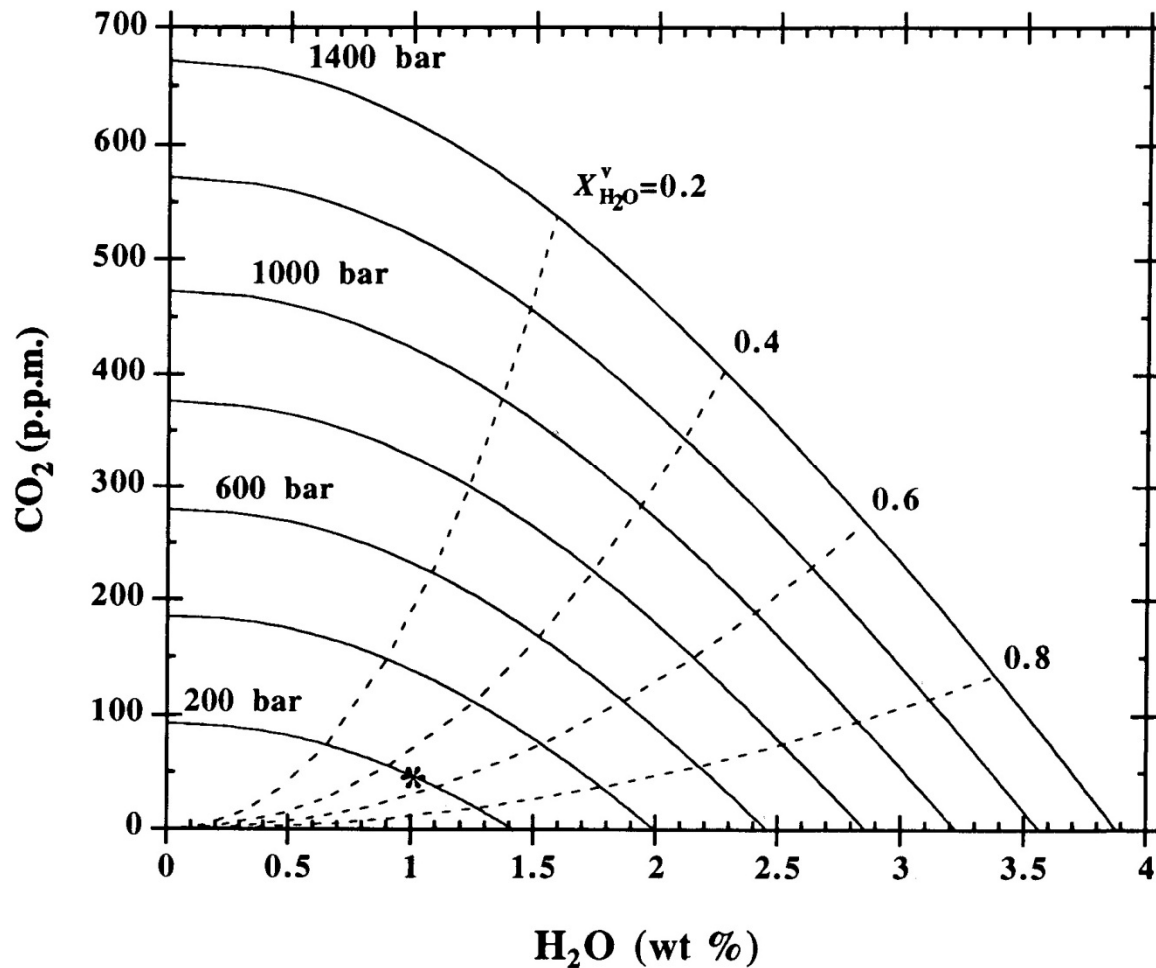


Understanding solubilities and saturation properties demands first experiments...then thermodynamics



- Solubilities are strongly pressure dependent
- Solubilities do not vary much with composition
- CO₂ has very low solubility compared to H₂O (~30x lower)

Solubilities with more than 1 volatile component present



Solid lines show solubility at different constant total pressures

Dashed lines show the vapor composition in equilibrium with melts of different H₂O & CO₂

From Dixon & Stolper (1995)

- In natural systems, melts are saturated with a multicomponent vapor phase
- H₂O and CO₂ contribute the largest partial pressures, so people often focus on these when comparing pressure & volatile solubility

- S solubility is more complicated because of multiple oxidation states
- Dissolved S occurs as either S^{2-} or S^{6+}

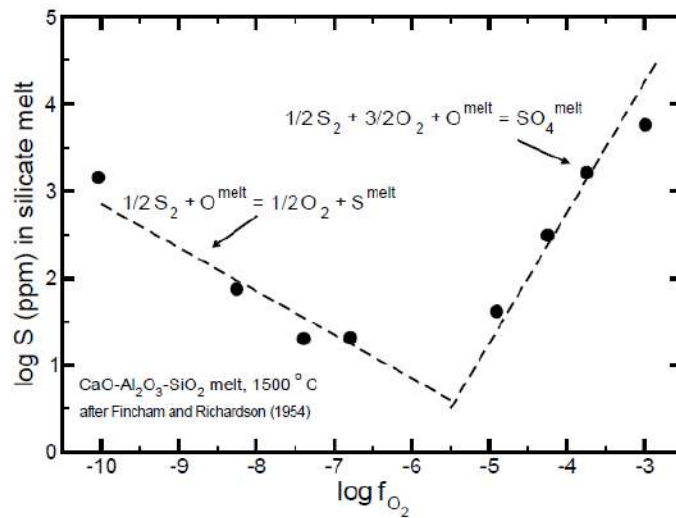
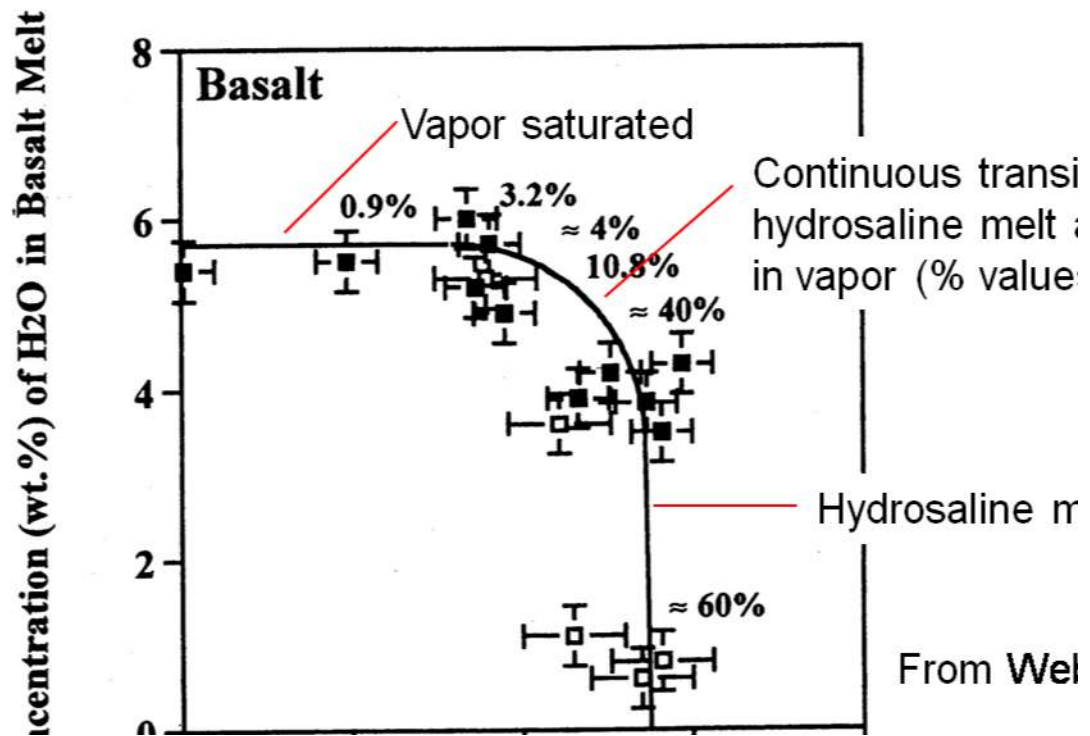


Figure 2. Solubility of sulfur in silicate melts at conditions of a fixed mole fraction of SO₂ in the input gas phase and varying f_{O_2} measured by Fincham and Richardson (1954) in a CaO-Al₂O₃-SiO₂ melt at 1 bar pressure. Please see text for further discussion of the reactions portrayed in these figures.

Baker and Moretti (2011)

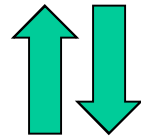
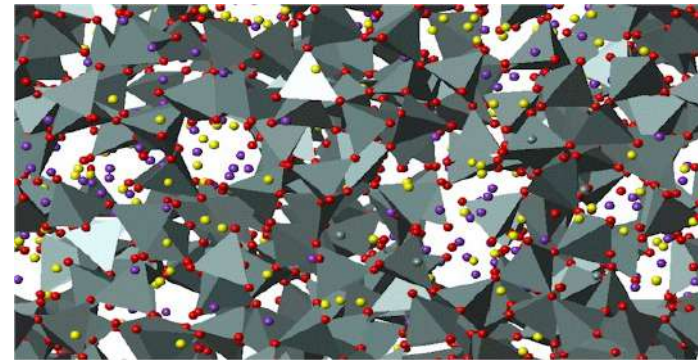
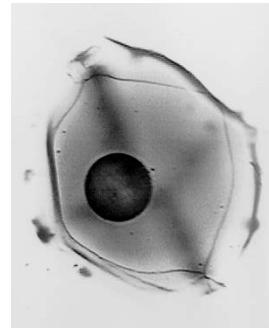
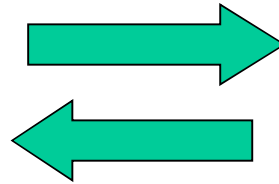
Jugo (2005)

Chlorine Solubility



→ In real basalts there is less chlorine (luckily!) → saturation with brine is avoided!

The message: Integrated and synergetic approach



$$\ln f_i^{oL}(P,T) = \ln f_i^{oL}(P^o, T^o) + \int_{P^o}^P \frac{v_i^o}{RT} dP - \int_{T^o}^T \frac{1}{RT^2} \int_{P^o}^P \left[v_i^o - T \left(\frac{\partial v_i^o}{\partial T} \right)_P \right] dPdT$$



Stromboli

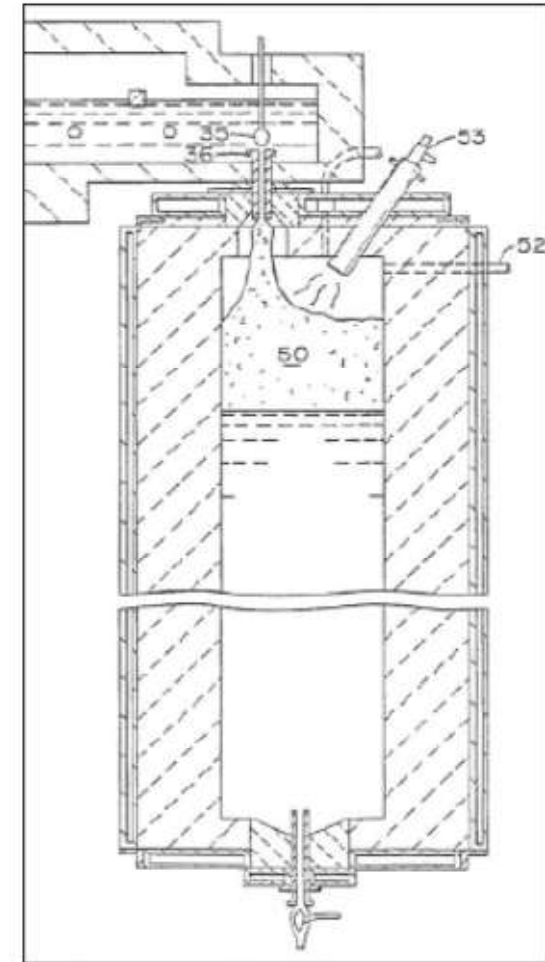
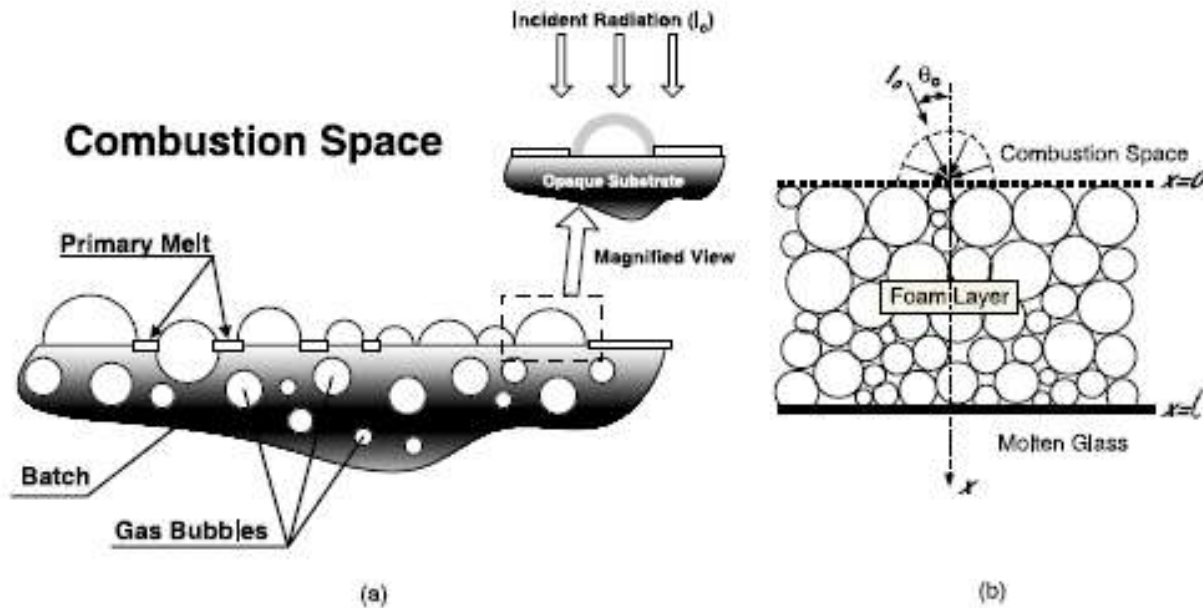


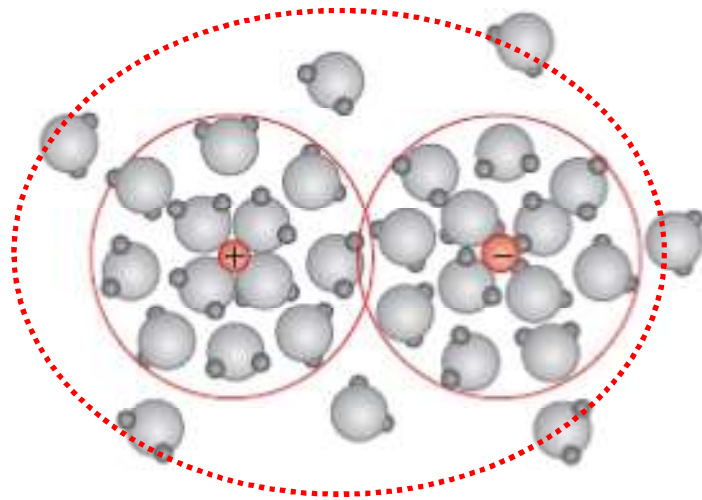
Fig. 2. Commercial vacuum-refining module [(35-36) is special valving arrangement, (52) is pressure maintenance tube, (50) is foam and (53) is gas burner].

Fedorov and Pilon
(2002; JNCS)

Fig. 2. (a) A layer of the primary foam formed on top of batch logs with a magnified view showing an idealized unit cell used for analysis of radiative transfer, and (b) an idealized layer of the secondary glass foam.

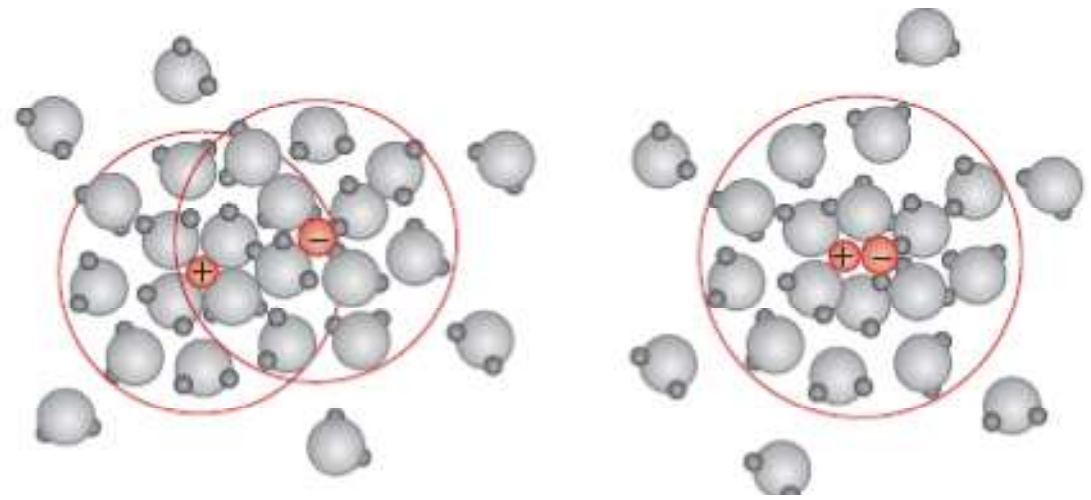
Silicate melts are not liquid water...

Outer sphere ion pair



Intact solvation shells

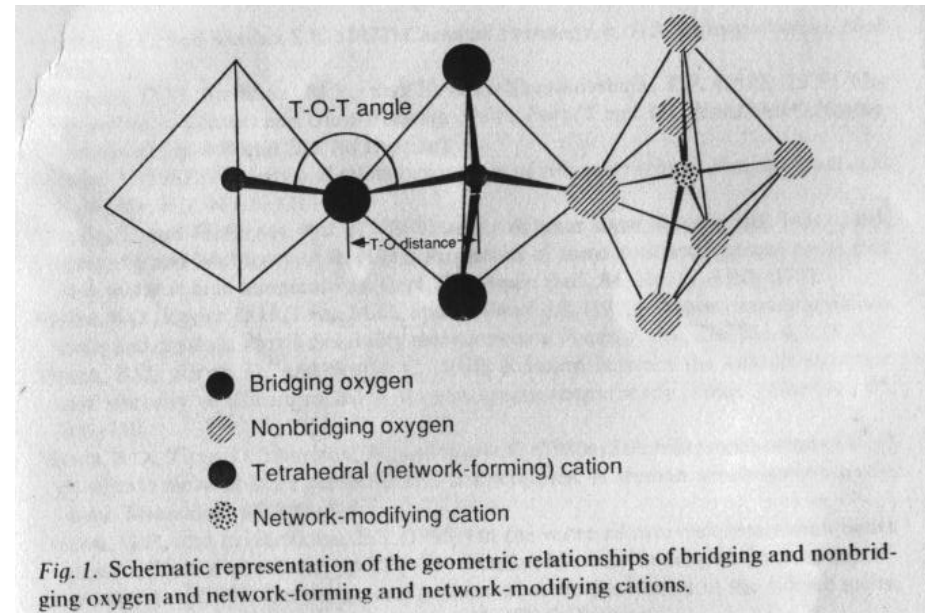
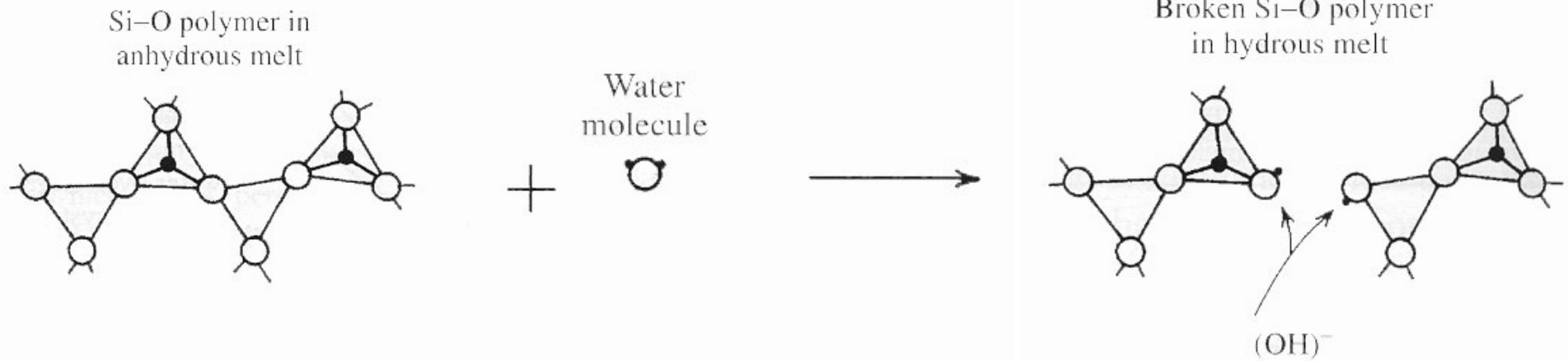
Inner sphere ion pair
(complex)



Partial disruption of
solvation shells

Disruption of solvation
shells

Depolymerization of Silicate Melts to accommodate volatiles (e.g. water)



Mysen and Richet, 2005

How deep need we to go with connections between structure and chemical thermodynamics ?

The “thermochemical knowledge” of a melt system does not seem to require the microstructural “complexity” that can be revealed by many spectroscopic investigations: the structural “characterization” exceeding that required for the **description of acid-base properties (e.g, in the Lux-Flood notation for oxide systems)** may be not useful.

Back to basics

In silicate melts acid-base properties are expressed in terms of Lux-Flood formalism:



(Ottonello et al., 2001; Moretti, 2005; Moretti and Ottonello, 2003; Ottonello, 1997: "Principles of Geochemistry"; Flood and Forland, 1947; Fraser, 1975; 1977).

In oxide systems, "reaction" 1 is the analogous of the Bronsted-Lowry one in aqueous solutions:



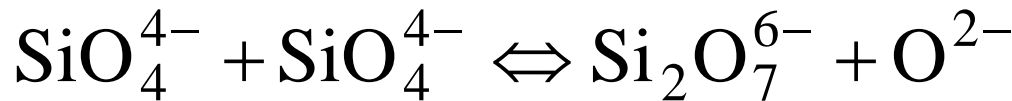
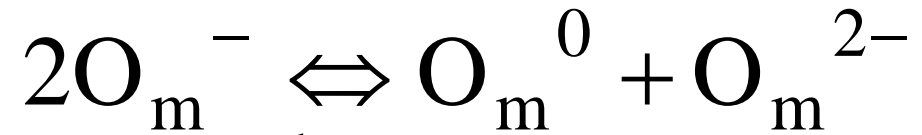
In aqueous solutions the electrode of reference is the "normal hydrogen electrode", whereas in silicate melts the reference electrode is the "normal oxygen electrode" (Ottonello et al., 2001), i.e.:



This is the main redox couple in oxide melts.

Polymeric nature of anion matrix: Toop-Samis model

In polymeric models for silicate melts, it is postulated that, at each composition, for given P-T values, the melt is characterized by an equilibrium distribution of several ionic species of oxygen, metal cations and ionic polymers of monomeric units SiO_4^{4-} .



$$K_{58} = \frac{(\text{O}^0)(\text{O}^{2-})}{(\text{O}^-)^2}$$

$$\Delta G_{\text{mixing}} = [(\text{O}^-)/2]RT \ln K_{\text{polym}}$$



Chemical Geology 174 (2001) 157–179

CHEMICAL
GEOLOGY
AN INTERNATIONAL JOURNAL OF
ISOTOPE GEOSCIENCE
www.elsevier.com/locate/chemgeo

ANNALS OF GEOPHYSICS, VOL. 48, N. 4/5, August/October 2005

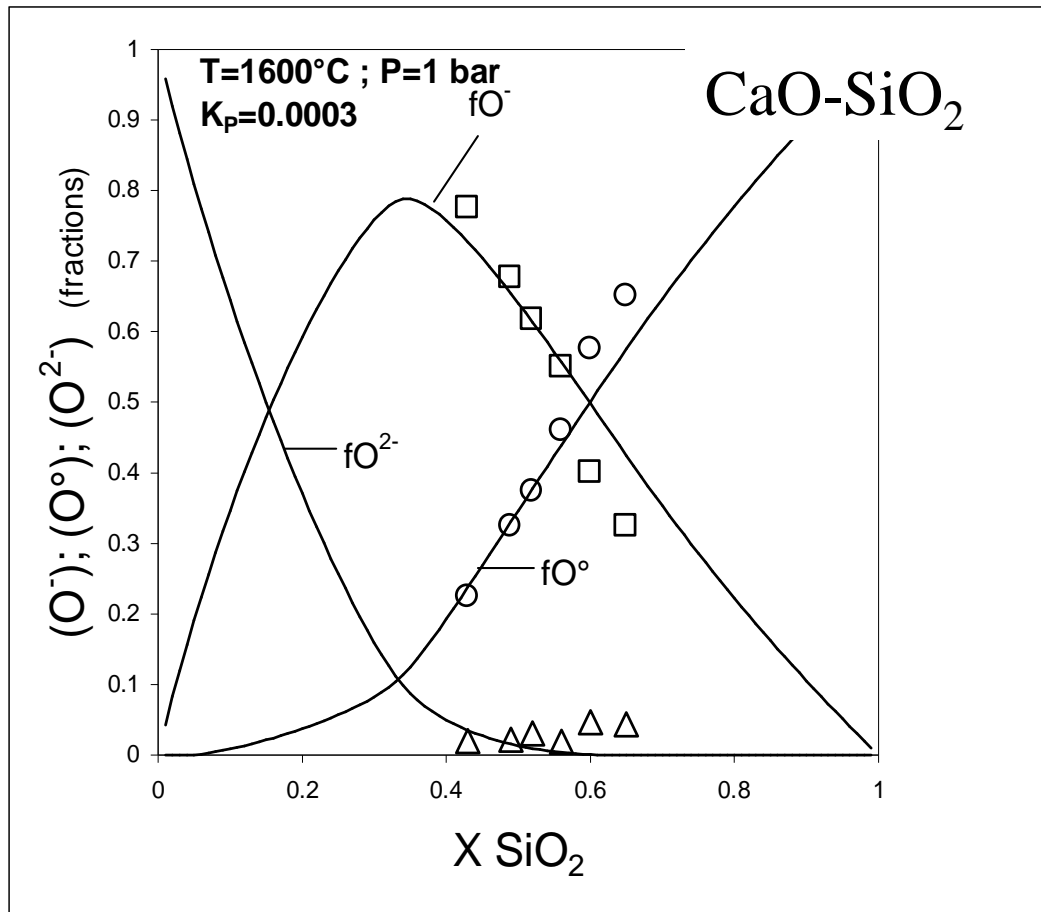
Polymerisation, basicity, oxidation state
and their role in ionic modelling
of silicate melts

Roberto Moretti

ISTITUTO NAZIONALE DI FISICA E VULCANOLOGIA, OSSERVATORIO VEVAIANO, VARESE, ITALY

Oxidation state of iron in silicate glasses and melts: a
thermochemical model

Giulio Ottonello ^{a,*}, Roberto Moretti ^b, Luigi Marini ^a, Marino Vetuschì Zuccolini ^a



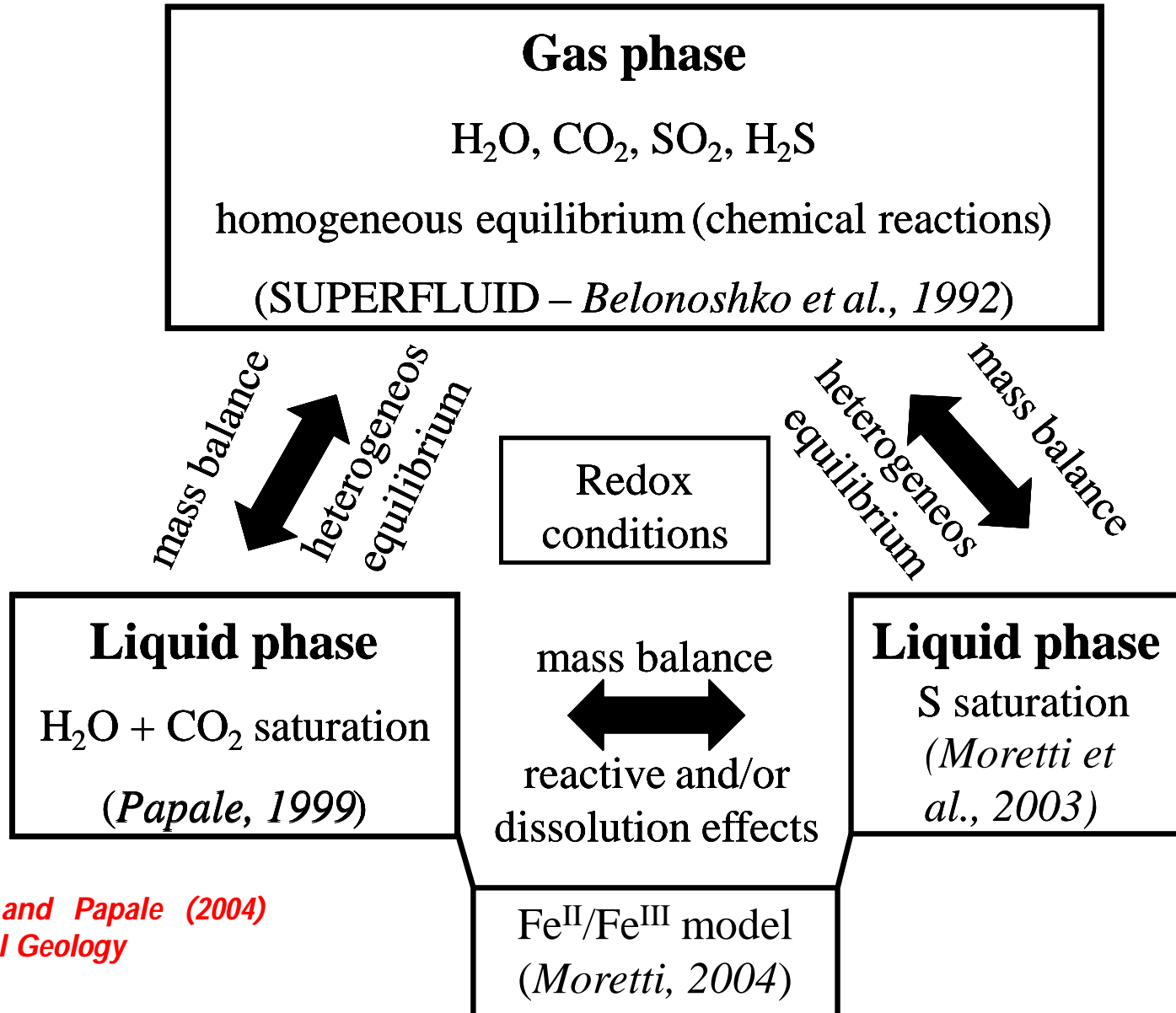
*Ottonello and Moretti
 (2004) J. Phys. Chem.
 Solids*

The message:

1. Silicate melts are polymerized liquids
2. Polymeric units are highly reactive

Polymerization and redox state are intimately interrelated. This affects melt properties, including oxidation state, volatile solubility *et cetera*.

The $H_2O-CO_2-H_2S-SO_2$ saturation model



Moretti and Papale (2004)
Chemical Geology

Theory of the revised and extended H_2O-CO_2 saturation model (Papale, Moretti & Barbato, 2006)

- Fully non-ideal
- Fluid phase of any composition in the system H_2O+CO_2
- Liquid phase of any composition from two/three components to natural (12 components)

Equilibrium equations

$$P^G = P^L = P$$

$$T^G = T^L = T$$

$$f_{H_2O}^G = f_{H_2O}^L \Rightarrow \phi_{H_2O} y_{H_2O} P = \gamma_{H_2O} x_{H_2O} f_{H_2O}^{oL}$$

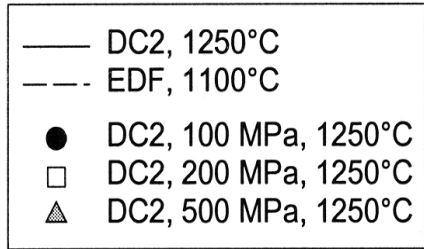
$$f_{CO_2}^G = f_{CO_2}^L \Rightarrow \phi_{CO_2} y_{CO_2} P = \gamma_{CO_2} x_{CO_2} f_{CO_2}^{oL}$$

Mass balance equations

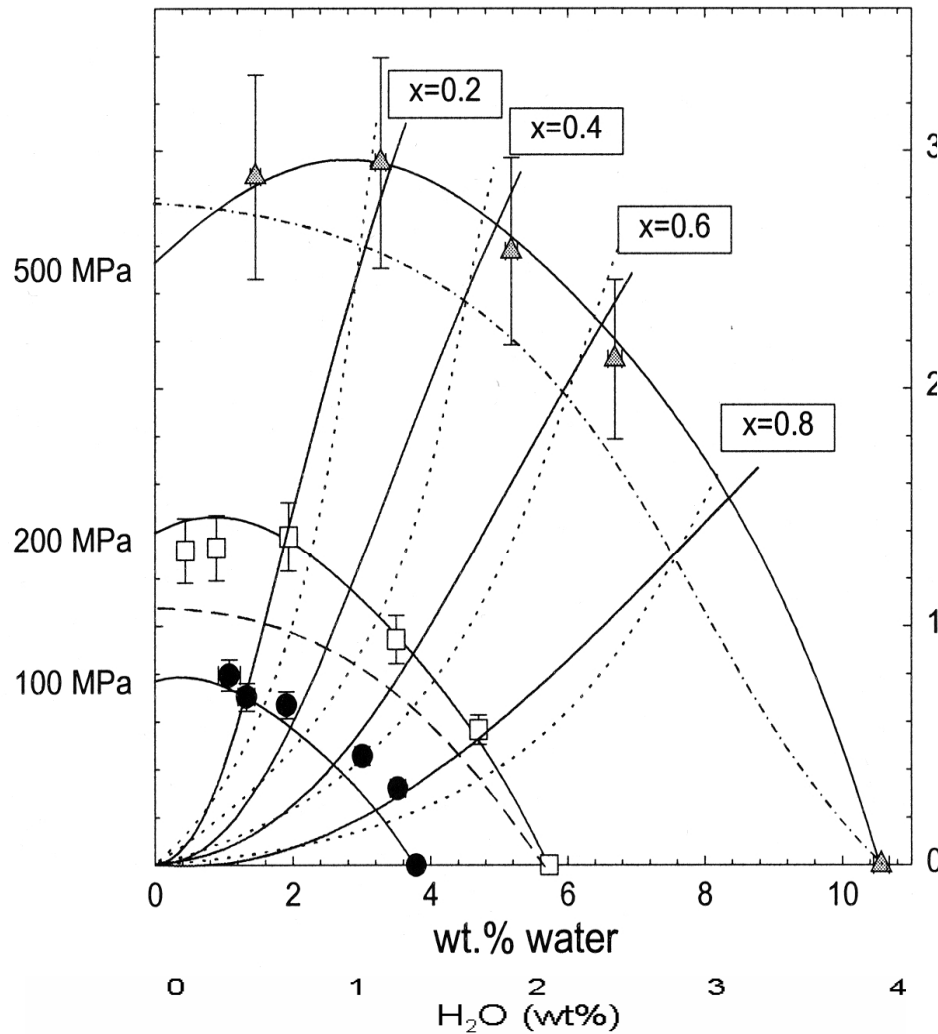
$$y_{H_2O} + y_{CO_2} = 1$$

$$\frac{x_{H_2O}^T - x_{H_2O}}{y_{H_2O} - x_{H_2O}} = \frac{x_{CO_2}^T - x_{CO_2}}{y_{CO_2} - x_{CO_2}}$$

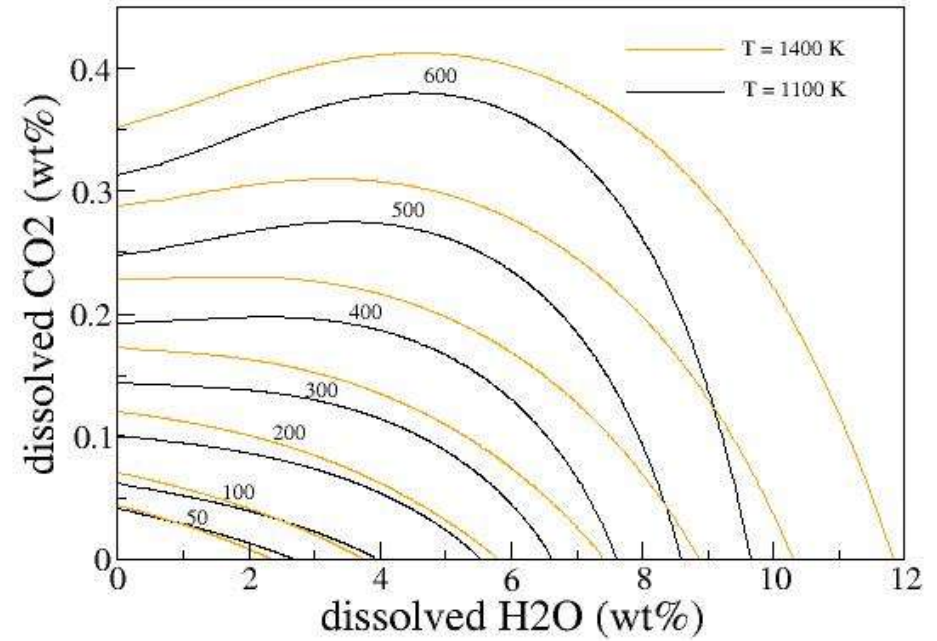
$$y_{H_2O} - x_{H_2O} = y_{CO_2} - x_{CO_2}$$



Tamic et al., 2001



Rhyolite (comp. from Blank et al. 1993)



Chemical Geology 229 (2006) 78–95

**CHEMICAL
GEOLOGY**
including
ISOTOPE GEOSCIENCE
www.elsevier.com/locate/chemgeo

The compositional dependence of the saturation surface of
 $H_2O + CO_2$ fluids in silicate melts

Paolo Papale^{a,b,*}, Roberto Moretti^{a,c}, David Barbato^{a,b}

^a Istituto Nazionale di Geofisica e Vulcanologia, Italy

^b Sezione di Pisa, Via della Faggiola 32, 56126 Pisa, Italy

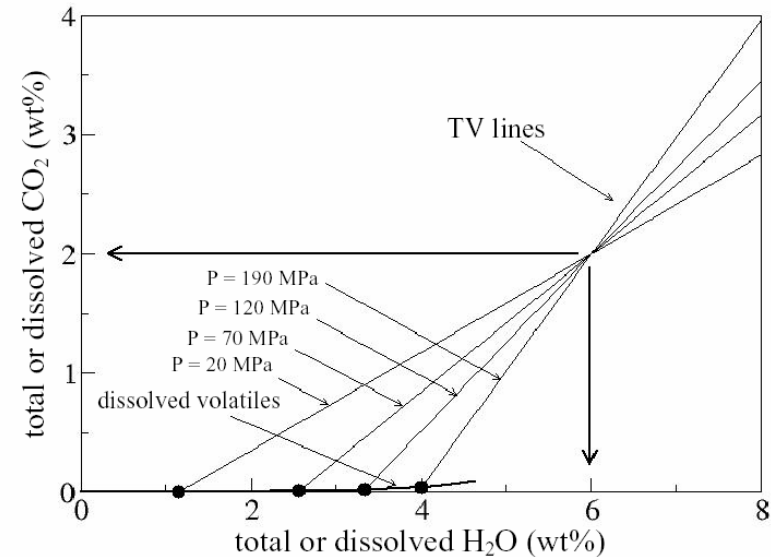
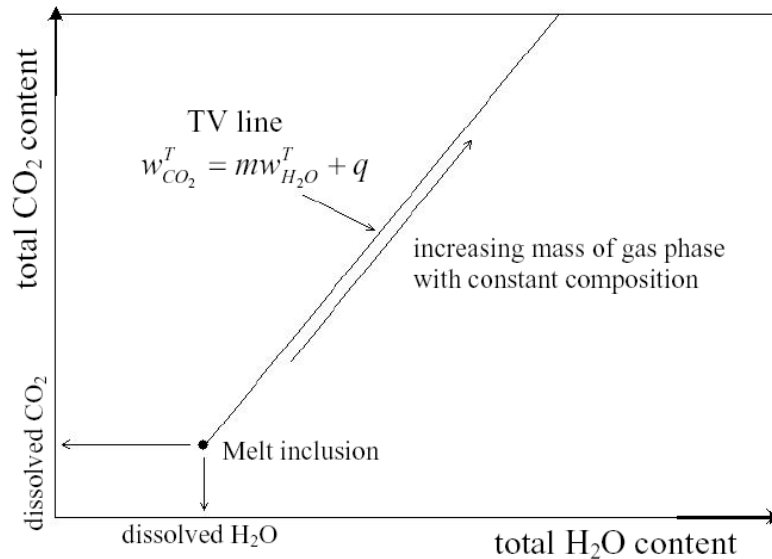
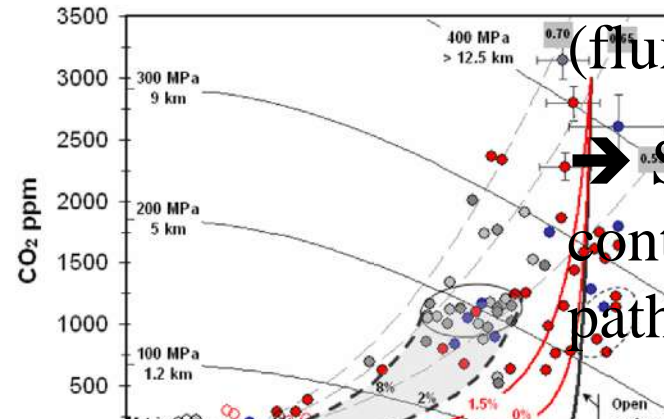
^c Sezione Osservatorio Vesuviano, Via Diocleziano 328, 80124, Napoli

(Papale et al., 2006)

MIs show processes of CO₂ addition and dehydration

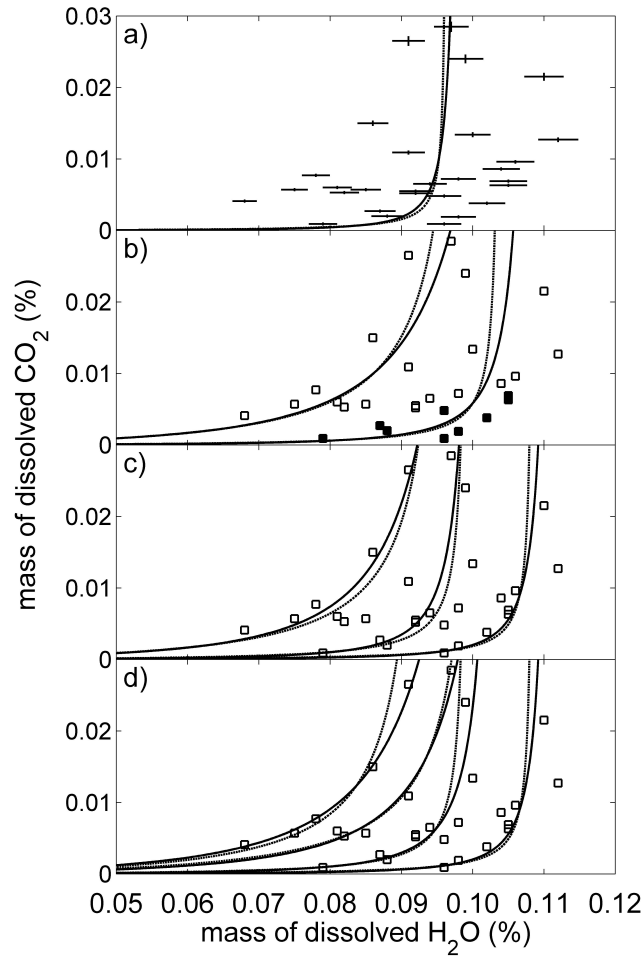
(fluxing)

→ Shift in total/initial volatile content → many degassing paths

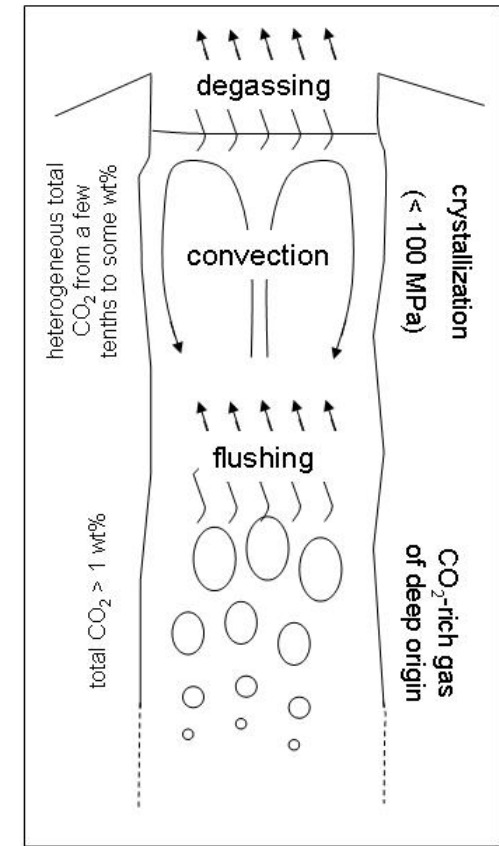
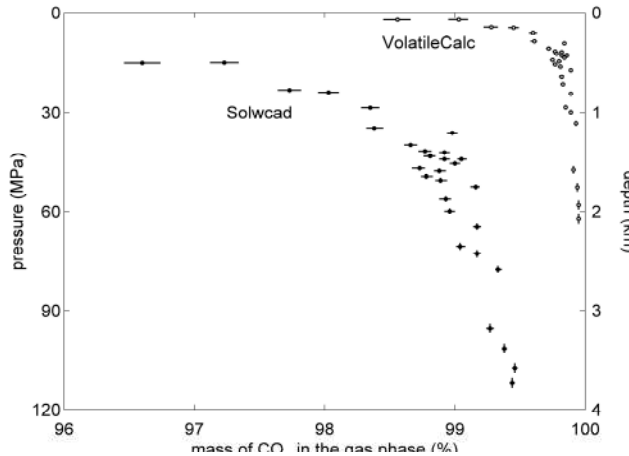


Papale, 2005

KILAUEA



Sat.Mod.	N. of curves	wTH2O (wt%)	wTCO2 (wt%)
SWCD 1	0.100	0.50	
SWCD 2	0.110	0.80	
SWCD 3	0.111	3.80	
		0.102	0.80
		0.105	3.10
SWCD 4	0.112	0.54	
		0.105	0.96
		0.110	2.82
	0.112	4.38	



JOURNAL OF GEOPHYSICAL RESEARCH, VOL. 114, B12201, doi:10.1029/2008JB006187, 2009



Heterogeneous large total CO₂ abundance in the shallow magmatic system of Kilauea volcano, Hawaii

Michele Barsanti,^{1,2} Paolo Papale,¹ David Barbato,^{1,3} Roberto Moretti,⁴ Enzo Boschi,^{1,4} Erik Hauri,⁵ and Antonella Longo¹

...shifting degassing paths...

S solubility: the Conjugated-Toop-Samis (CTSFG) model

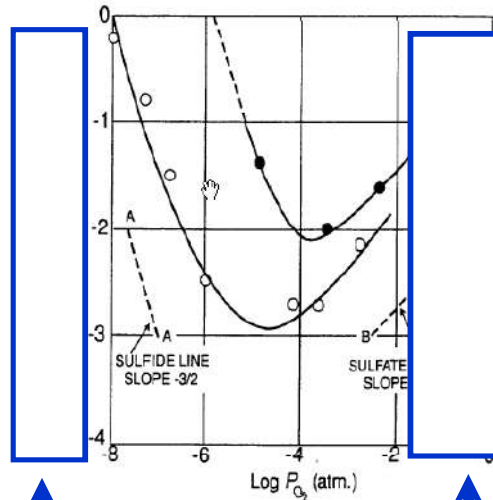


Geochimica et Cosmochimica Acta, Vol. 69, No. 4, pp. 801-823, 2005
 Copyright © 2005 Elsevier Ltd
 Printed in the USA. All rights reserved
 0016-7037/05 \$30.00 + .00

doi:10.1016/j.gca.2004.09.006

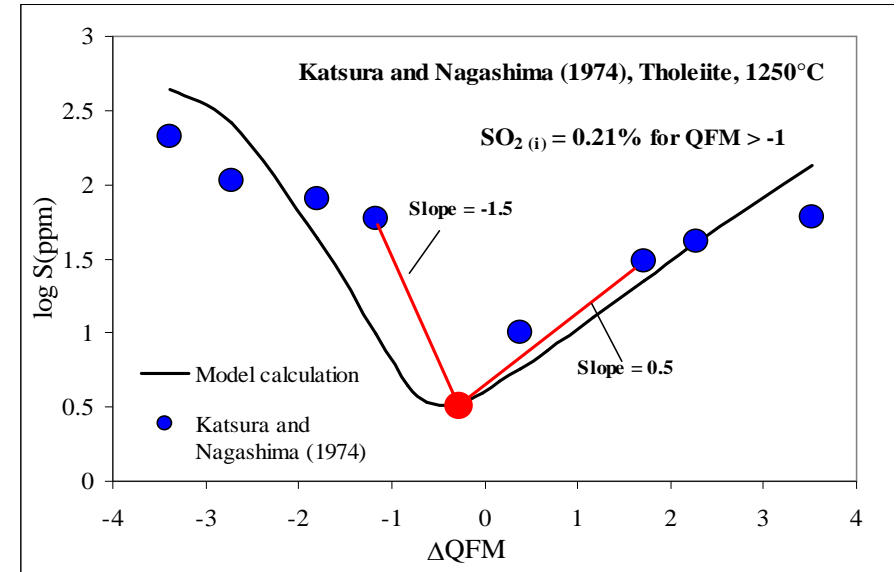
Solubility and speciation of sulfur in silicate melts: The Conjugated Toop-Samis-Flood-Grjotheim (CTSFG) model

ROBERTO MORETTI^{1,*} and GIULIO OTTONELLO²



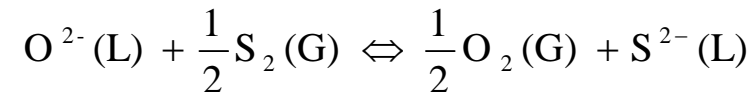
S as sulphide

S as sulphate

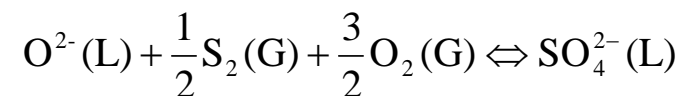


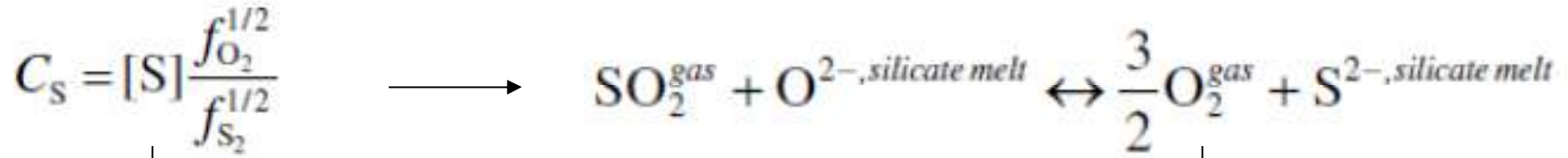
Moretti and Ottonello (2005 GCA)

Sulfide equilibrium:



Sulfate equilibrium:



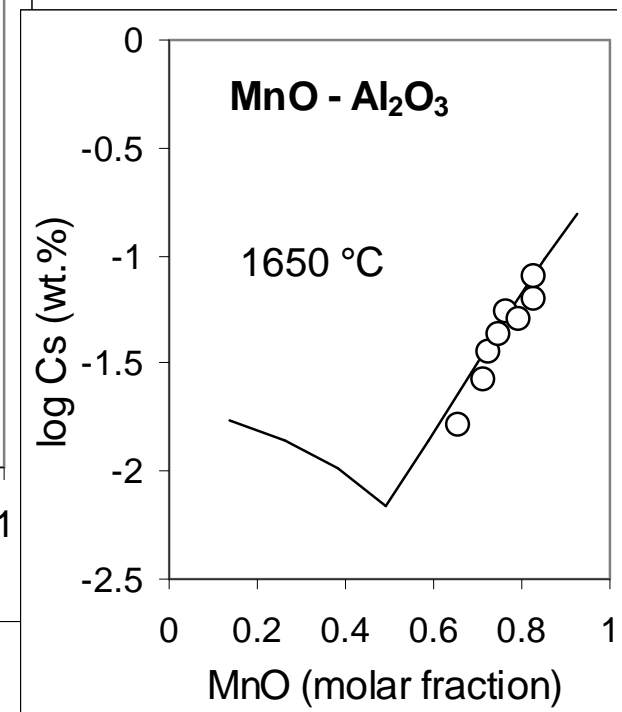
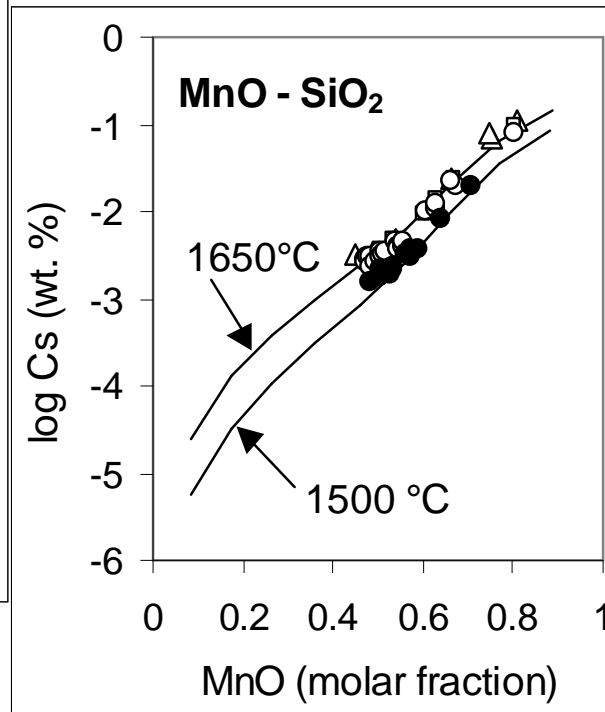
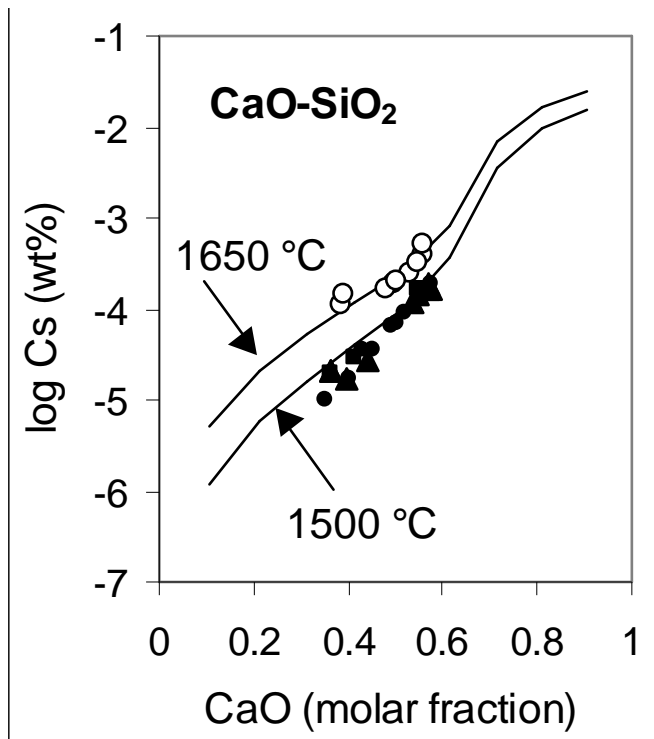


$$C_{S,c} = K'_{O-S,M} (O^{2-}) \left(\frac{f_{O_2}^{\circ}}{f_{S_2}^{\circ}} \right)^{1/2} M_S \sum_{mol} oxides \longleftarrow \ln K'_{O-S,M} = A'_{O-S,M} + \frac{B'_{O-S,M}}{T}$$

A Polymeric Approach to the Sulfide Capacity of Silicate Slags and Melts

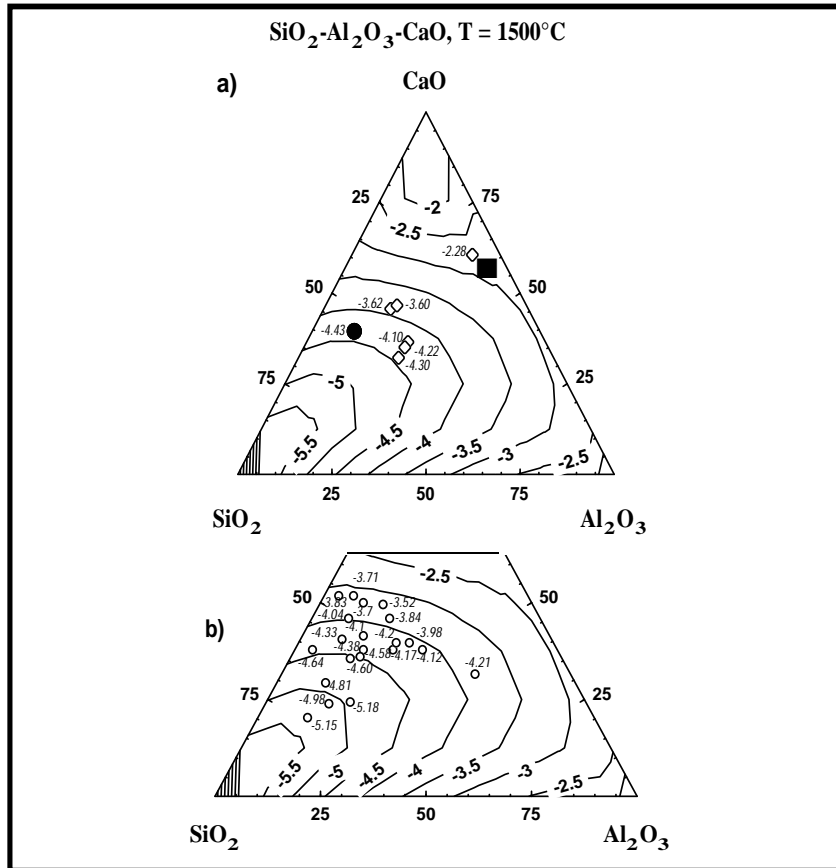
ROBERTO MORETTI and GIULIO OTTONELLO

METALLURGICAL AND MATERIALS TRANSACTIONS B



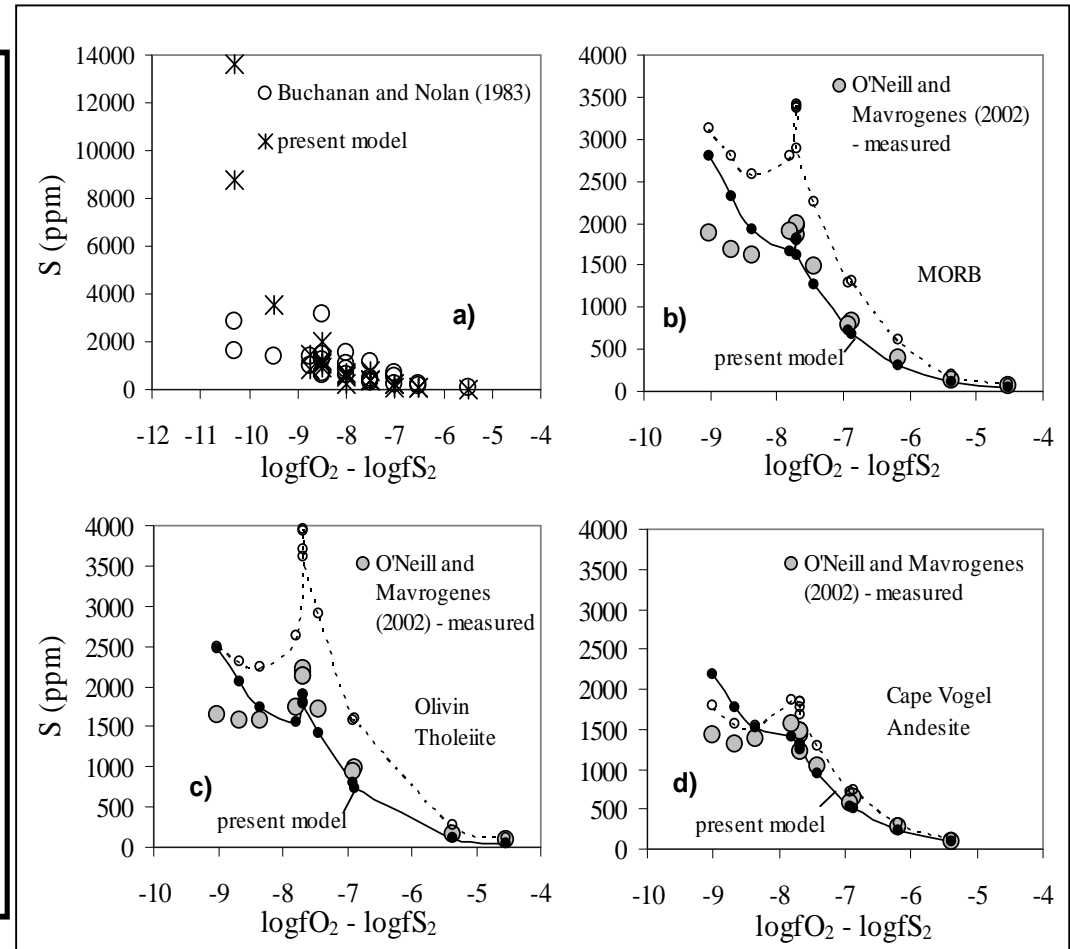
Moretti and Ottonello, 2003 MMTB

Simple metallurgical slags (log Cs contouring)



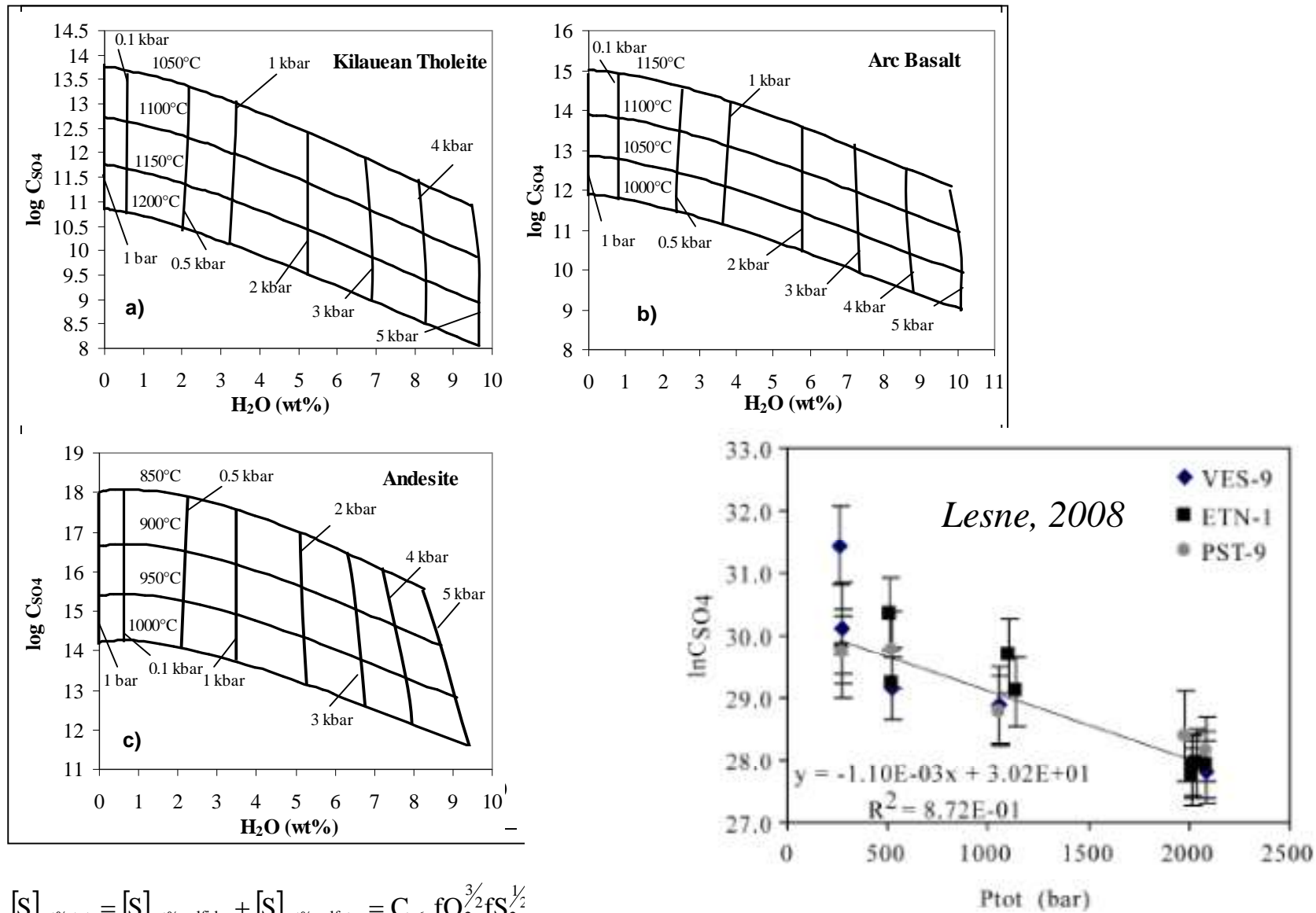
Moretti and Ottonello (2003), *Metall. Mat. Trans. B*

Natural-like melts (sulfur content)



Moretti and Ottonello (2005)

The CTSFG solubility model: features of the sulfide and sulfate capacity surfaces



$$[S]_{wt\%,tot} = [S]_{wt\%,sulfide} + [S]_{wt\%,sulfate} = C_{S^{6+}} fO_2^{3/2} fS_2^{1/2}$$

Figure III.10: $\ln C_{S04}$ calculated as explained in the text, versus total pressure.

Modeling the Solubility of Sulfur in Magmas: A 50-Year Old Geochemical Challenge

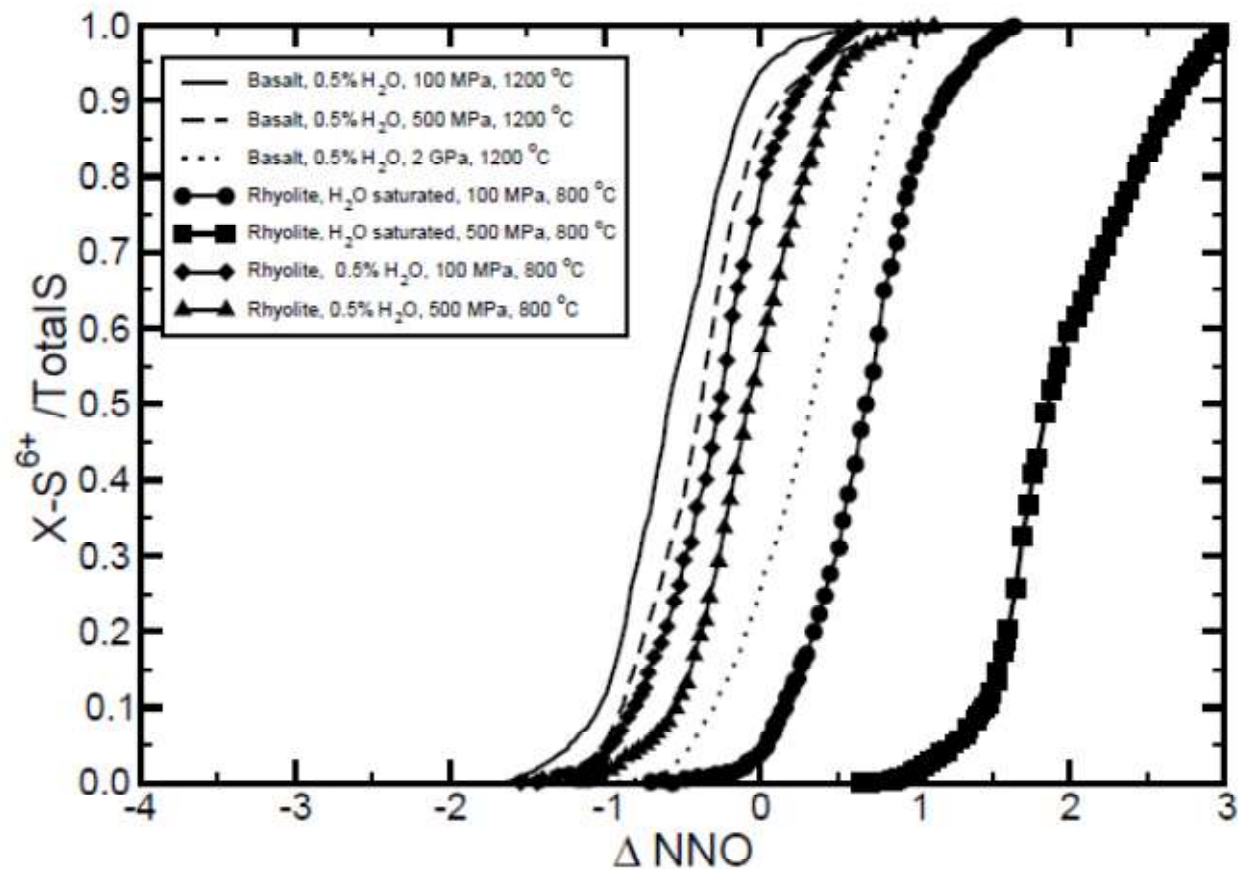
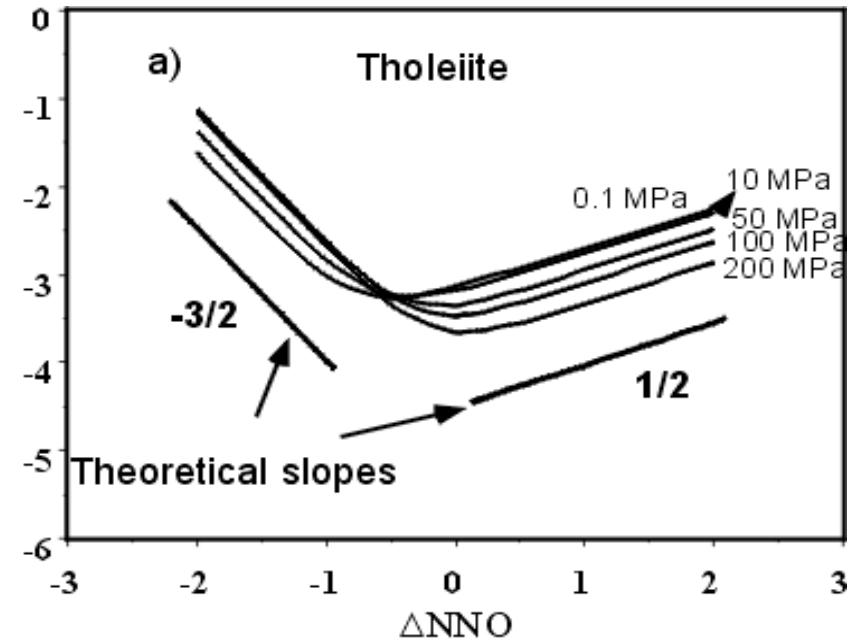
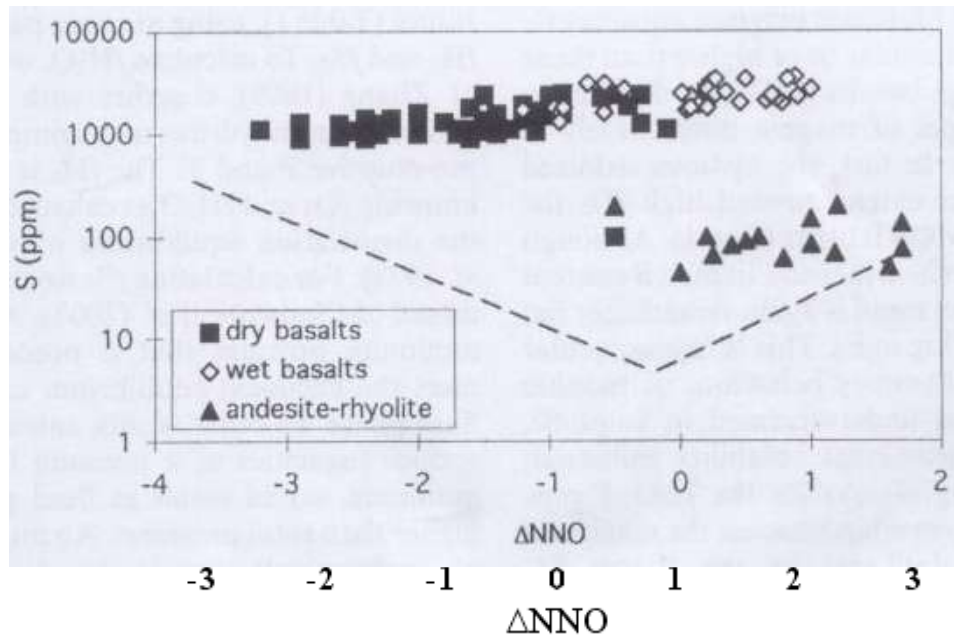


Figure 13. Comparison of the calculated molar ratio of S⁶⁺/Total S ($X-S^{6+}/\text{Total S}$) in melts as a function of ΔNNO for basaltic and rhyolitic melts at different temperatures, pressures and water concentrations in the melt. Drawn after Moretti and Baker (2008). Note how unlike in Figure 8, the curves are functions of the intensive thermodynamic variables describing the melt, e.g., pressure, temperature and composition. Please see the text for further discussion.

Baker and Moretti (2011)

Tholeiite, 1400K . H₂O^{tot}=3%wt; CO₂^{tot}=1%wt; S^{tot}=0.5%wt



Moretti et al. (2003) Geol. Soc. Spec. Publ. 213

Mass partitioning in Nature is non-linear. The expected linearity required by theory (stoichiometry in this case) is embodied, not cancelled. Models must account for it.

A Model for the Saturation of C–O–H–S Fluids in Silicate Melts

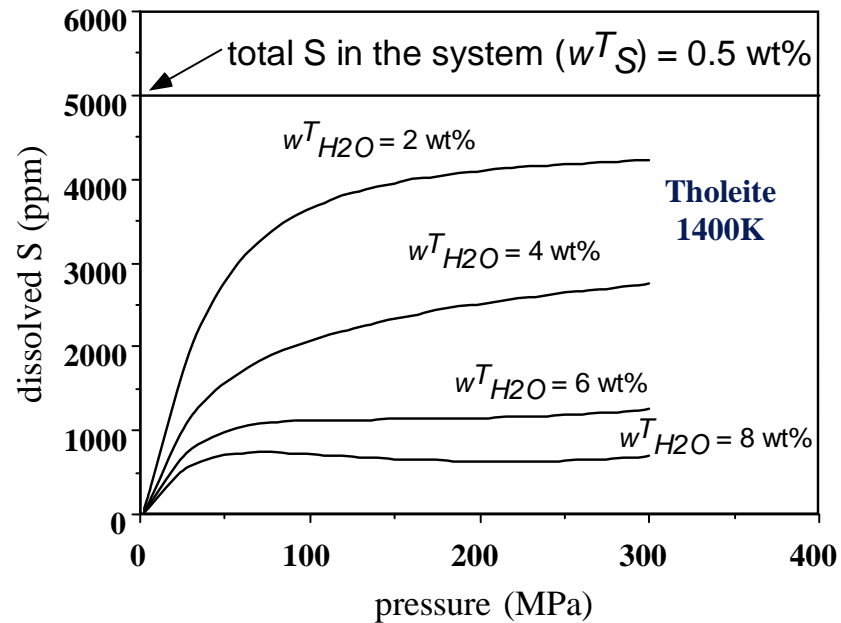
R. MORETTI¹, P. PAPALE^{2,*} & G. OTTONELLO³

¹Istituto Nazionale di Geofisica e Vulcanologia, Osservatorio Vesuviano, Naples, Italy.

²Istituto Nazionale di Geofisica e Vulcanologia, Via della Faggiola 32, I 56126 Pisa, Italy.
(e-mail: papale@pi.ingv.it)

³Dipartimento per lo Studio del Territorio e delle sue Risorse, Genoa, Italy.

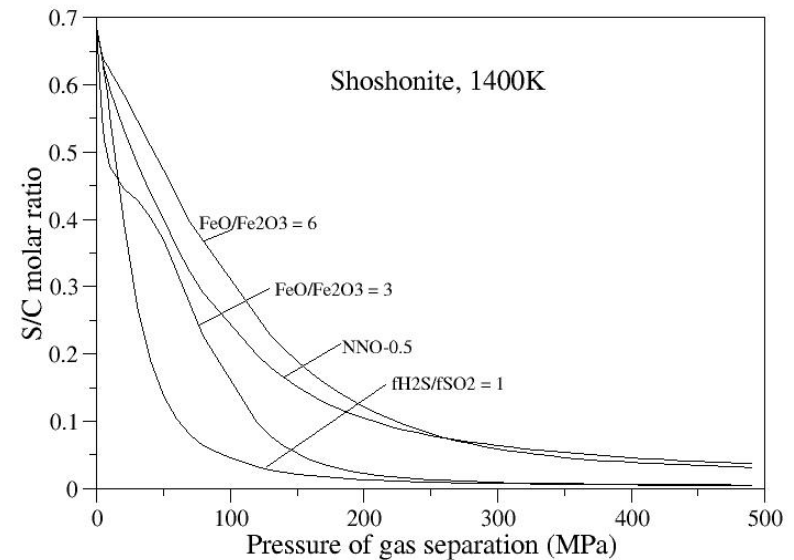
Volatile mixed "solubility"



(applicable to glass inclusions)

Moretti et al. (2003) Geol. Soc. Spec. Publ. 213

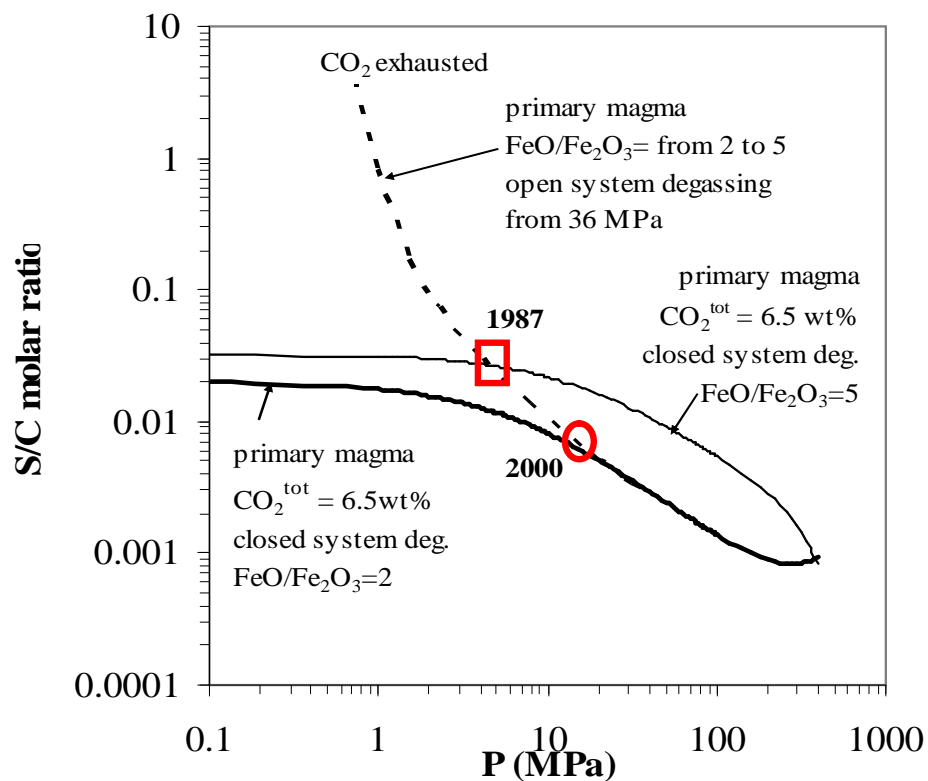
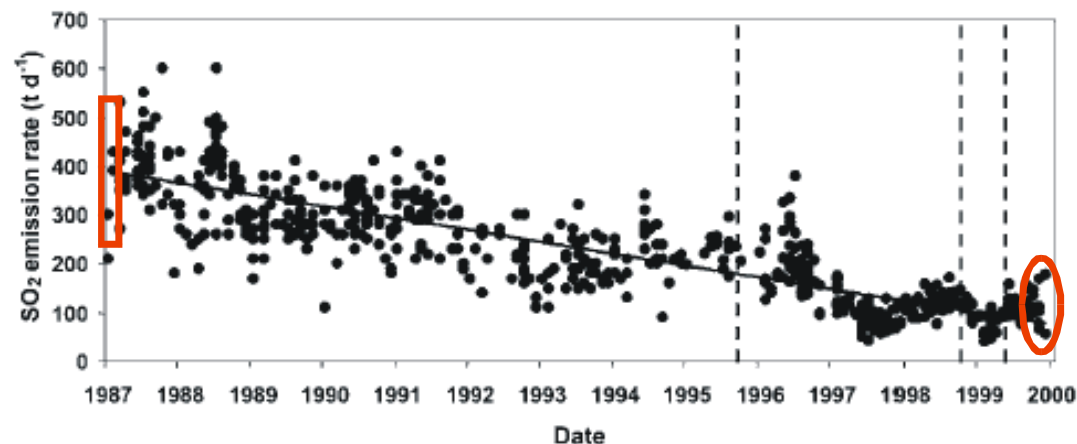
Single-step volatile separation



*(applicable to the geochemical
sensing of volcanoes)*

The Kilauea example...

Summit SO₂ emission rates (1987-2000; Elias et al., 1998, Gerlach et al., 2002).

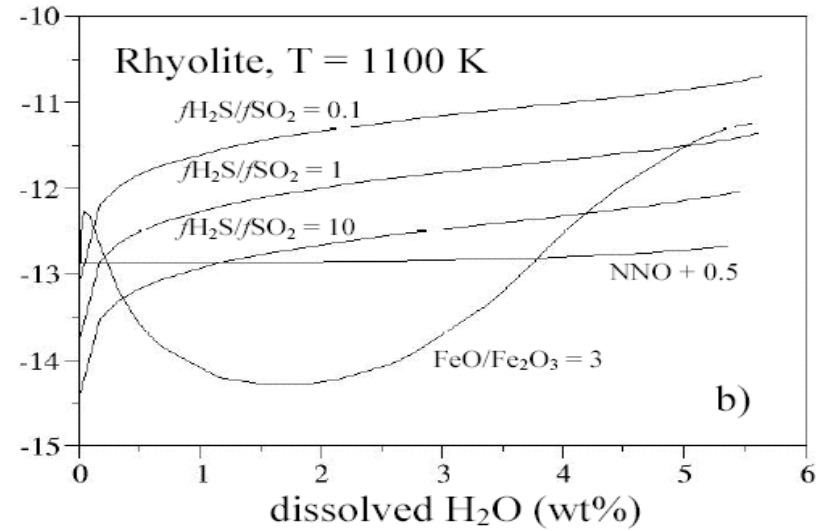
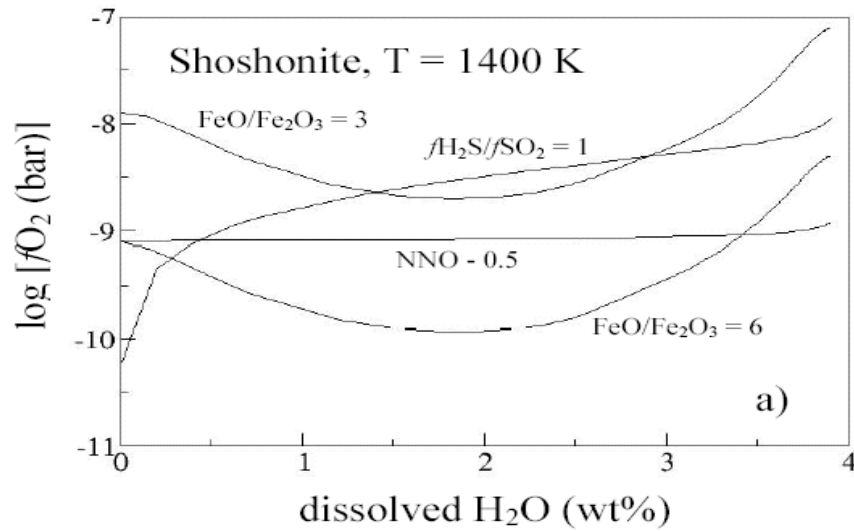
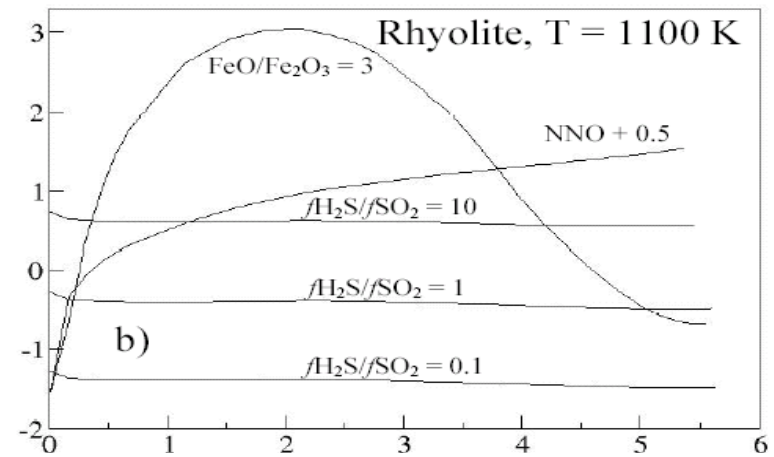
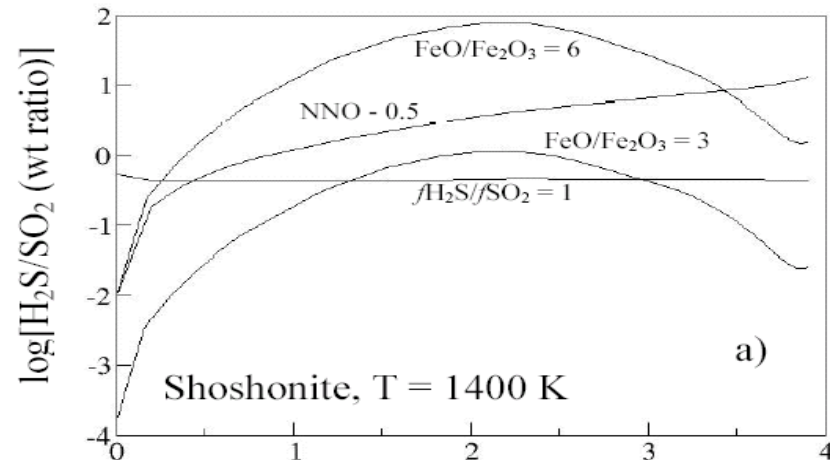


By assuming a CO₂ flux of 9000 tons/day, constant through years (Gerlach, 2002), the following S/C molar average ratios can be computed:

year 1987: S/C = 0.03

year 2000: S/C = 0.0075

→ From 1987 to 2000: downward migration of 7 Mpa (about 300 m.) of the main degassing surface (i.e., fresh magma arrival?) and onset of more oxidized conditions



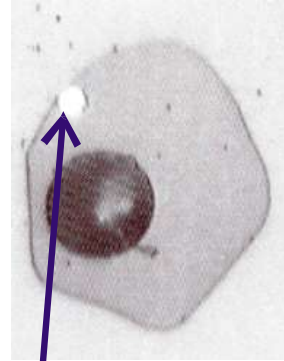
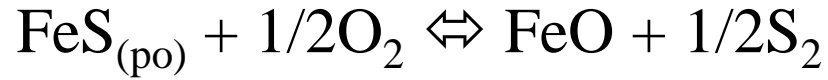
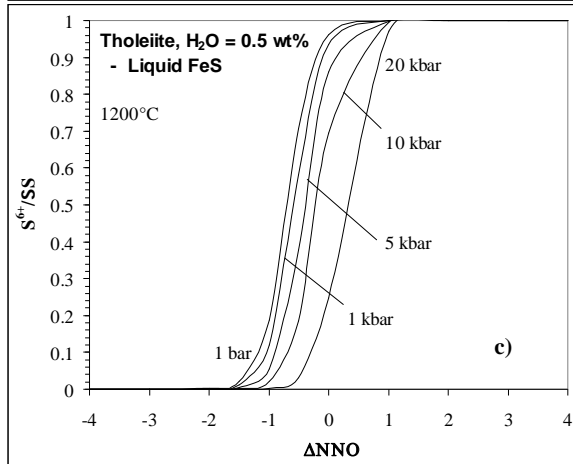
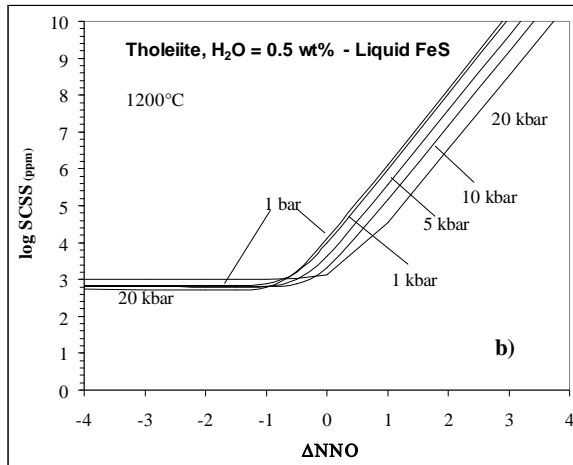
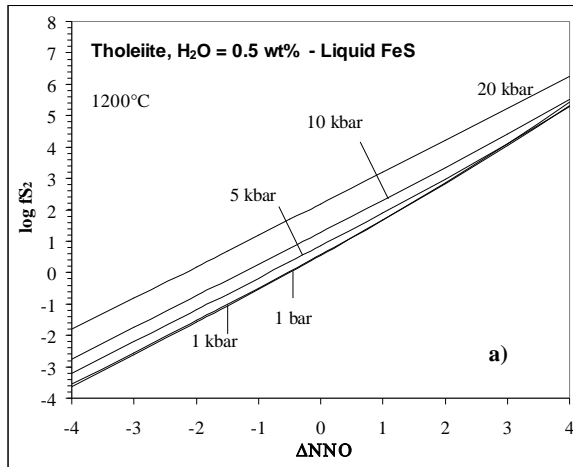
Chemical Geology 213 (2004) 265–280



Moretti and Papale (2004) *Chem. Geol.*

On the oxidation state and volatile behavior in multicomponent gas–melt equilibria

Roberto Moretti^{a,*}, Paolo Papale^b



Sulfide globule

$$\bar{H}_{i,P_r,T,\text{melt}}^0 = \bar{H}_{i,P_r,T_r,\text{crystal}}^0 + \int_{T_r}^{T_i} C_{P,i,\text{crystal}} dT$$

$$+ \Delta \bar{H}_{i,\text{fusion}} + \int_{T_r}^T C_{P,i,\text{melt}} dT$$

$$\bar{S}_{i,P_r,T,\text{melt}}^0 = \bar{S}_{i,P_r,T_r,\text{crystal}}^0 + \int_{T_r}^{T_i} C_{P,i,\text{crystal}} \frac{dT}{T}$$

$$+ \Delta \bar{S}_{i,\text{fusion}} + \int_{T_r}^T C_{P,i,\text{melt}} \frac{dT}{T}$$

Moretti and Baker (2008, Chemical Geology)

$\bar{0}$ $\bar{70}$ $\bar{80}$

Chemical Geology 256 (2008) 285–297



ELSEVIER

Contents lists available at ScienceDirect

Chemical Geology

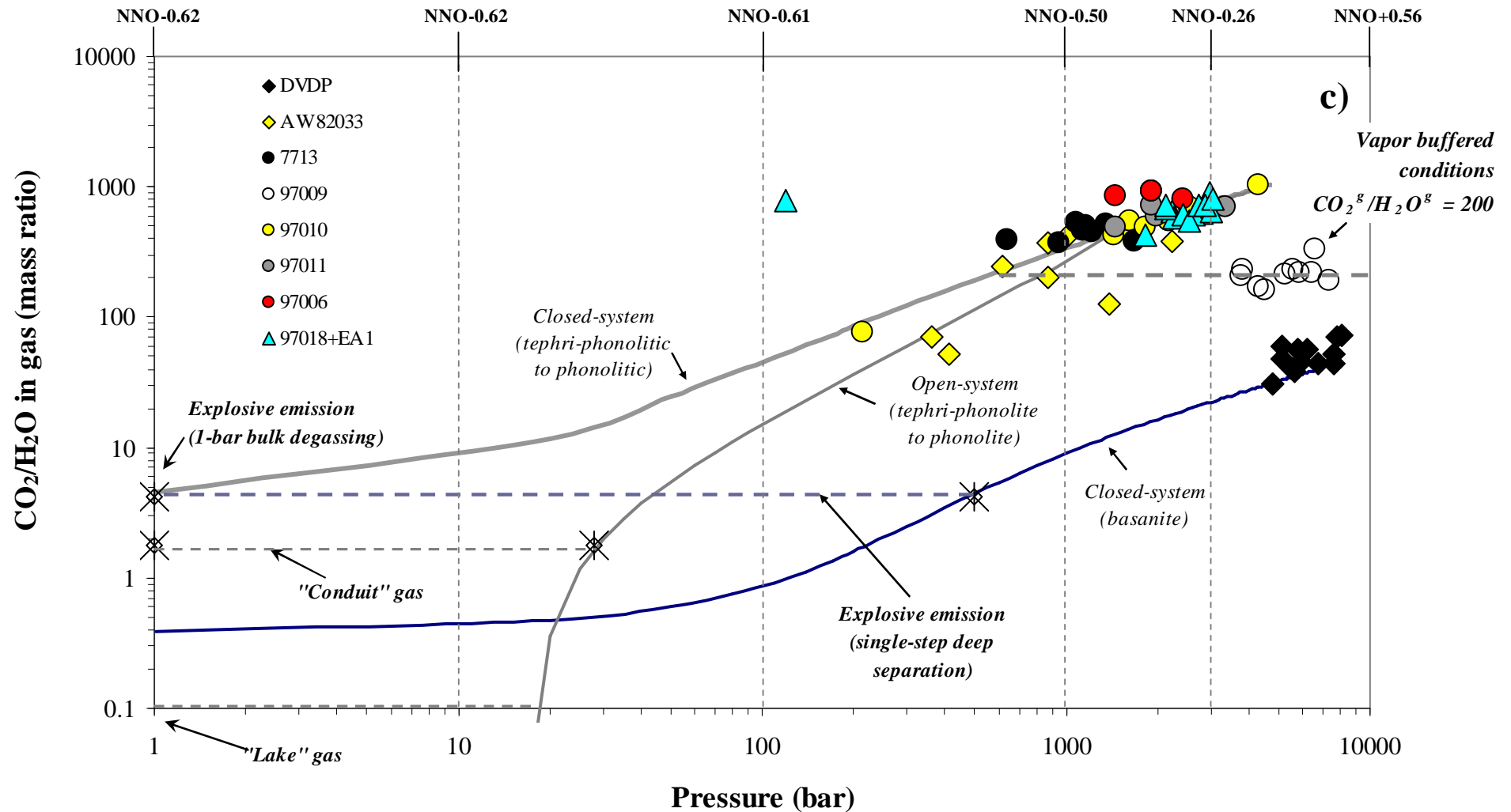
journal homepage: www.elsevier.com/locate/chemgeo



Modeling the interplay of $f\text{O}_2$ and $f\text{S}_2$ along the FeS-silicate melt equilibrium

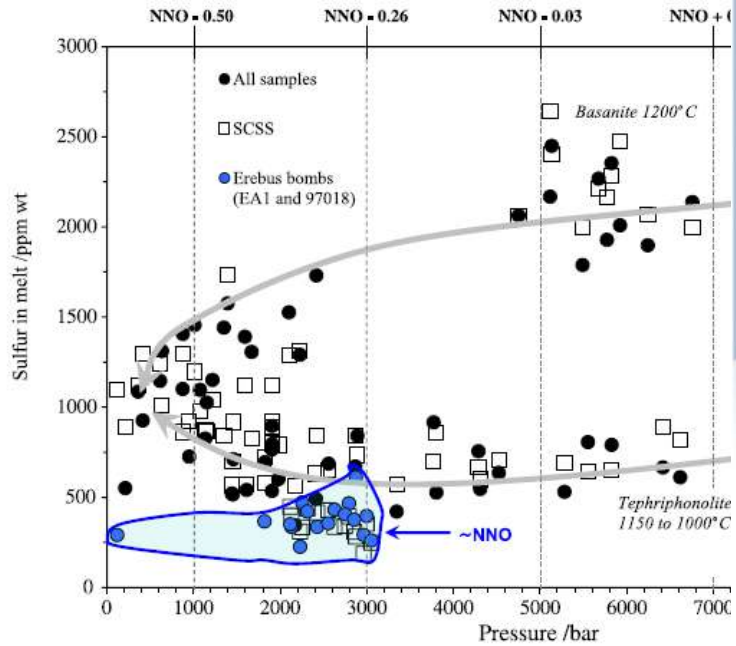
Roberto Moretti ^{a,*}, Don R. Baker ^{b,c}

Open-conduit conditions (e.g., Erebus)



Modelled CO₂^{gas}/H₂O^{gas} mass ratios

Oppenheimer et al. (2011)



$$[S]_{wt.\%SCSS} = [S]_{wt.\%sulfide} +$$

Earth and Planetary Science Letters 306 (2011) 261–271

Contents lists available at ScienceDirect

Earth and Planetary Science Letters

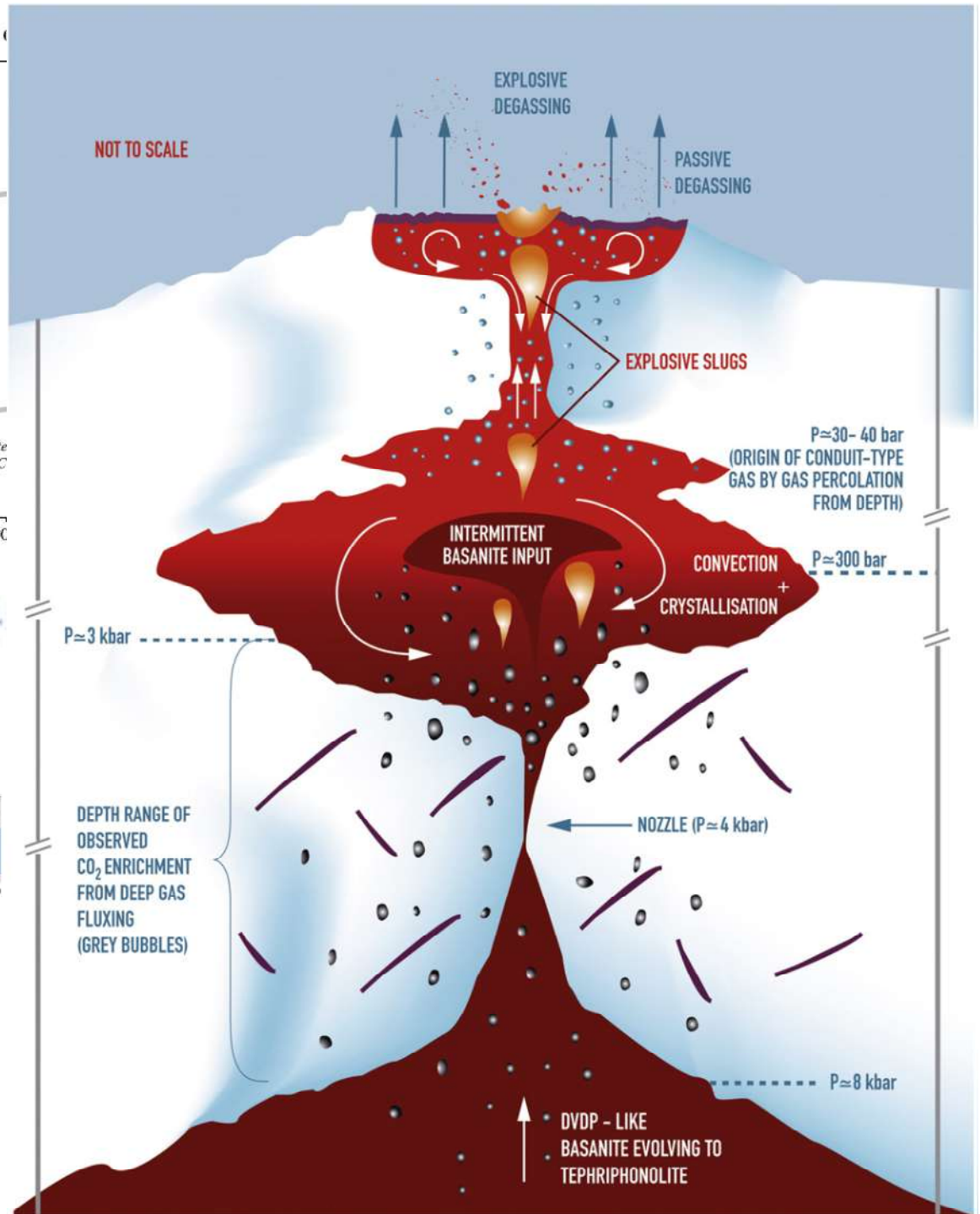
journal homepage: www.elsevier.com/locate/epsl




Mantle to surface degassing of alkalic magmas at Erebus volcano, Antarctica

Clive Oppenheimer^{a,b,c,*}, Roberto Moretti^{d,e}, Philip R. Kyle^f, Al Eschenbacher^f, Jacob B. Lowenstern^g, Richard L. Hervig^h, Nelia W. Dunbarⁱ

Oppenheimer et al. (2011)



Montserrat – Soufrière Hills

Click Here for Full Article

Excess volatiles supplied by mingling of mafic magma at an andesite arc volcano

M. Edmonds
 COMET, National Centre for Earth Observation, Earth Science Department, University of Cambridge, Cambridge CB2 3EQ, UK (m.e2010@cam.ac.uk)

A. Aiuppa
 Dipartimento CFTA, Università di Palermo, Via archirafi 36, I-90123 Palermo, Italy

M. Humphreys
 Earth Science Department, University of Cambridge, Cambridge CB2 3EQ, UK

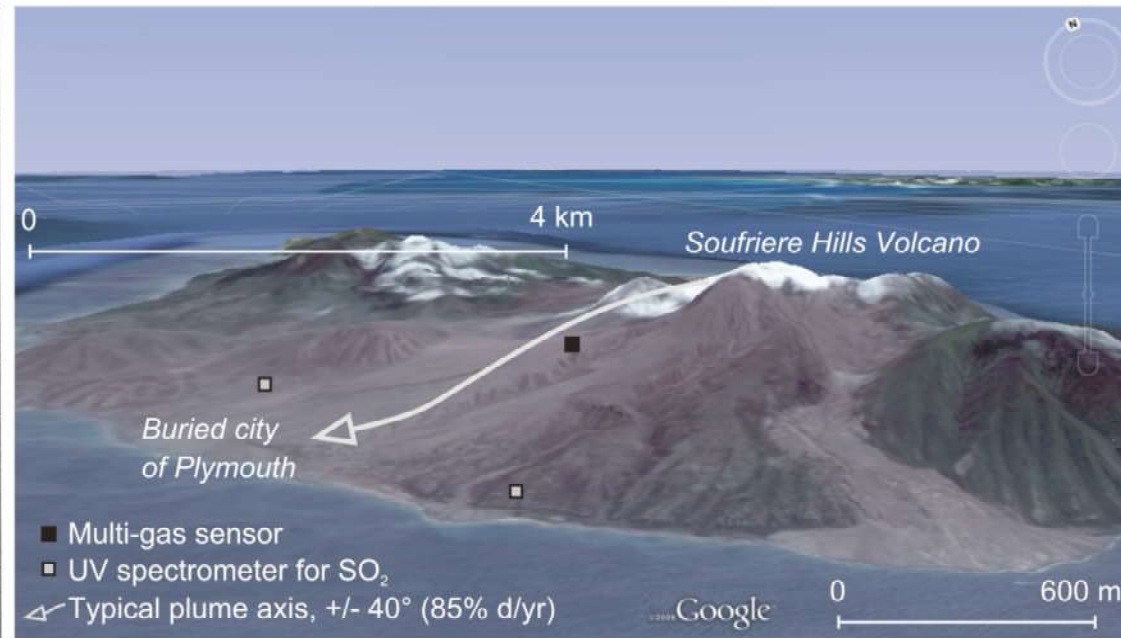
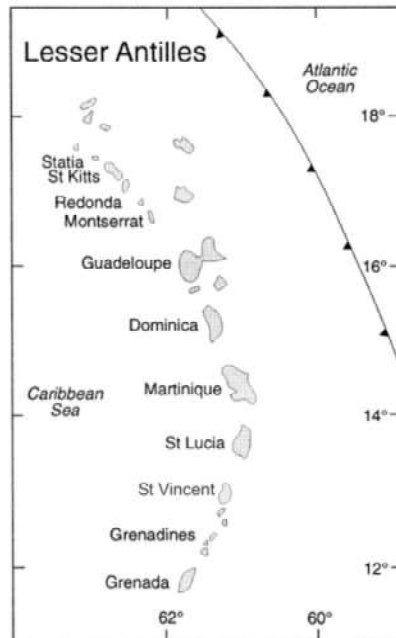
R. Moretti
 Osservatorio Vesuviano, Istituto Nazionale di Geofisica e Vulcanologia, Via Diadolziani, 328, I-80124 Naples, Italy

G. Giudice
 Sezione di Palermo, Istituto Nazionale di Geofisica e Vulcanologia, Via Ugo La Malfa, 153, I-90146 Palermo, Italy

R. S. Martin
 Earth Science Department, University of Cambridge, Cambridge CB2 3EQ, UK

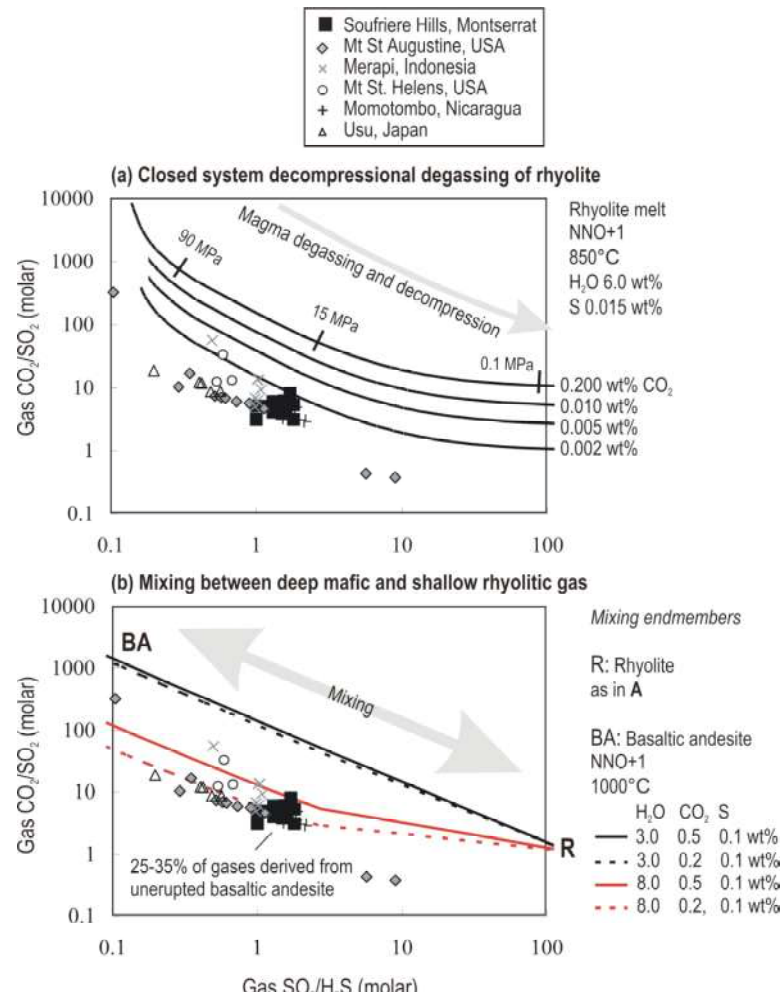
R. A. Herd
 School of Environmental Sciences, University of East Anglia, Norwich, NR4 7TJ, UK

T. Christopher
 Montserrat Volcano Observatory, Montserrat, West Indies



Problem: mafic enclaves \leftrightarrow excess volatiles \leftrightarrow high plume $\text{SO}_2/\text{H}_2\text{S}$

Edmonds et al. (2008)



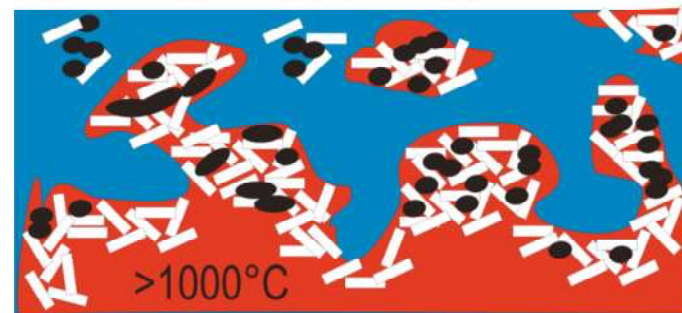
Excess volatiles and high H₂S/SO₂



Vapour-permeable bubble and fracture networks



H₂S and CO₂ (and H₂O) gases supplied to andesite



Vesiculation-induced mixing and enclave formation

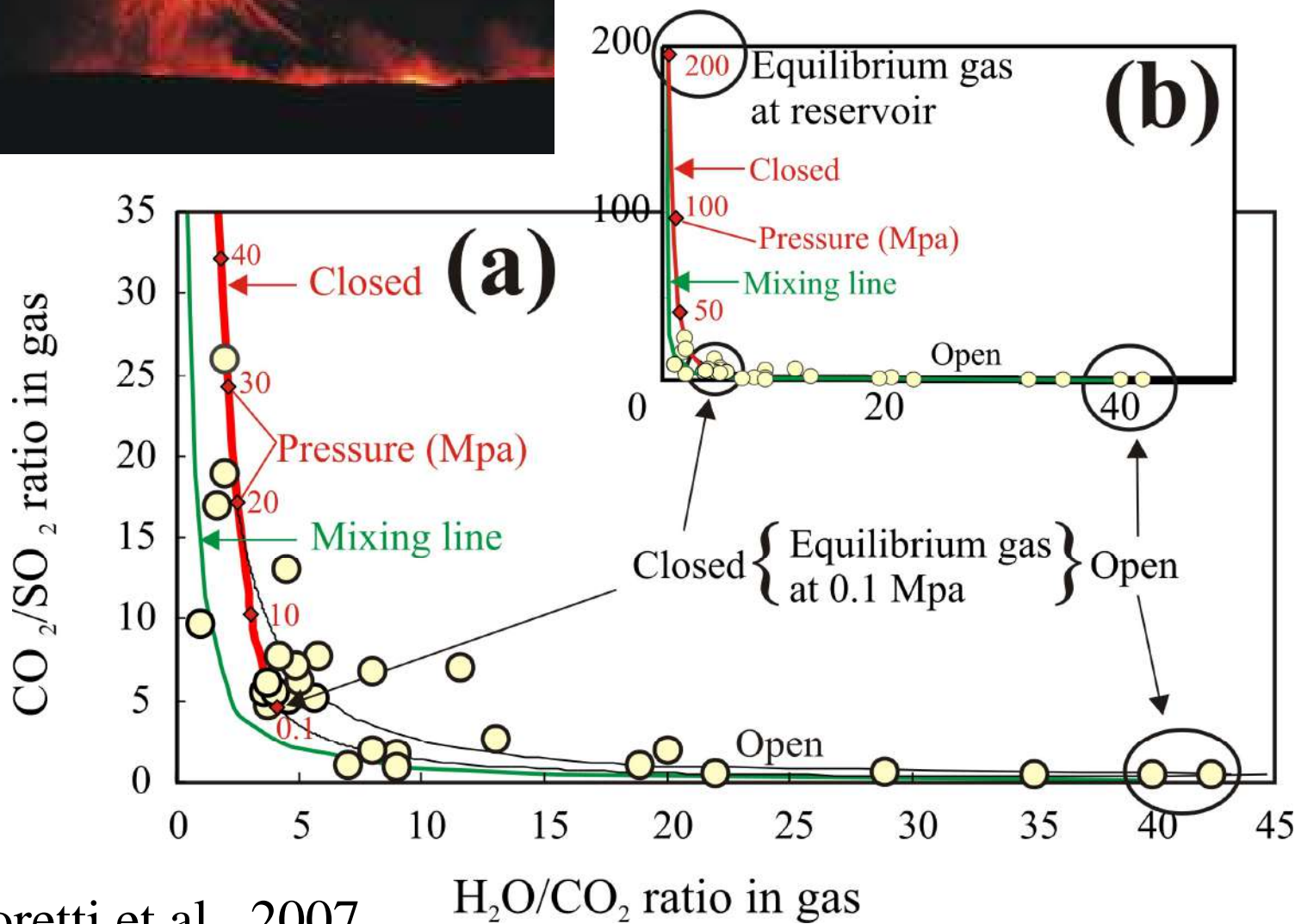
“...volatiles are supplied from a quenching, vesiculating mafic magma against a cooler, more crystalline andesitic magma in the crust “

Open-conduit conditions (e.g., Etna...)

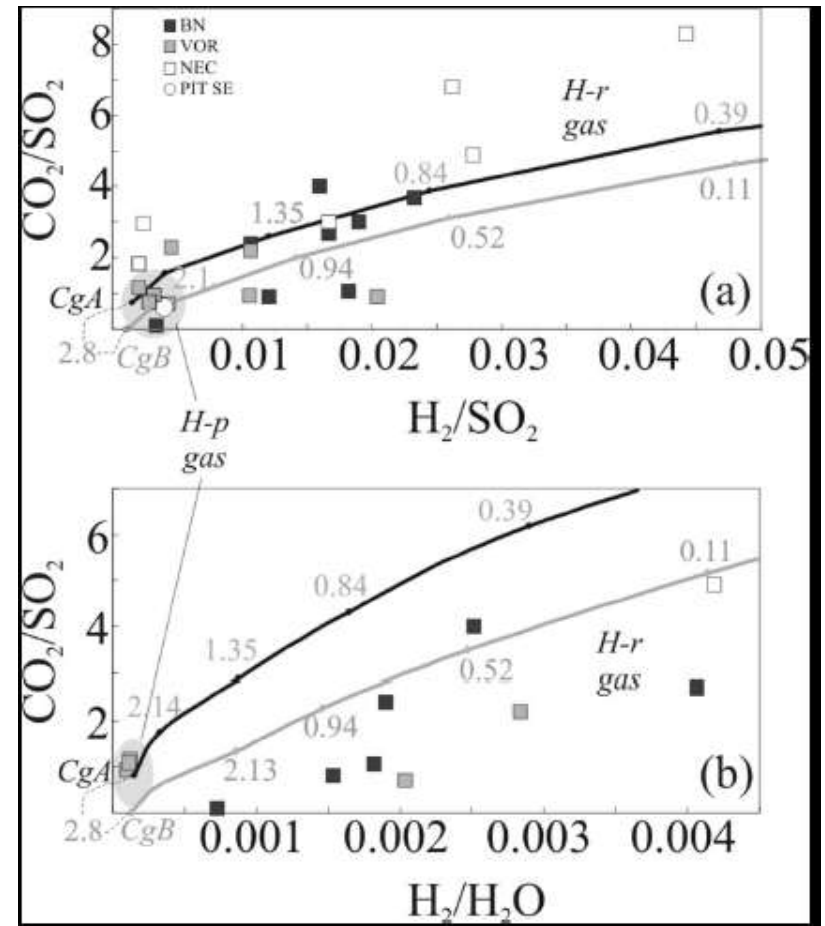
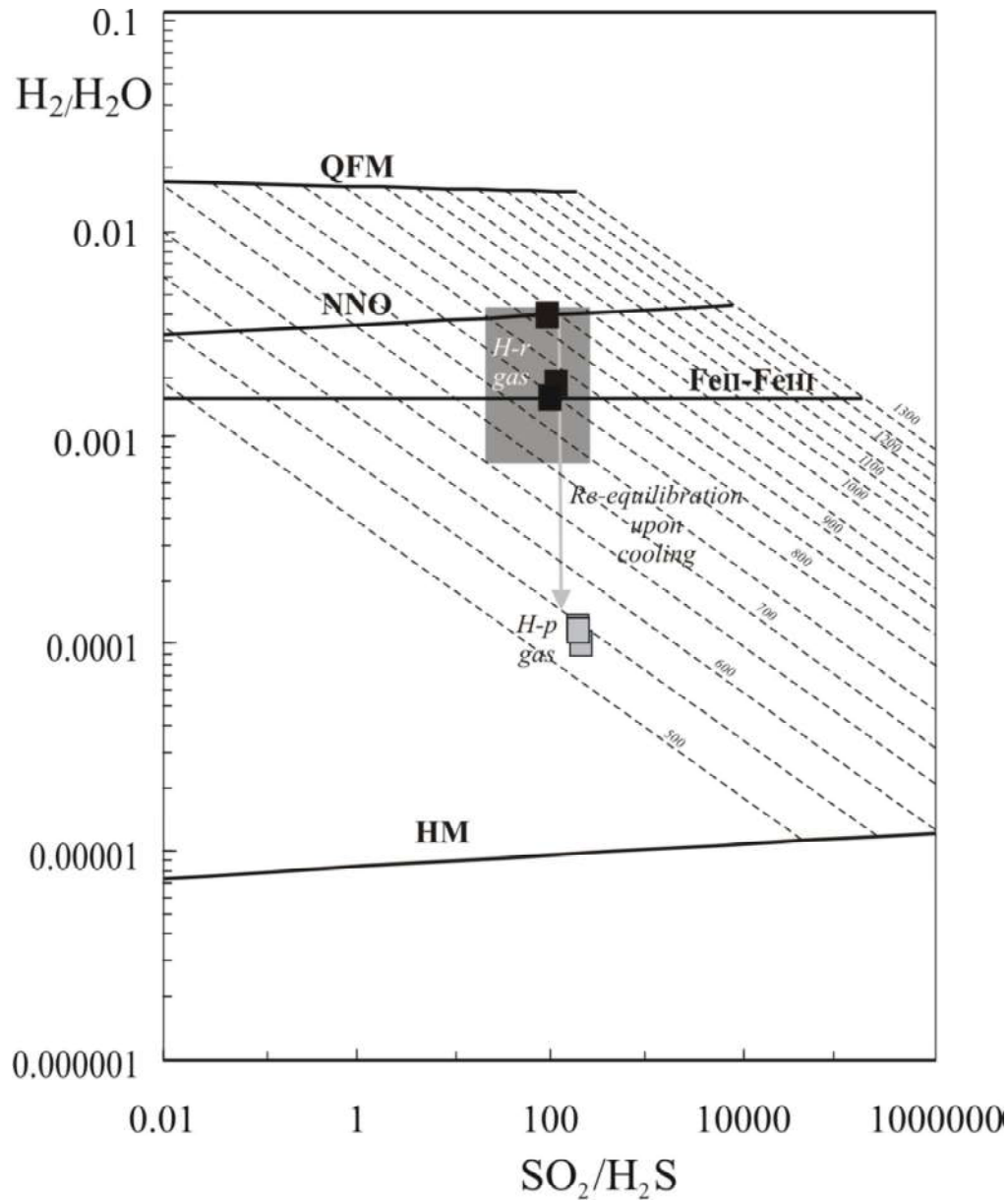
Aiuppa, Moretti et al., 2007



Open-conduit conditions (e.g., Etna...)



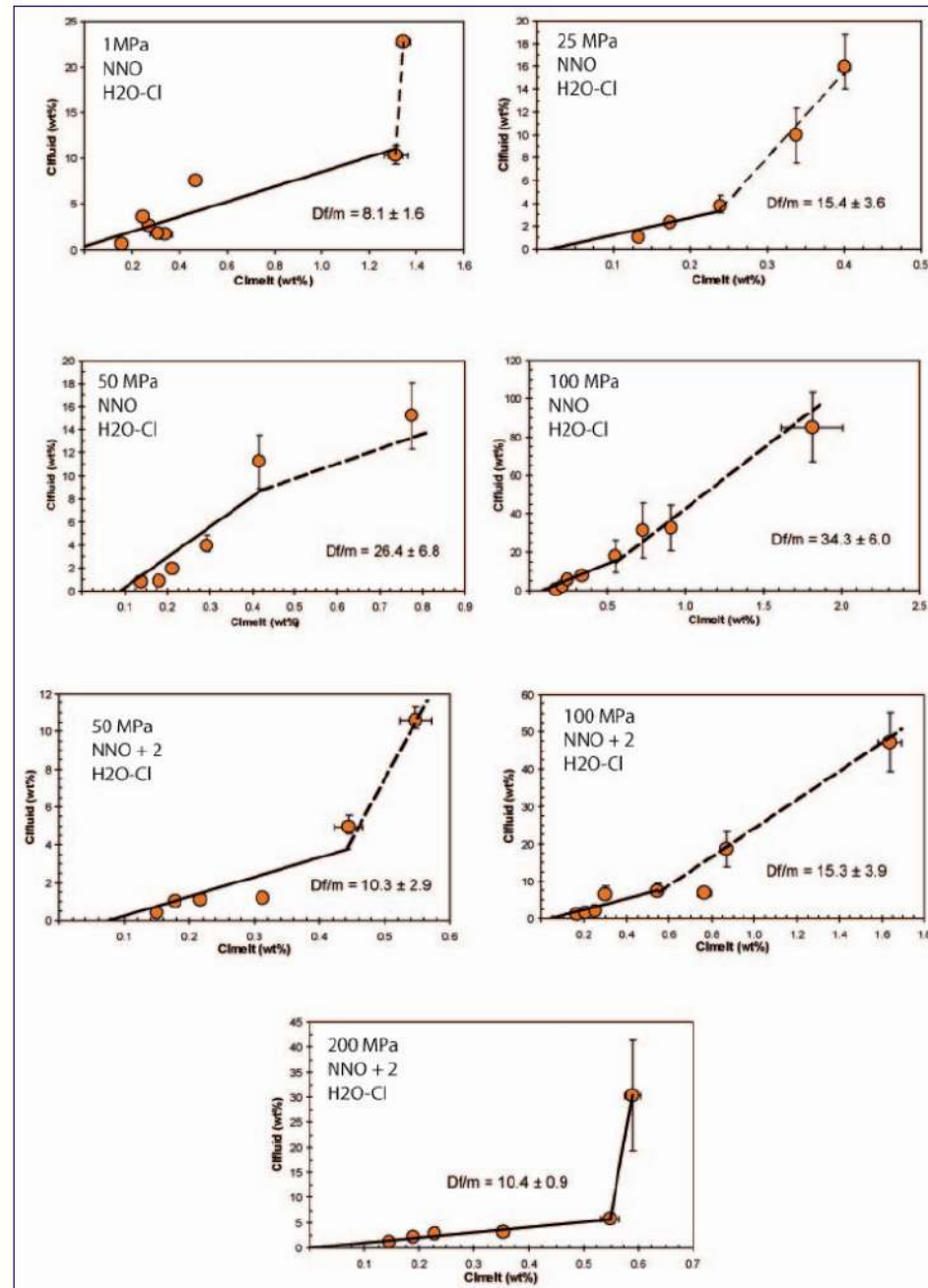
Aiuppa, Moretti et al., 2007



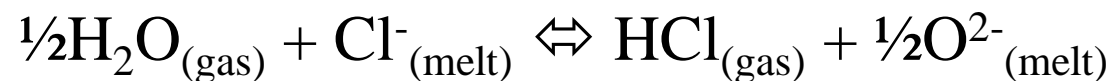
Aiuppa, Shinohara, Giudice, Liuzzo, Moretti (2011, JGR)

Partition coefficients (H₂O-Cl exps)

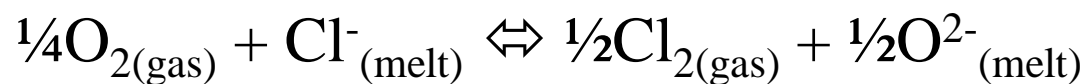
Alletti et al, 2009



In the ionic-polymeric approach we set the following equilibria:

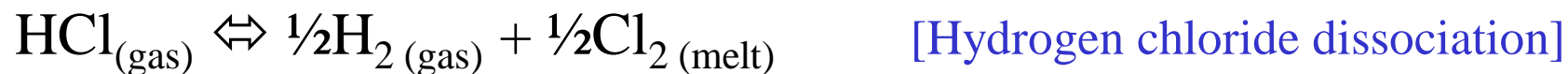
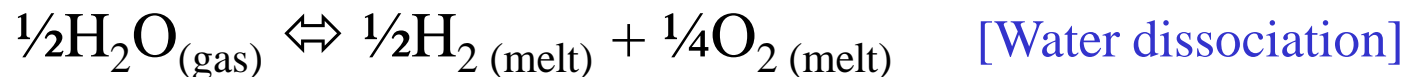


which can be also derived from:



*Hirosumi and Morita (2000;
for chlorine)*

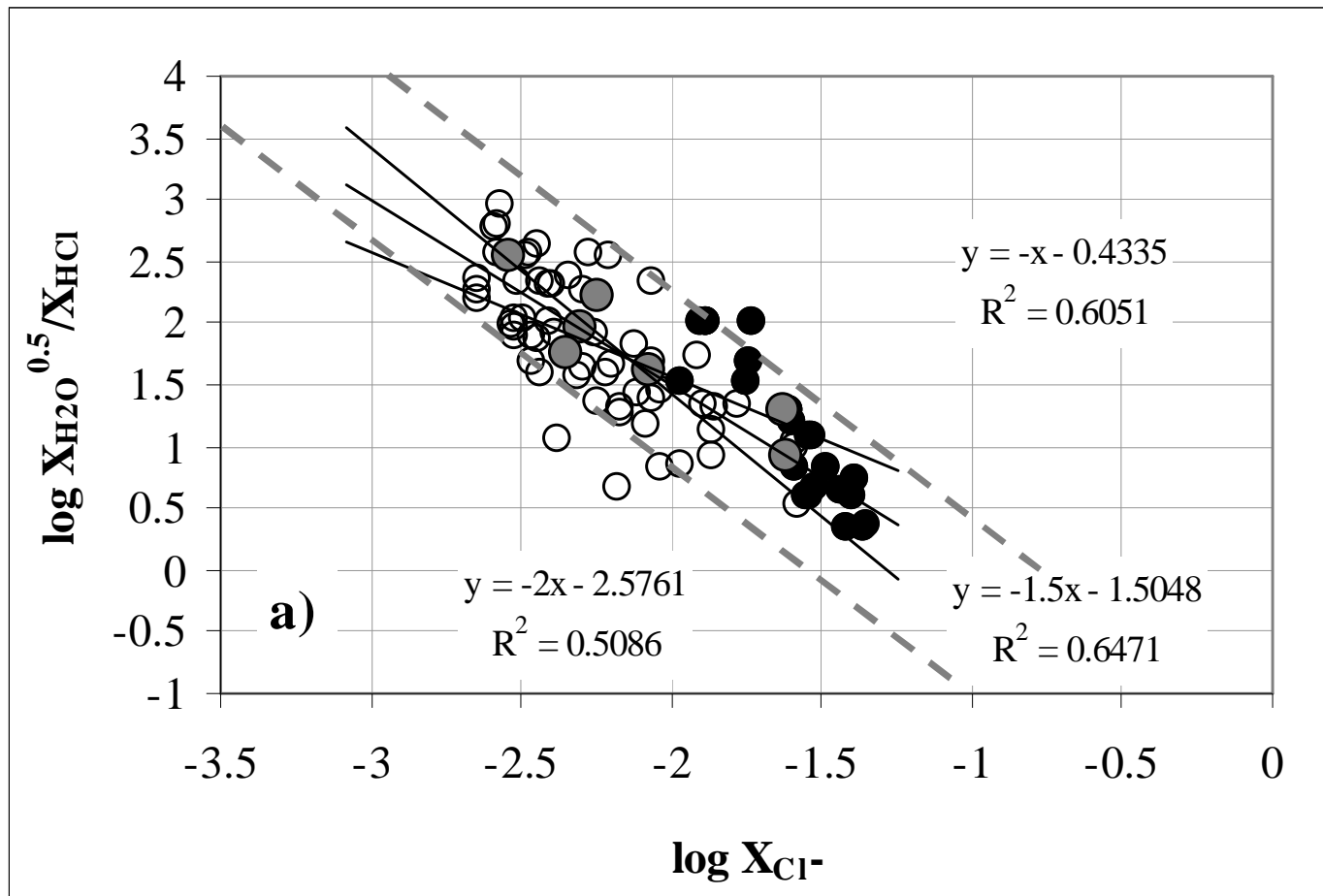
by considering the following dissociations and redox couples:

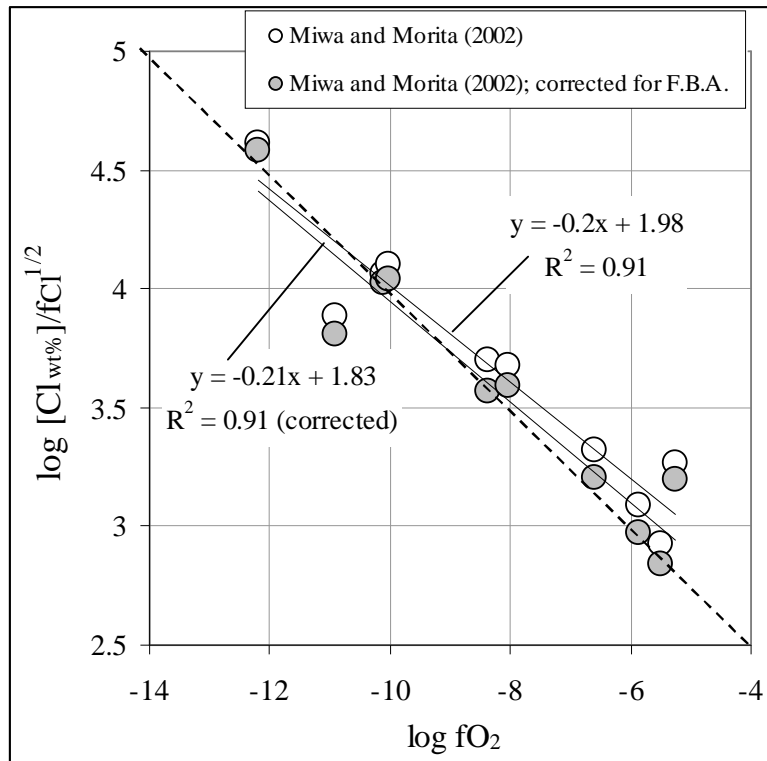
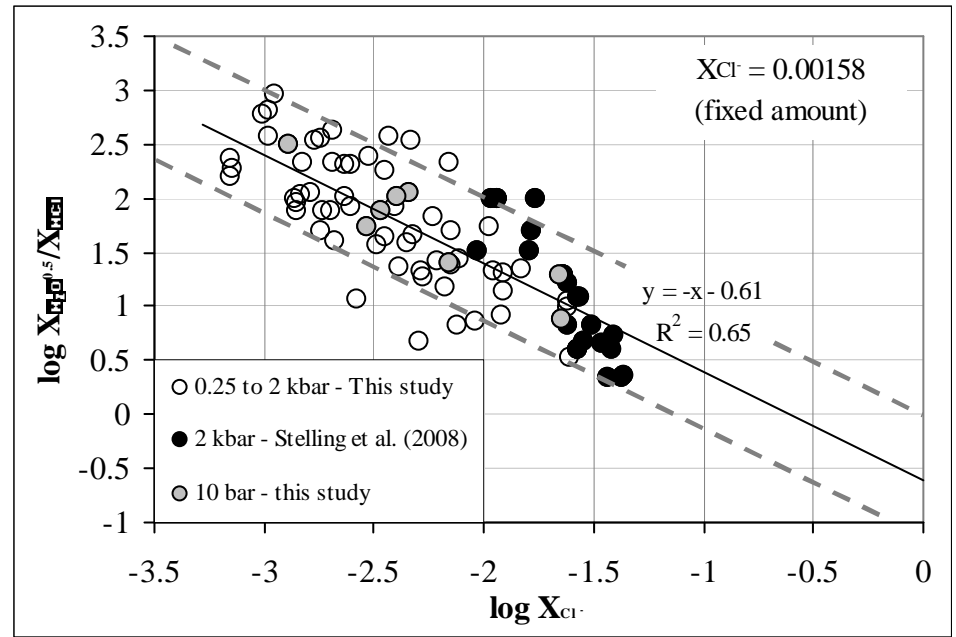
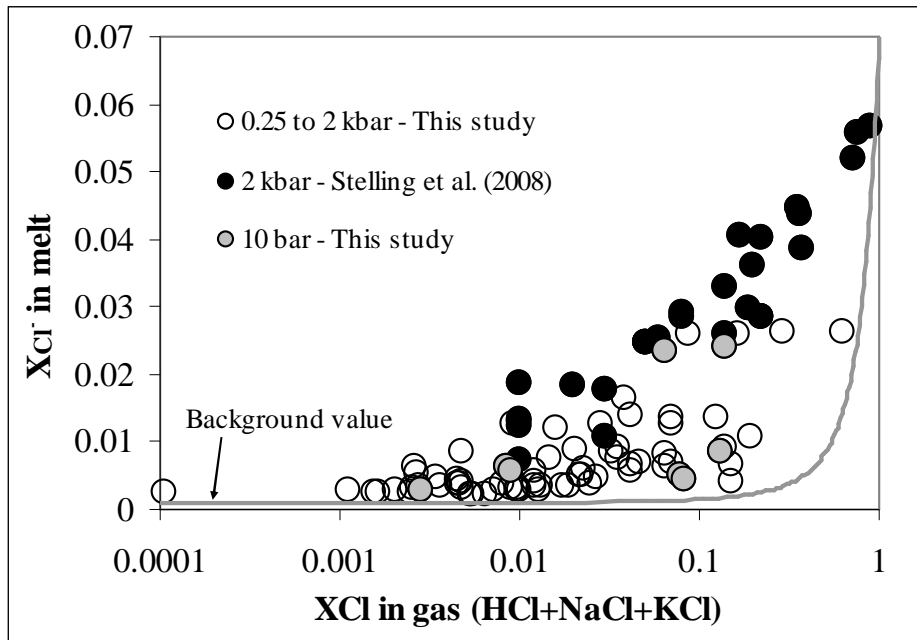


Moretti et al., in prep.



$$\log \frac{X_{\text{H}_2\text{O},\text{gas}}^{1/2}}{X_{\text{HCl},\text{gas}}} = -\log K_3^* - \log X_{\text{Cl}^-}^{\text{melt}}$$





$$D^* = \frac{X_{HCl}}{X_{Cl^-}^2} = X_{H_2O}^{1/2} \cdot 10^{2.5761}$$

Moretti et al., in progress

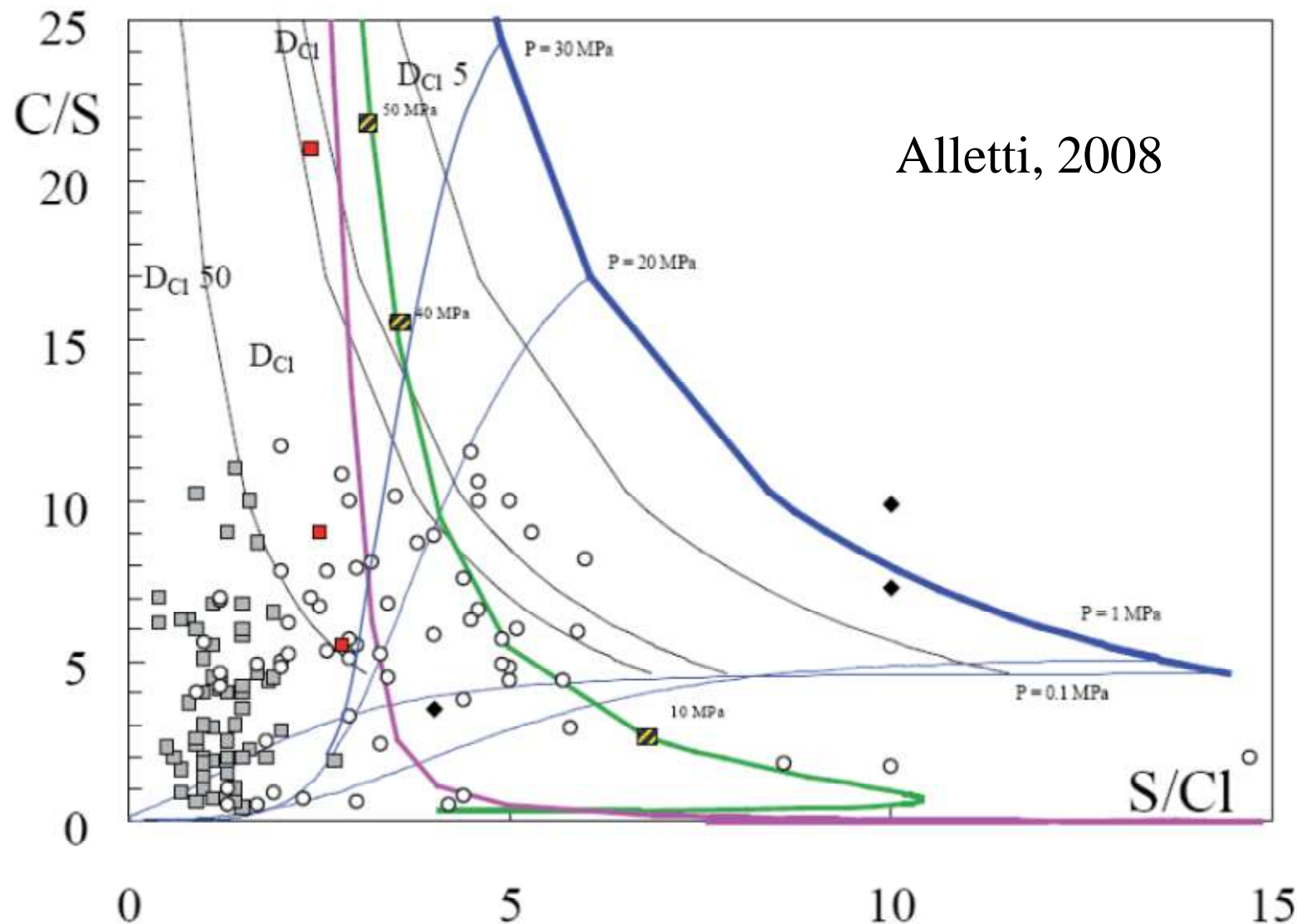
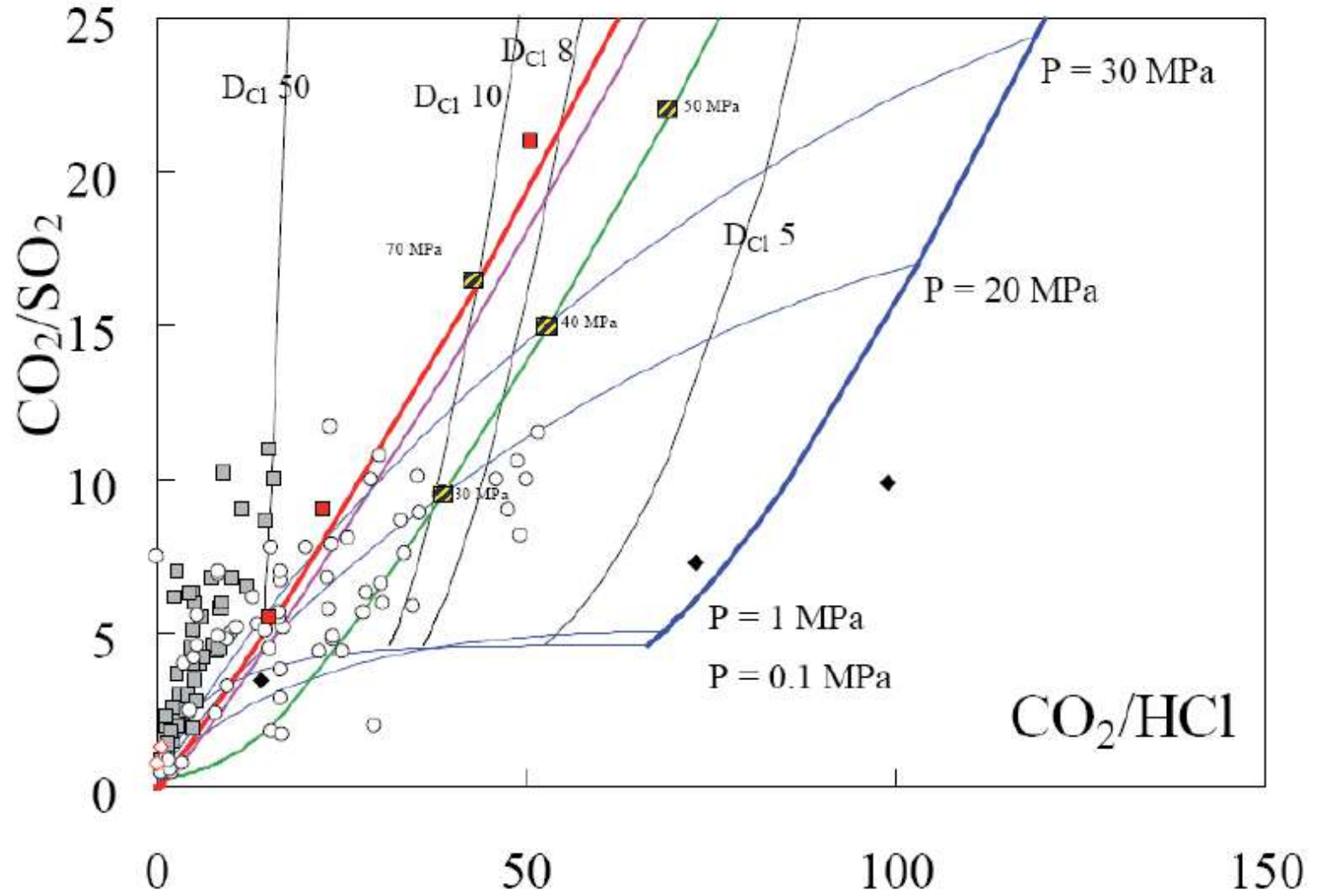


Fig. 30: SO_2/HCl vs. CO_2/SO_2 molar ratios in Etna's volcanic gas plume, contrasted against model results for the magmatic gas phase (symbols as in Fig. 25).

Alletti, 2008



Gas fluxing determines the detected K-enrichment by stripping K to the gas phase as KCl.

=> the measured K variability reflects the **K-gain**, by some portions of the magmatic system, that **superimposes to the normal trend of fractional crystallization**.

By considering KCl and HCl as the most important gas species, the following chemical reactions can be written:



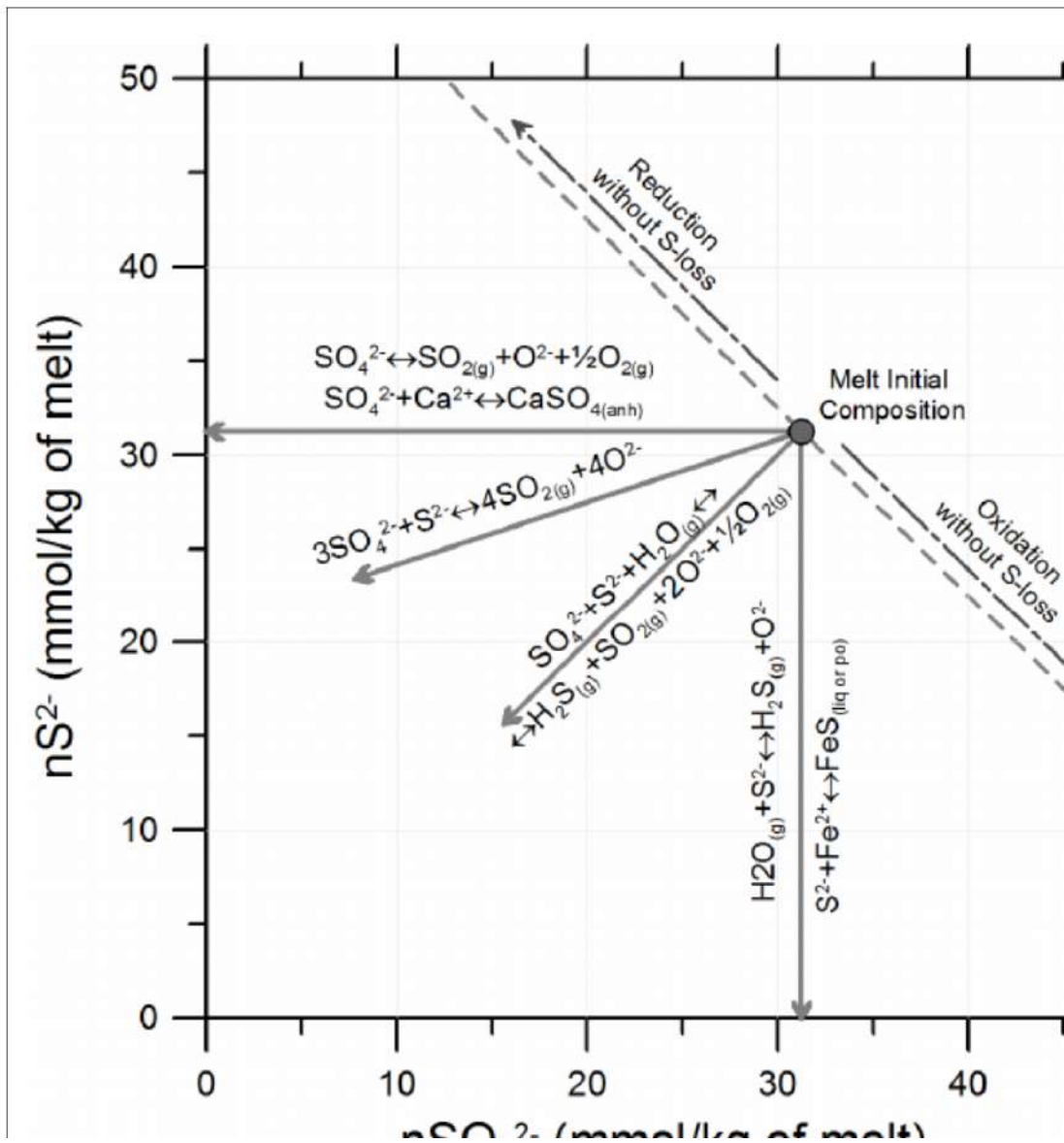
From their equilibrium constants:

$$\log a_{\text{KCl}_{\text{melt}}} = \log a_{\text{KCl}_{\text{gas}}} - \log K_2 = \log \frac{a_{\text{HCl}_{\text{gas}}}}{a_{\text{H}_2\text{O}_{\text{gas}}^{1/2}} + \log a_{\text{K}_2\text{O}_{\text{melt}}} + \log K_1$$

Moretti et al. JPet (accepted)

If $\text{K}_2\text{O}=\text{const}$ $\rightarrow \frac{a_{\text{HCl}_{\text{gas}}}}{a_{\text{H}_2\text{O}_{\text{gas}}^{1/2}}$ increases due to CO_2 -fluxing and dehydration

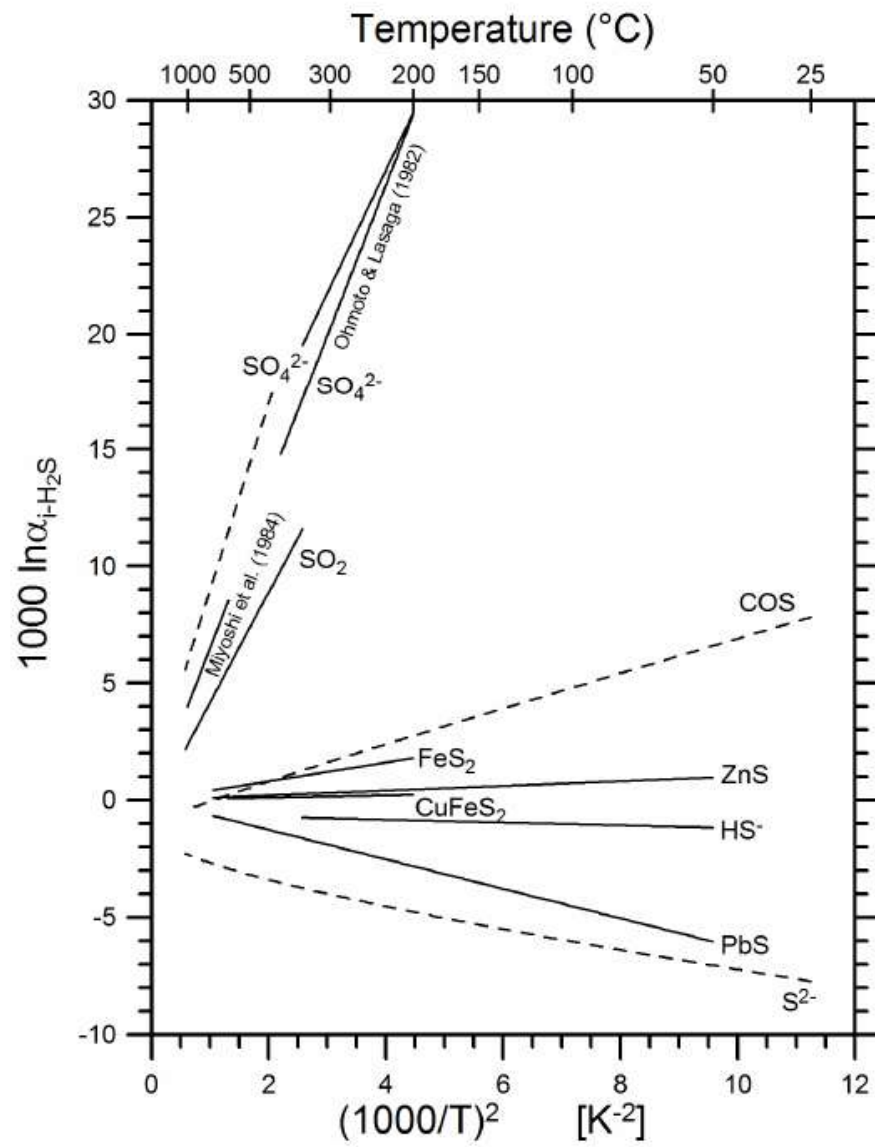
$\rightarrow a_{\text{KCl}_{\text{melt}}}$ increases, hence $X_{\text{KCl}_{\text{melt}}}$ increases



S-species and reactions involved in the full tracking of volcanic degassing...

High reactivity
 ↓
many degassing paths

Marini, Moretti & Accornero (2011) RiMG 73



Ohmoto-Rye, 1979


$$\delta^{34}\text{S}_{\Sigma\text{S}} = \delta^{34}\text{S}_{\text{SO}_2} \cdot y_{\text{SO}_2(\text{g})} + \delta^{34}\text{S}_{\text{H}_2\text{S}} \cdot (1 - y_{\text{SO}_2(\text{g})}),$$

$$y_{\text{SO}_2(\text{g})} = X_{\text{SO}_2(\text{g})} / (X_{\text{SO}_2(\text{g})} + X_{\text{H}_2\text{S}(\text{g})}).$$

$$1000 \ln \alpha_{\text{SO}_2-\text{H}_2\text{S}} = \delta^{34}\text{S}_{\text{SO}_2} - \delta^{34}\text{S}_{\text{H}_2\text{S}}$$

Degassing...

$$\delta^{34}\text{S}_{\Sigma\text{S},f} = \delta^{34}\text{S}_{\Sigma\text{S},i} - (1 - F) \cdot 1000 \ln \alpha_{\text{gas-melt}} \quad (\text{closed s.})$$

$$\delta^{34}\text{S}_{\Sigma\text{S},f} = \delta^{34}\text{S}_{\Sigma\text{S},i} + 1000 \cdot \left(F^{\alpha_{\text{gas-melt}}^{-1}} - 1 \right)$$


$$F = C_{\Sigma\text{S},\text{melt},f} / C_{\Sigma\text{S},\text{melt},i}$$

Marini et al.
(2011)



Nordstrom and Munoz, 1986

Degassing...

$$\begin{aligned}
 1000\ln\alpha_{\text{gas-melt}} &\cong \delta^{34}\text{S}_{\Sigma\text{S,gas}} - \delta^{34}\text{S}_{\Sigma\text{S,melt}} = \\
 &= \left[Y_{\text{SO}_2} \cdot \delta^{34}\text{S}_{\text{SO}_2} + (1 - Y_{\text{SO}_2}) \cdot \delta^{34}\text{S}_{\text{H}_2\text{S}} \right] - \left[Y_{\text{SO}_4^{2-}} \cdot \delta^{34}\text{S}_{\text{SO}_4^{2-}} + (1 - Y_{\text{SO}_4^{2-}}) \cdot \delta^{34}\text{S}_{\text{S}^{2-}} \right] = \\
 &= Y_{\text{SO}_2} \cdot 1000\ln\alpha_{\text{SO}_2-\text{H}_2\text{S}} + Y_{\text{SO}_4^{2-}} \cdot 1000\ln\alpha_{\text{S}^{2-}-\text{SO}_4^{2-}} + 1000\ln\alpha_{\text{H}_2\text{S}-\text{S}^{2-}}
 \end{aligned}$$

where $Y_{\text{SO}_4^{2-}}$ and Y_{SO_2} are defined as:

$$Y_{\text{SO}_4^{2-}} = X_{\text{SO}_4^{2-}} / (X_{\text{SO}_4^{2-}} + X_{\text{S}^{2-}}); \quad Y_{\text{SO}_2} = X_{\text{SO}_2} / (X_{\text{SO}_2} + X_{\text{H}_2\text{S}})$$

$$1000\ln\alpha_{\text{SO}_2-\text{H}_2\text{S}} = -0.42 \cdot (10^3/T)^3 + 4.367 \cdot (10^3/T)^2 - 0.105 \cdot (10^3/T) - 0.41$$

$$1000\ln\alpha_{\text{H}_2\text{S}-\text{S}^{2-}} = 1.1 \cdot (10^3/T)^2 - 0.19.$$

Taylor, 1986

We MUST know how $Y_{\text{SO}_4^{2-}}$ and $Y_{\text{S}^{2-}}$ are related to P, T and composition

Sulfide separation...

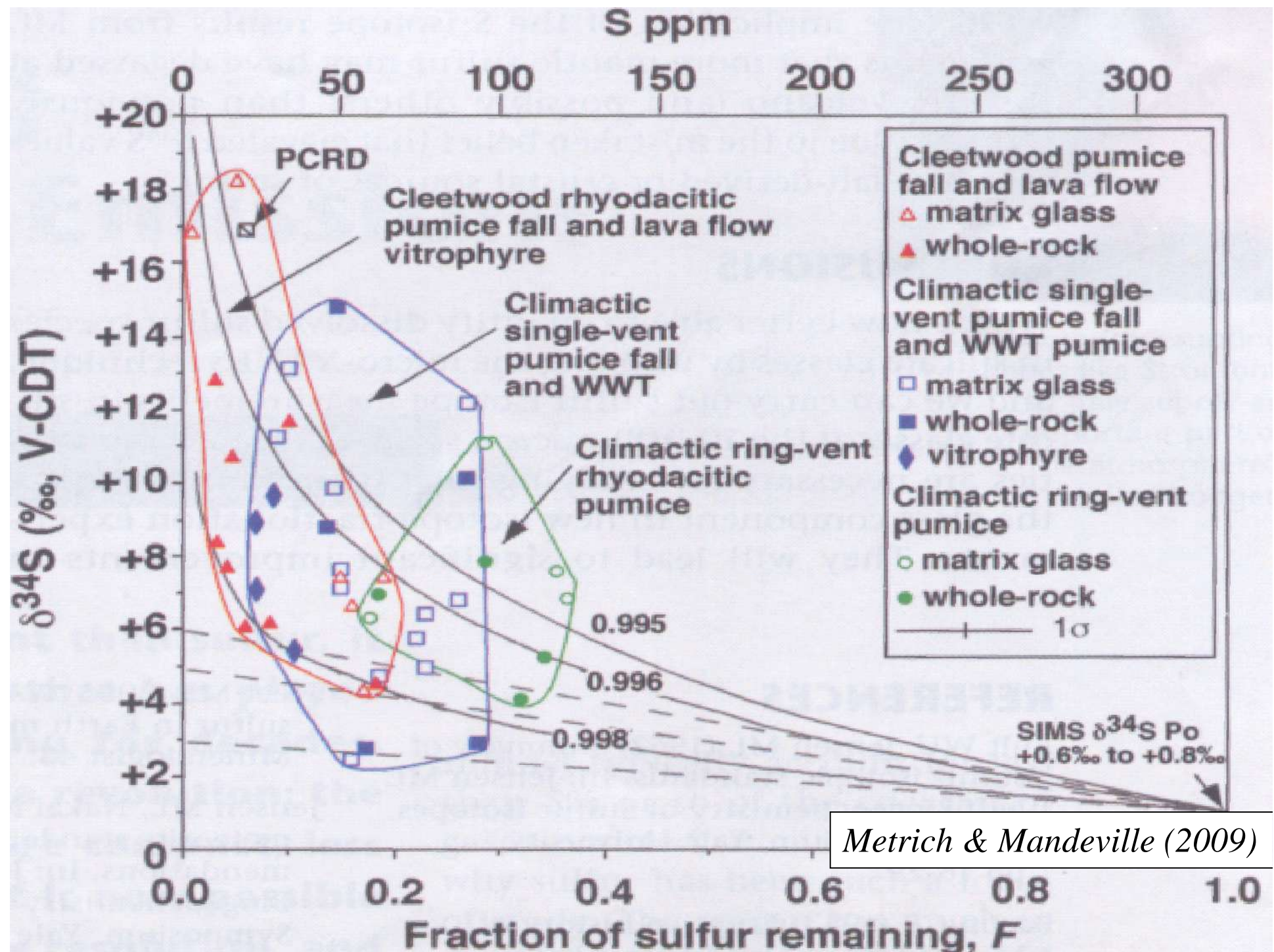
$$\begin{aligned} 1000\ln\alpha_{\text{FeS-melt}} &\cong \delta^{34}\text{S}_{\text{FeS}} - \delta^{34}\text{S}_{\Sigma\text{S,melt}} = \\ &= \delta^{34}\text{S}_{\text{FeS}} - \left[Y_{\text{SO}_4^{2-}} \cdot \delta^{34}\text{S}_{\text{SO}_4^{2-}} + (1 - Y_{\text{SO}_4^{2-}}) \cdot \delta^{34}\text{S}_{\text{S}^{2-}} \right] = \\ &= Y_{\text{SO}_4^{2-}} \cdot 1000\ln\alpha_{\text{S}^{2-}-\text{SO}_4^{2-}} + 1000\ln\alpha_{\text{FeS-H}_2\text{S}} + 1000\ln\alpha_{\text{H}_2\text{S-S}^{2-}} \end{aligned}$$

Set by taking pyrrhotite...

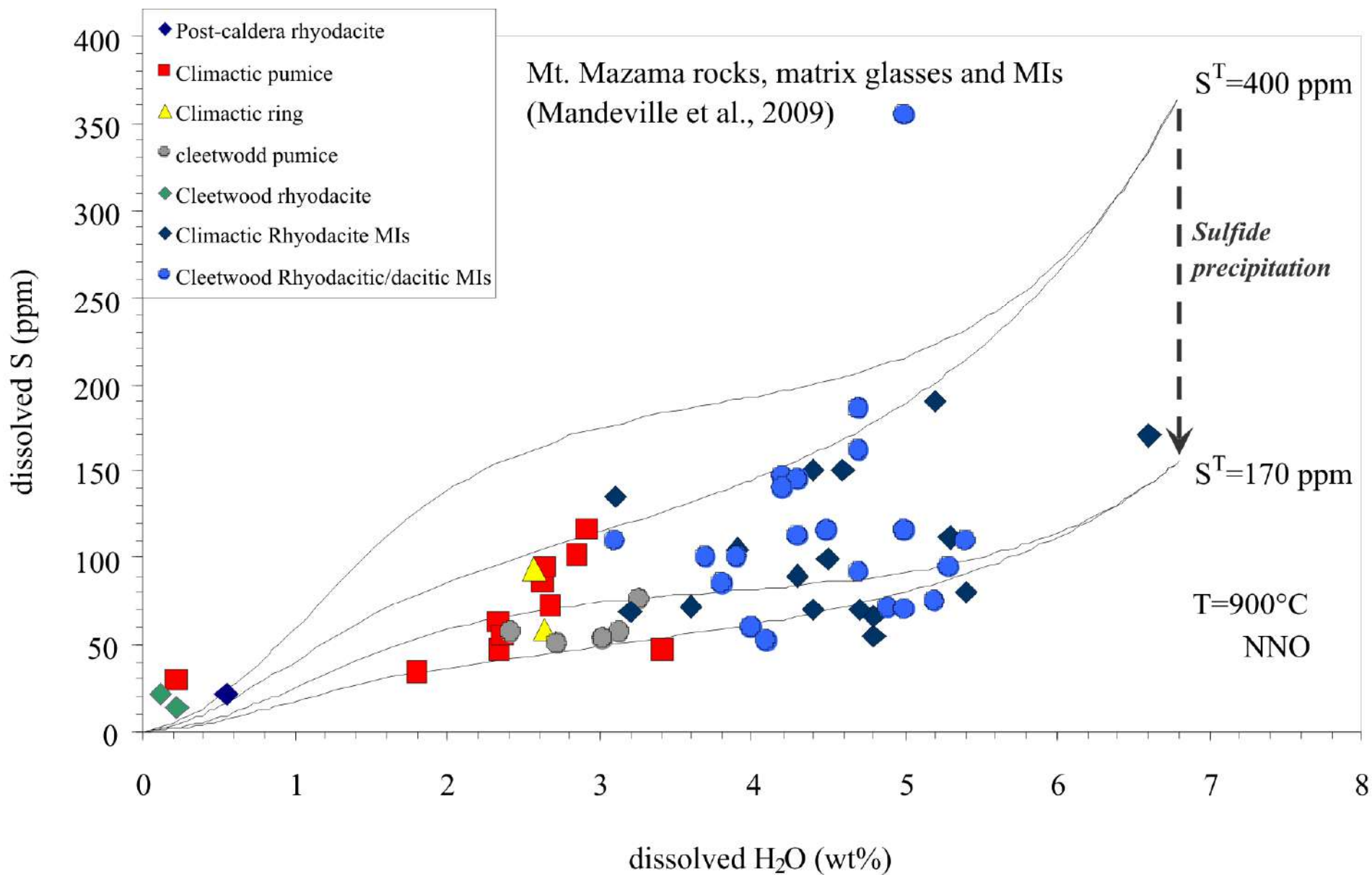
Considered to be valid for FeS liquids (...it also approximates FeOS liquids)

$$1000\ln\alpha_{\text{FeS-H}_2\text{S}} = 0.10 \cdot (10^3 / T)^2 \quad \text{Ohmoto and Rye, 1979}$$

...as for degassing: depends on $f\text{O}_2$ conditions for FeS saturation!

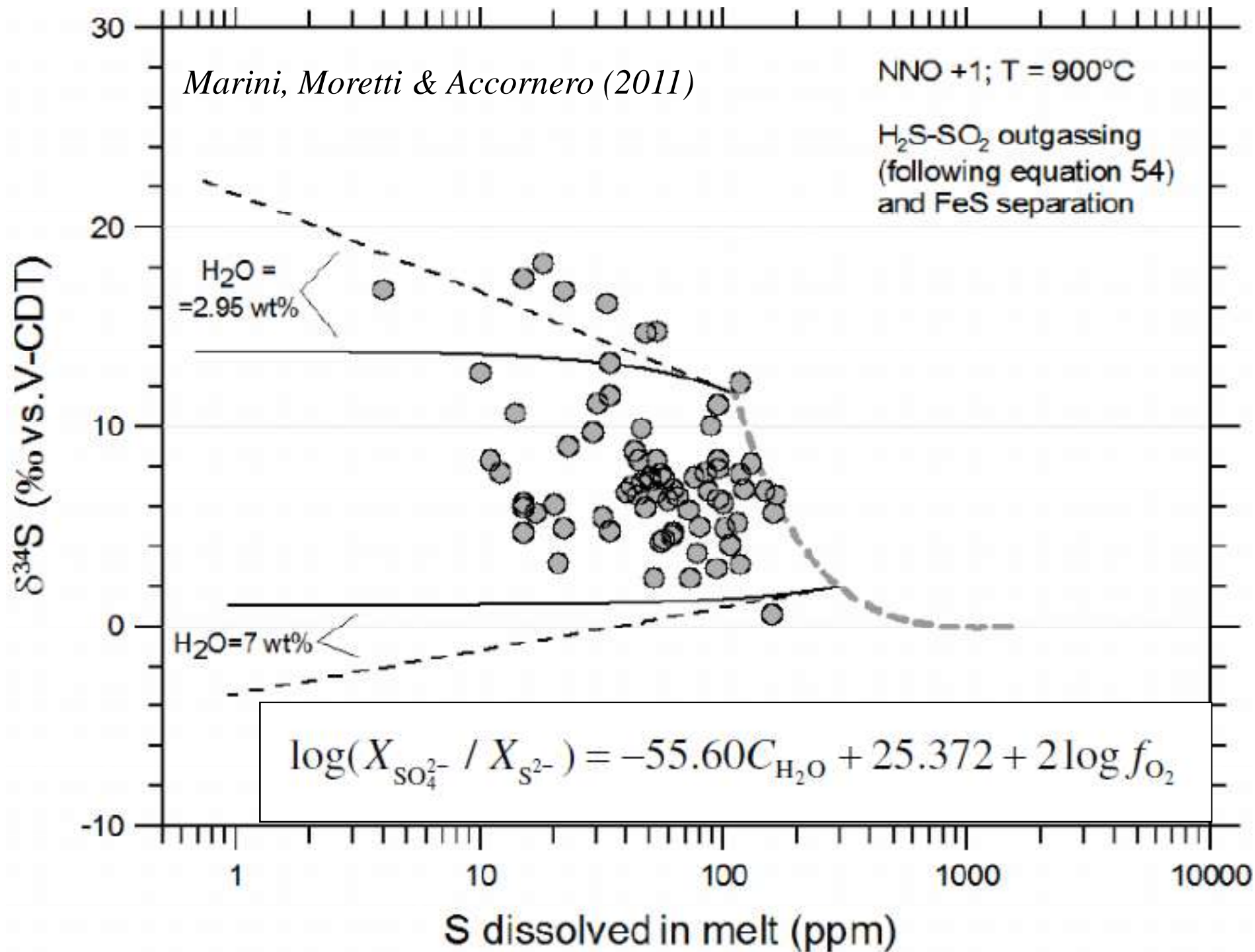


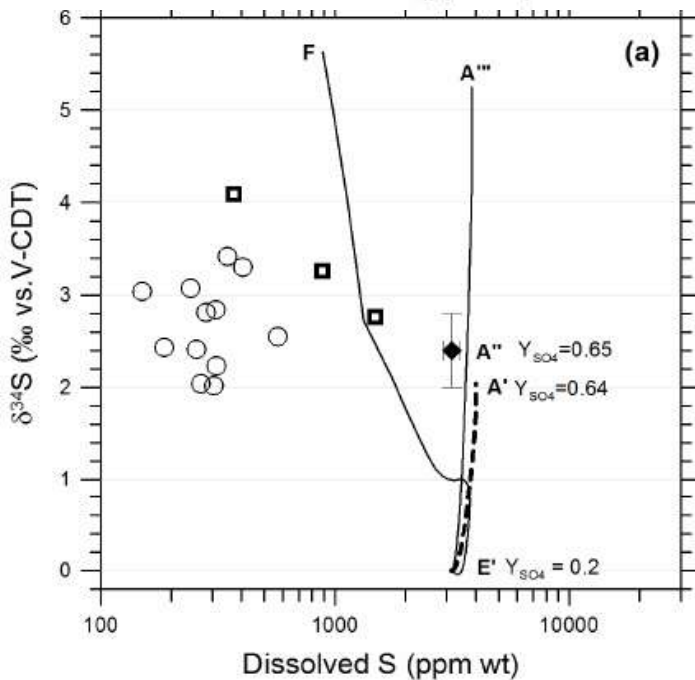
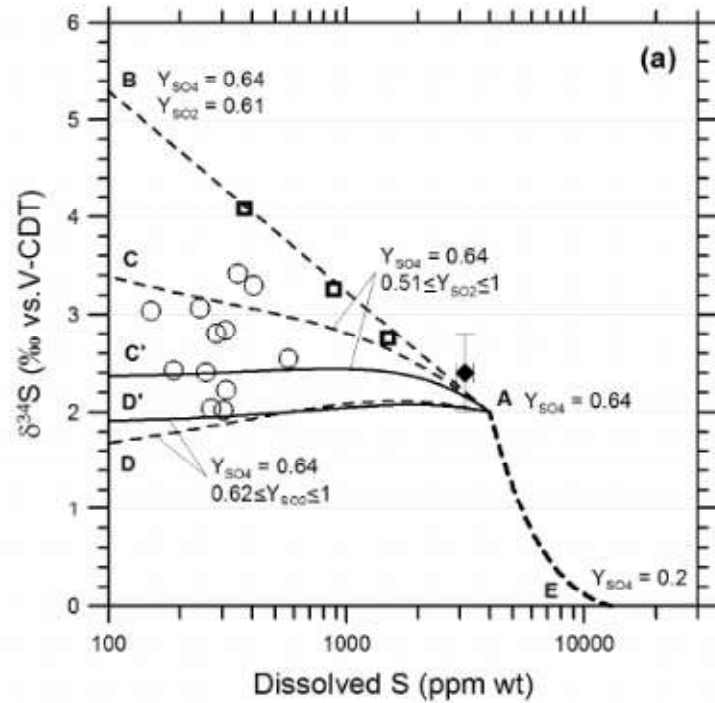
Metrich & Mandeville (2009)



$$\log(X_{\text{SO}_4^{2-}} / X_{\text{S}^{2-}}) = -55.60C_{\text{H}_2\text{O}} + 25.372 + 2\log f_{\text{O}_2}$$

Marini, Moretti & Accornero (2011)





$$m_{XX} (\text{wt}\%) = -0.0075 P(\text{bar}) + 30$$



**Sulfur Isotopes in Magmatic-Hydrothermal Systems,
 Melts, and Magmas**

Luigi Marini

Laboratory of Geochemistry, Dip. Te. Ris
 University of Genova, Corso Europa 26, I-16132 Genova, Italy
 and
 Institute of Geosciences and Georesources, CNR
 Area della Ricerca, Via G. Moruzzi 1, I-56124 Pisa, Italy
 lmarini@diptex.unige.it

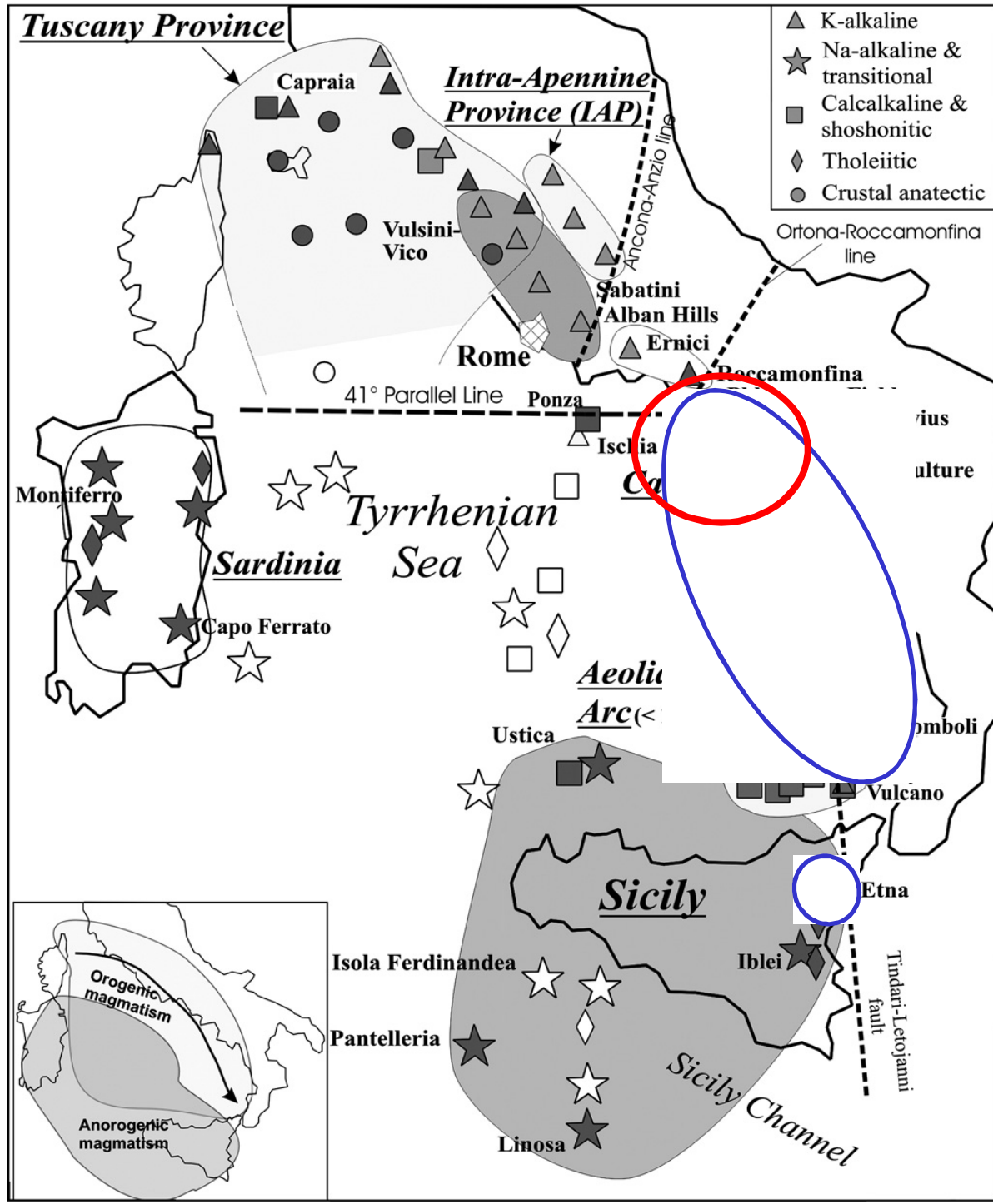
Roberto Moretti

Dipartimento di Ingegneria Civile, Seconda Università degli Studi di Napoli
 Real Casa Santa dell'Annunziata
 Via Roma 29, I-81031 Aversa (CE), Italy
 and
 Istituto Nazionale di Geofisica e Vulcanologia, sezione di Napoli 'Osservatorio Vesuviano'
 Via Diocleziano 328, I-80124 Naples, Italy
 rmoretti@unina2.it

Marina Accornero

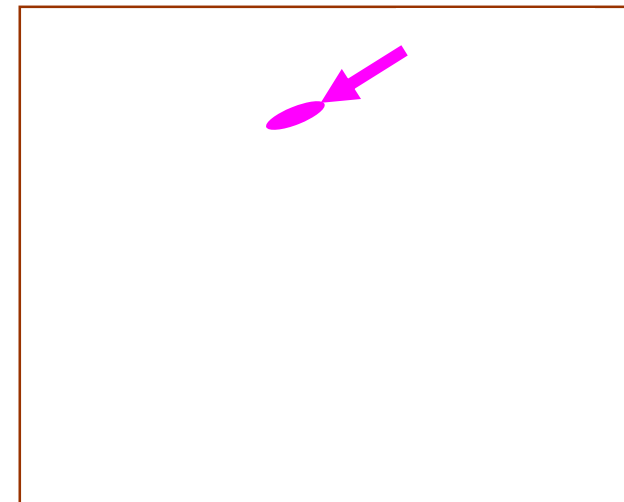
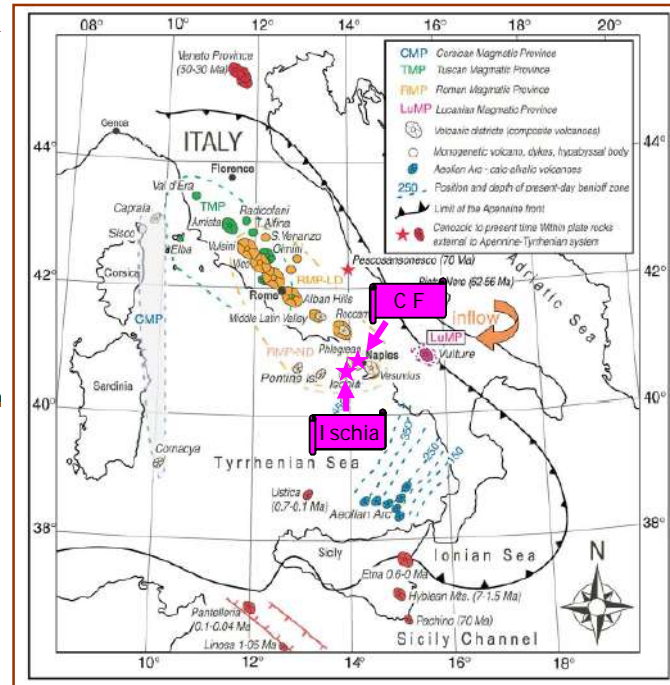
D'Appolonia S.p.A. Via S. Nazaro 19, I-16145 Genova, Italy
 marina.accornero@dappolonia.it

Marini, Moretti & Accornero (2011)

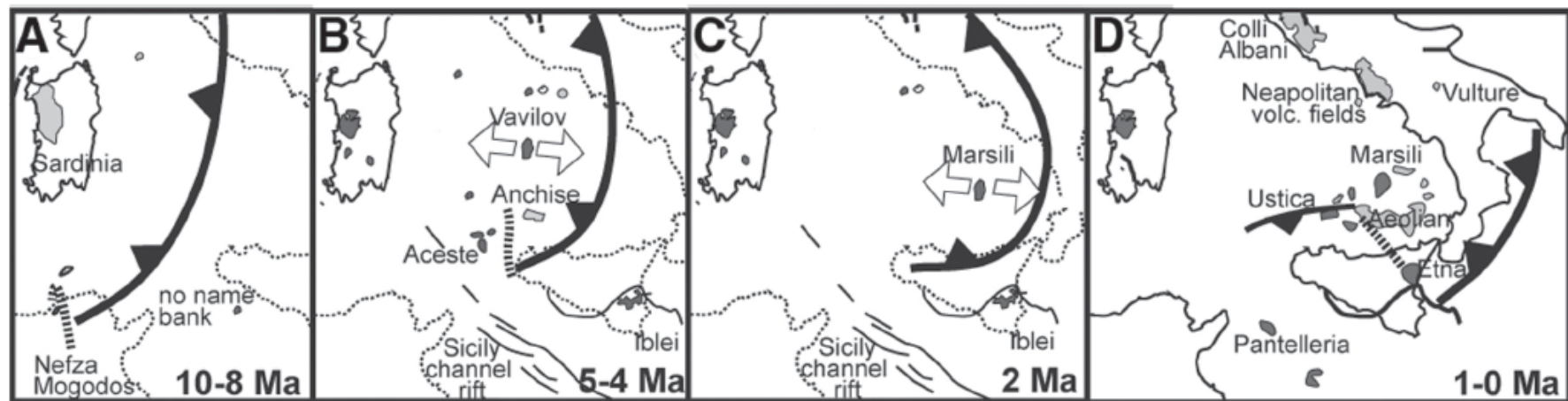


The magmatism of the **Neapolitan area** (**Phlegraean district** = Ischia + Procida + Campi Flegrei and **Somma-Vesuvius**) is related to the NW subducting Ionian plate

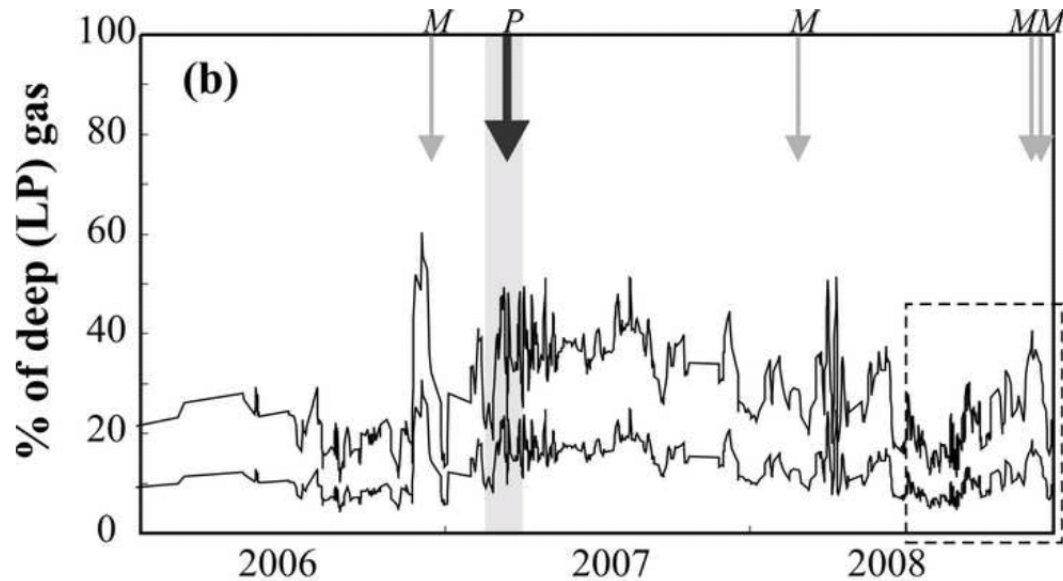
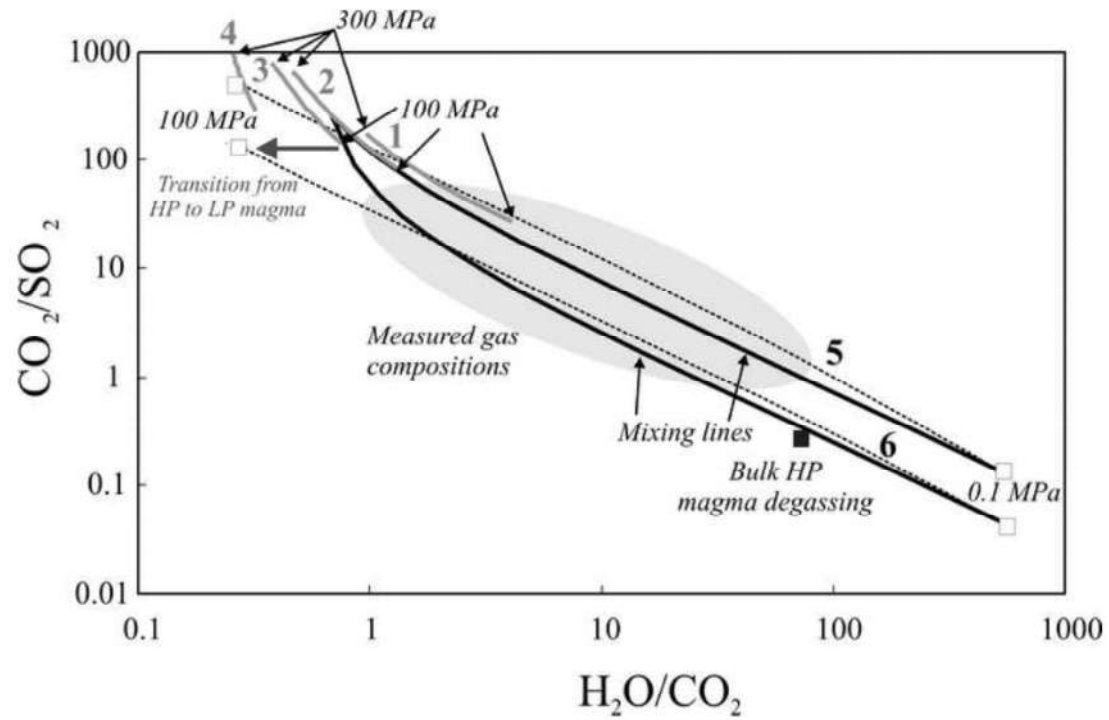
The Plio-Quaternary Italian magmatism is related to the complex geodynamics of the Mediterranean basin induced by convergence between African and Eurasian plates



Faccenna et al., 2004



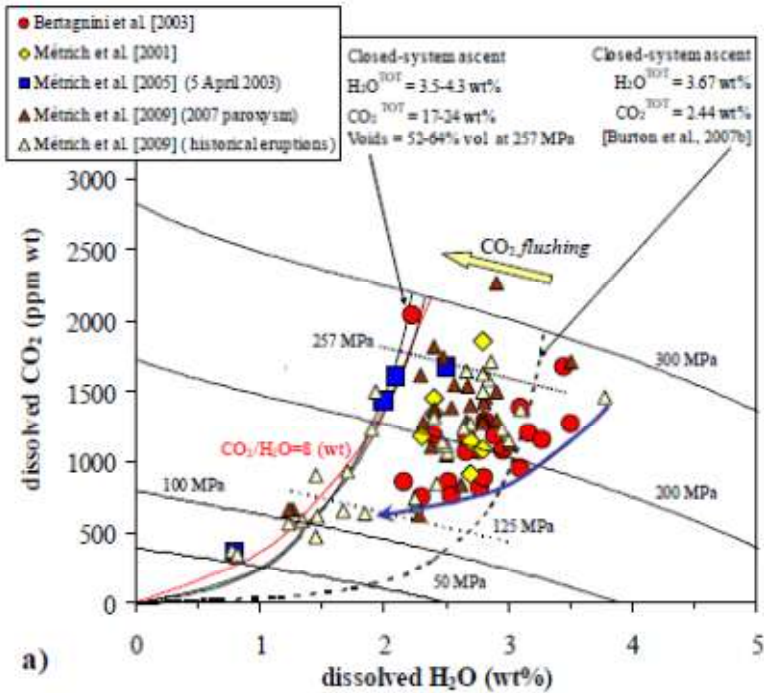




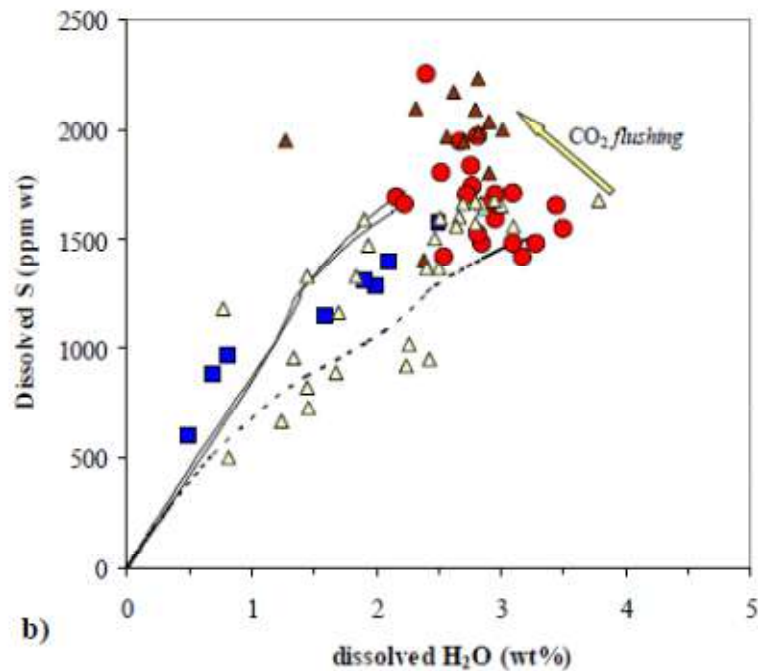
A model of degassing for Stromboli volcano

A. Aiuppa^{a,b,*}, A. Bertagnini^c, N. Métrich^{c,d}, R. Moretti^c, A. Di Muro^f, M. Liuzzo^b, G. Tamburello^a

Aiuppa, Bertagnini, Métrich, Moretti, Di Muro, Liuzzo, Tamburello (2010)



a)



b)

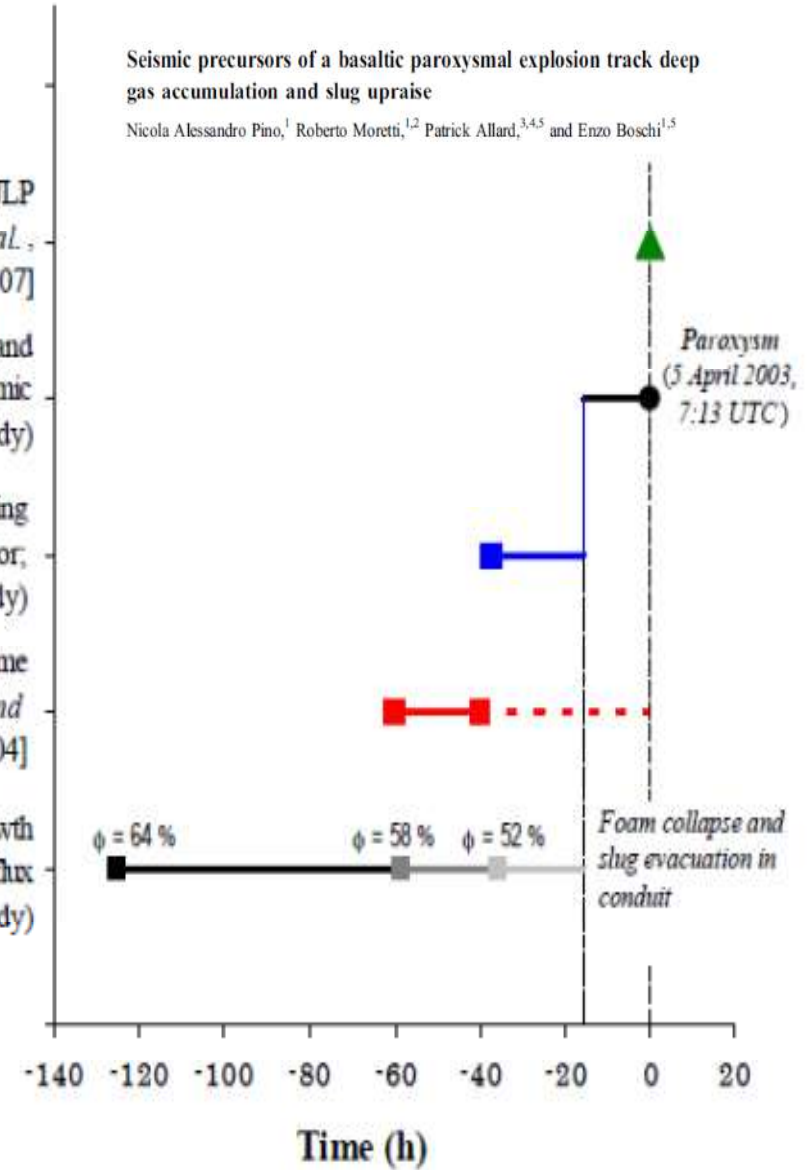
Shallow phase VLP-ULP signals [D'Auria et al., 2006; Cesca et al., 2007]

Slug release and ascent (ULP seismic signal; this study)

Vigorous degassing (seismic tremor; this study)

Anomalous plume degassing [Ahippa and Federico, 2004]

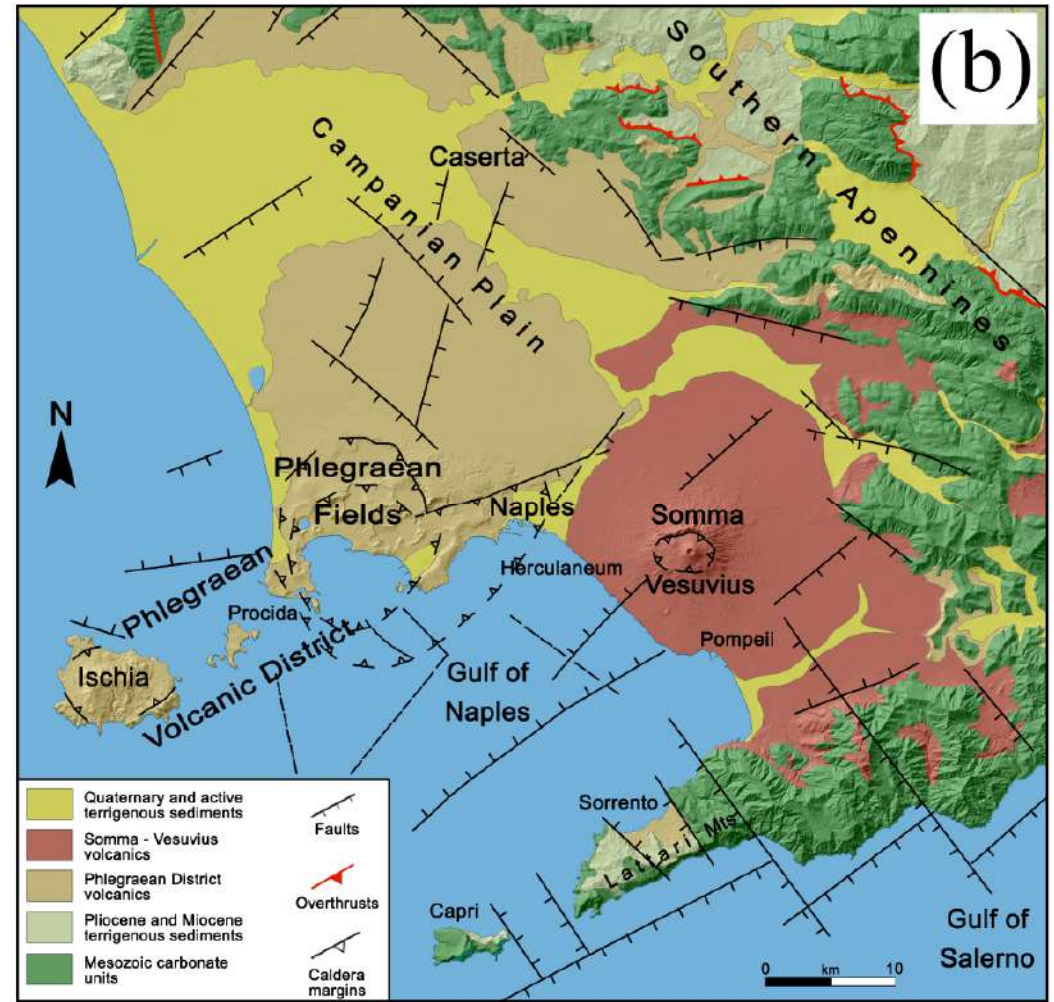
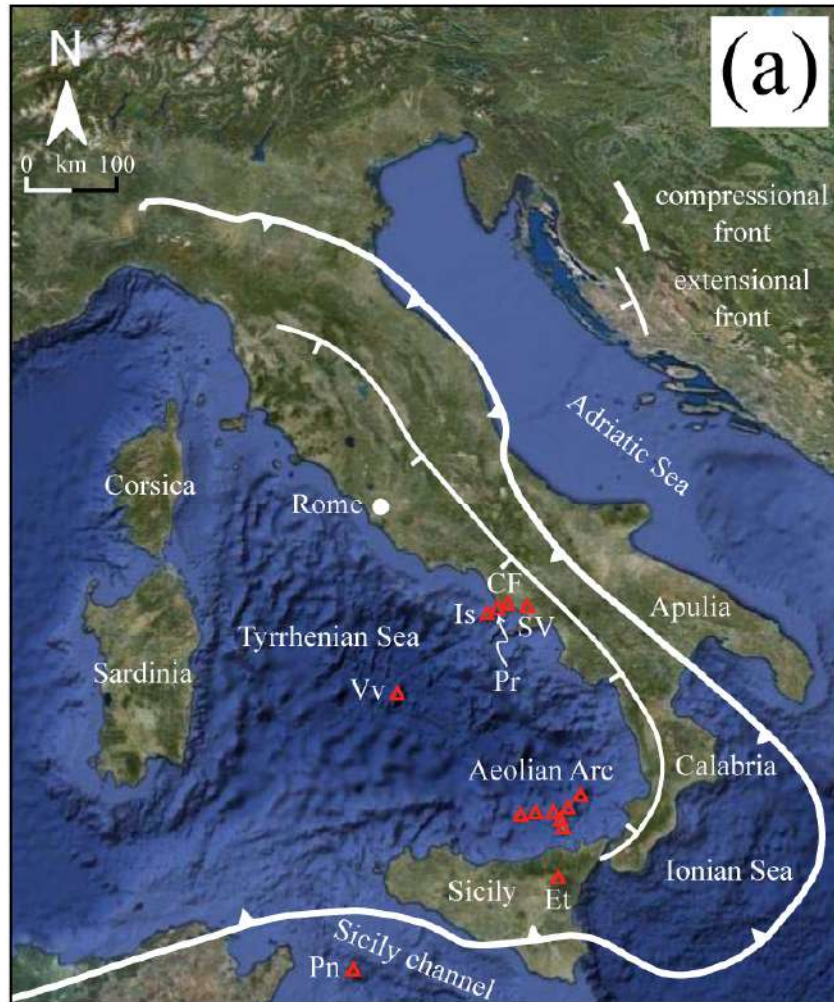
Bubble foam growth under critical gas flux (this study)



Seismic precursors of a basaltic paroxysmal explosion track deep gas accumulation and slug upraise

Nicola Alessandro Pino,¹ Roberto Moretti,^{1,2} Patrick Allard,^{3,4,5} and Enzo Boschi^{1,5}

Pino, Moretti, Allard, Boschi (2011, JGR)



Panel a): traces of the subduction-related compression and extension fronts along the Apennines chain (modified after Acocella and Funiciello, 2006); Is = Ischia; Pr = Procida; CF = Campi Flegrei; SV = Somma-Vesuvius; Vv = Vavilov; Et = Etna; Pn = Pantelleria.

Panel b): structural sketch map of the Campanian Plain and surrounding Apennines (modified after Orsi et al., 2003).

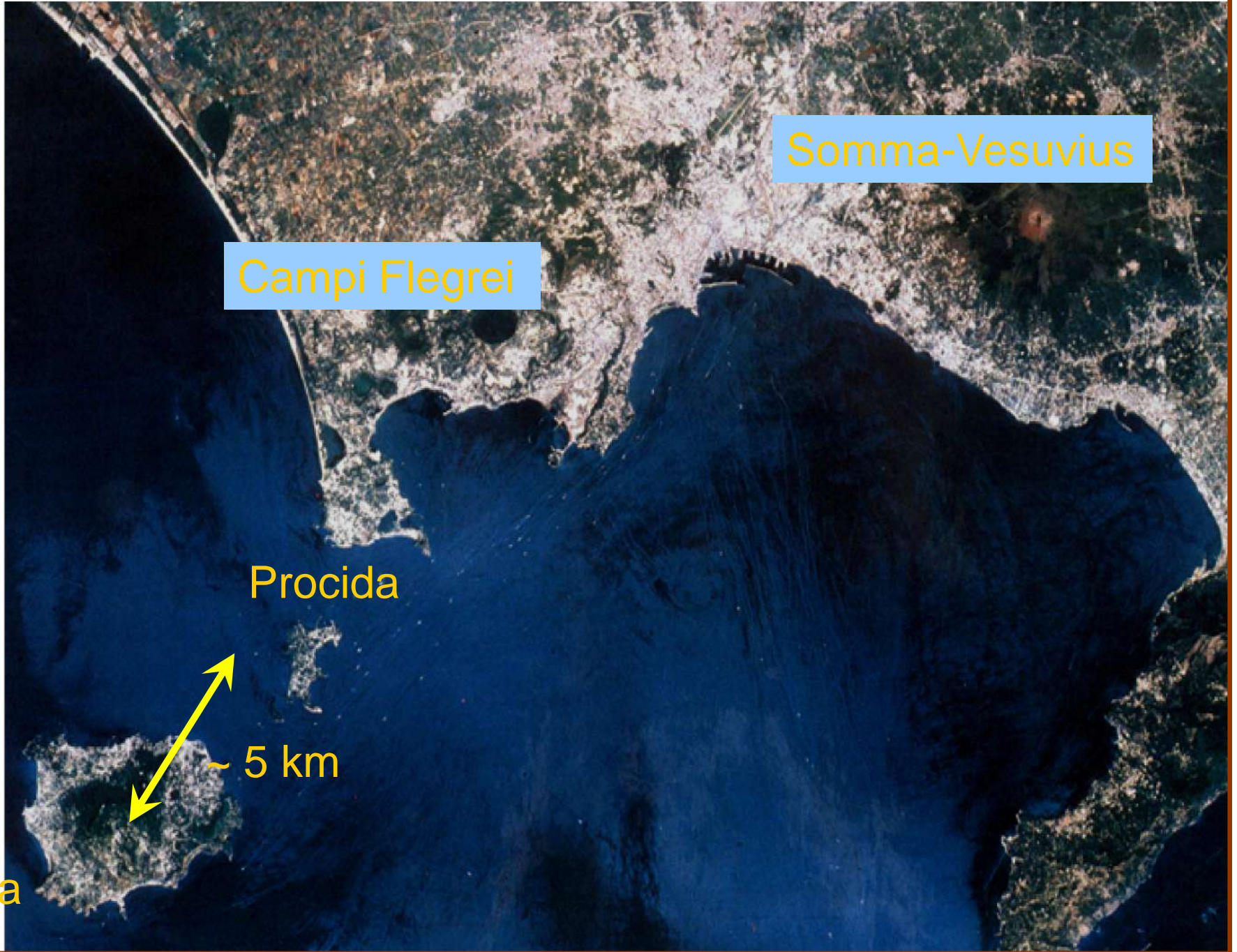
Somma-Vesuvius

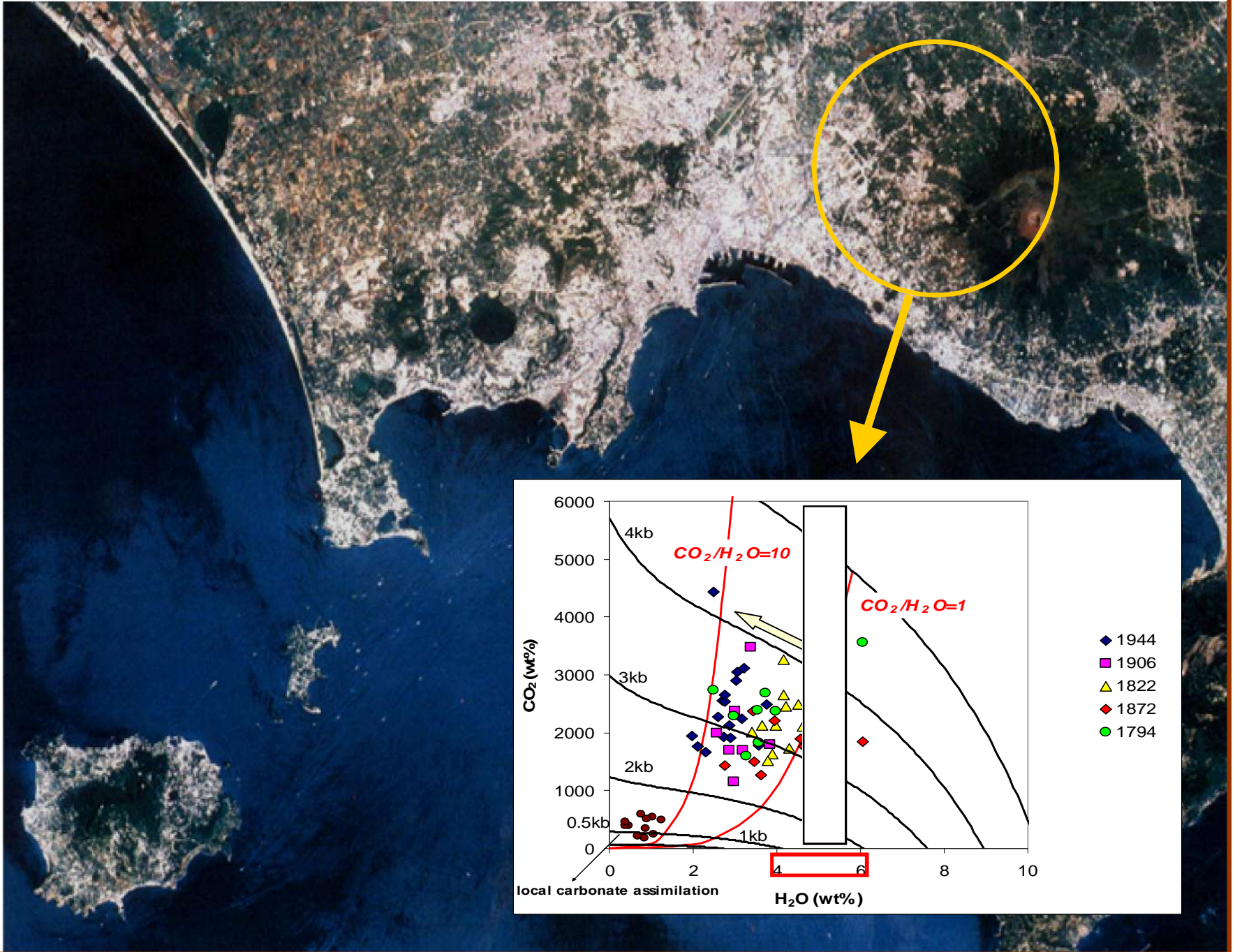
Campi Flegrei

Procida

~ 5 km

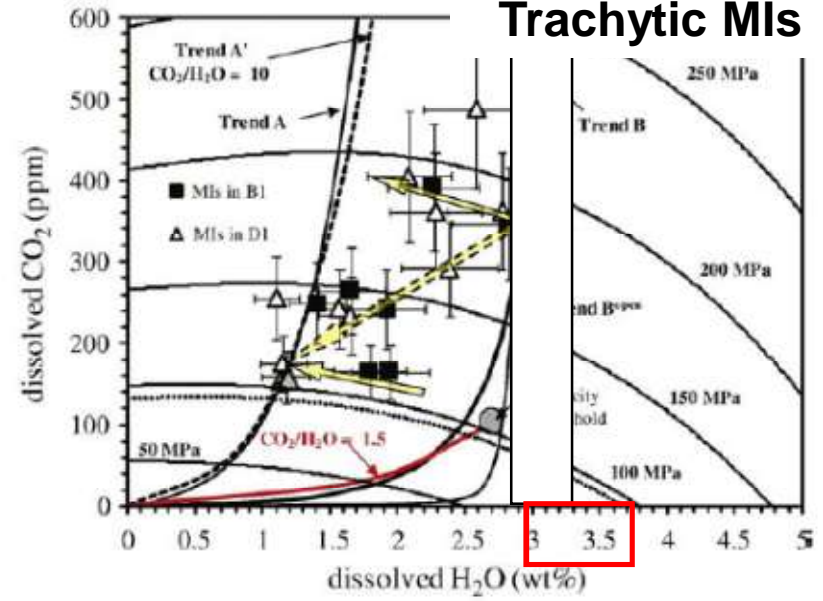
Ischia



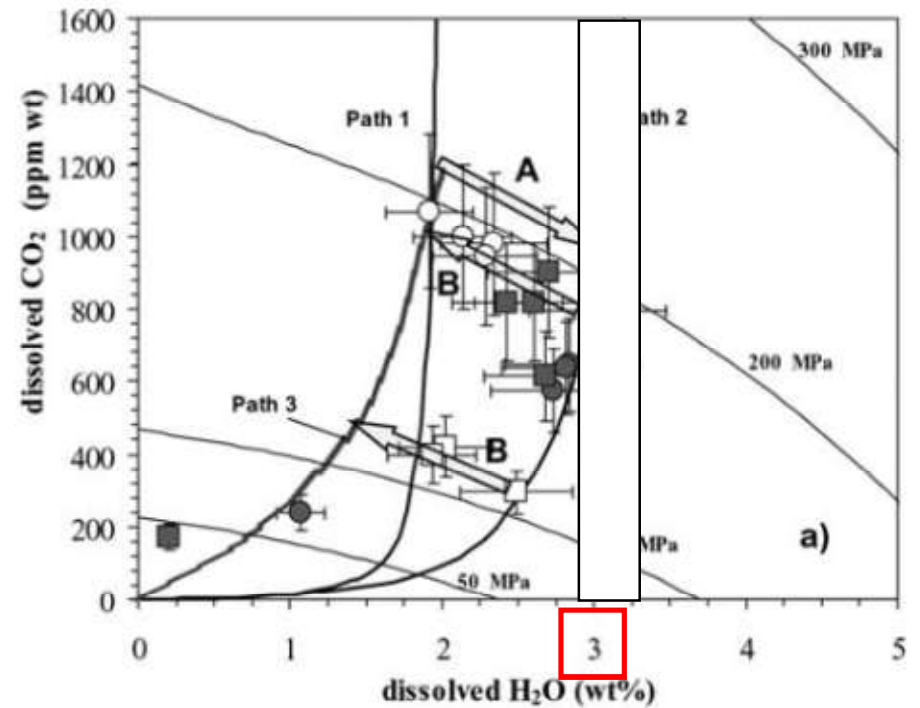


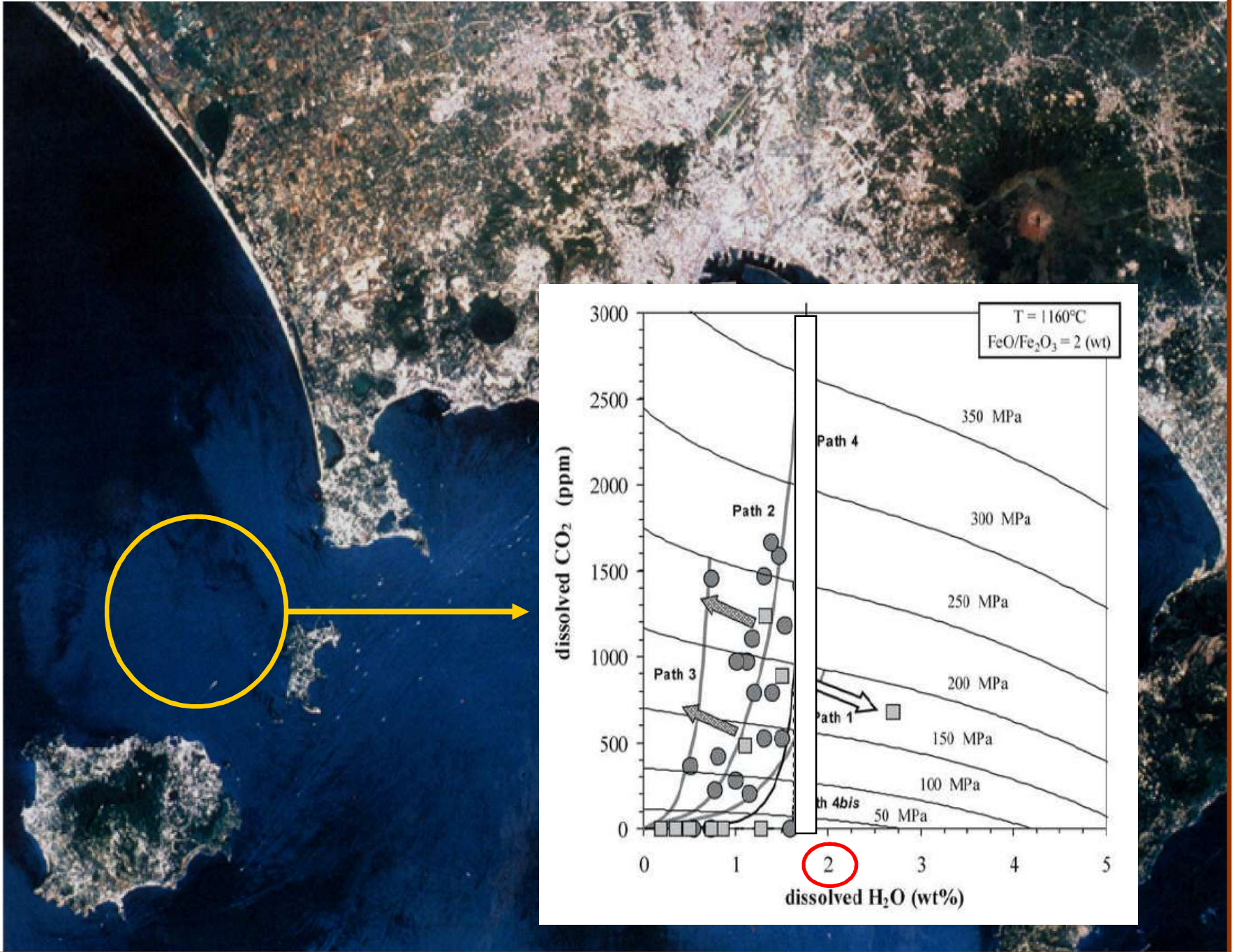


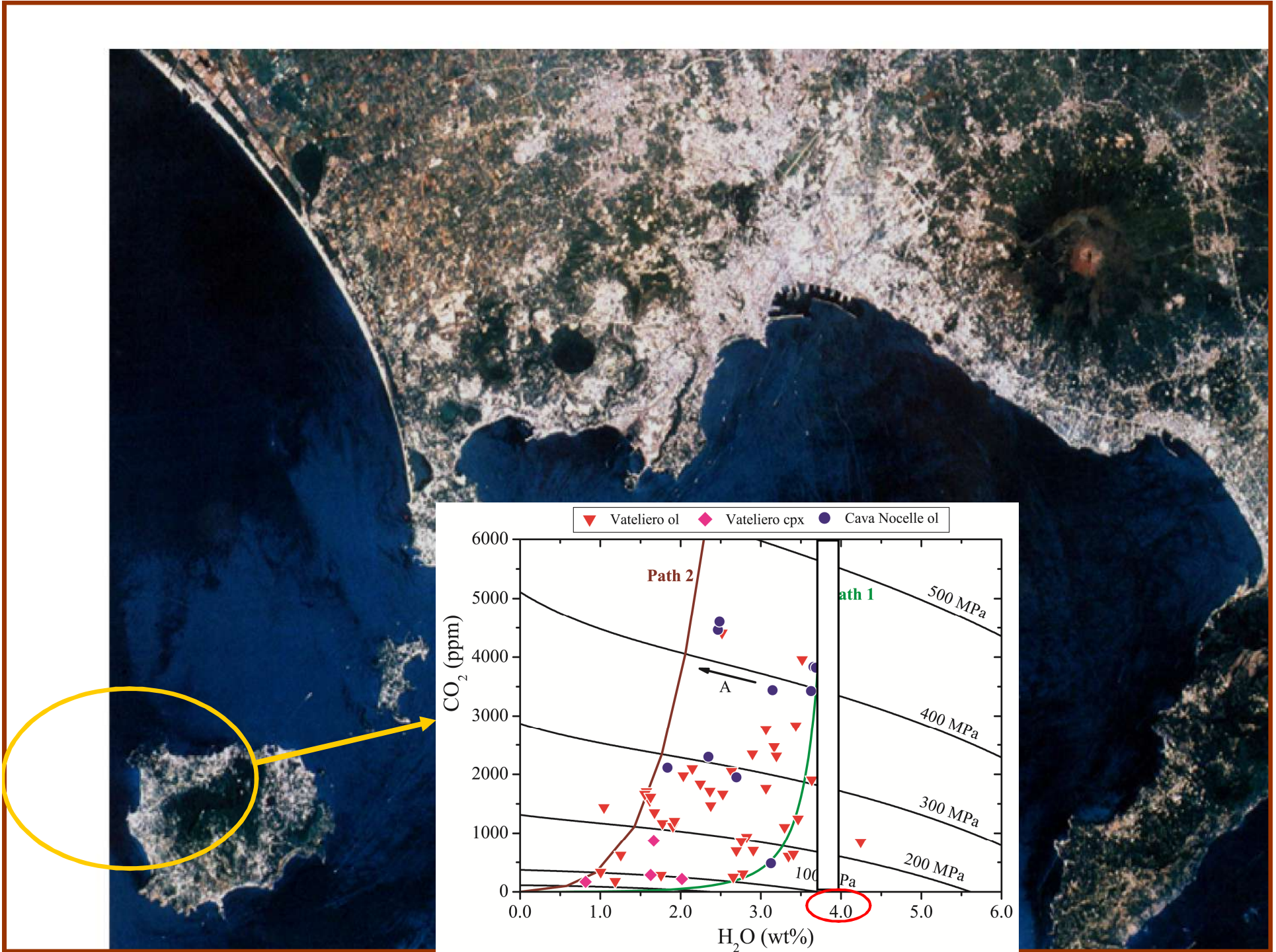
Trachytic MIs

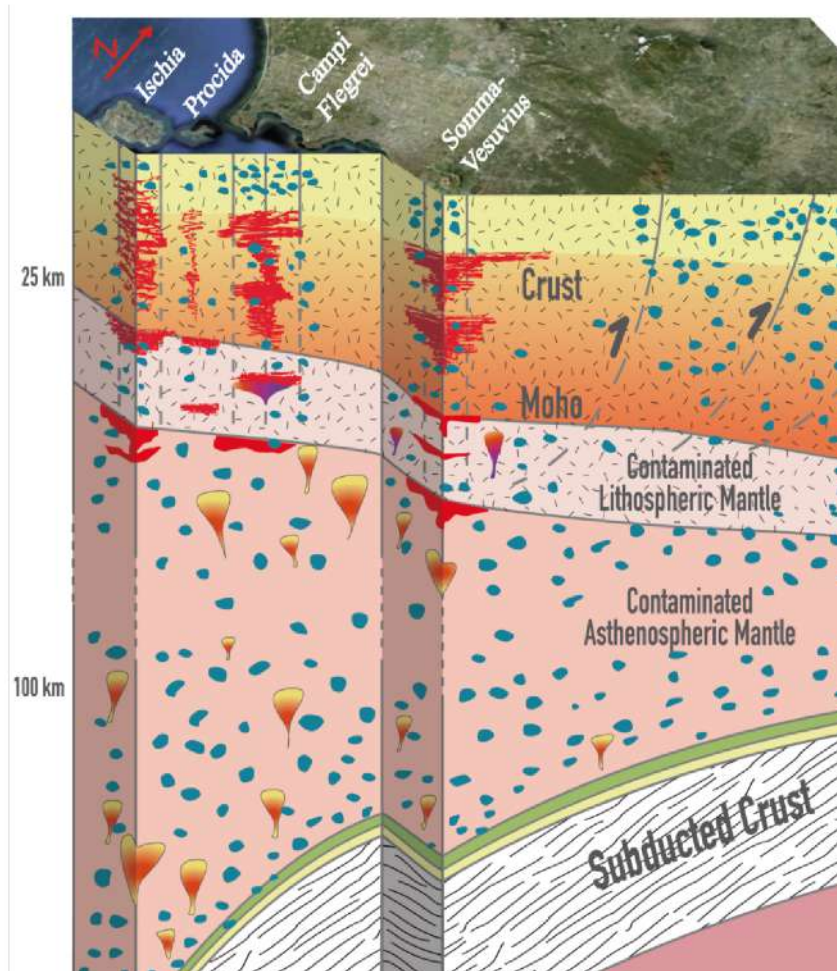


Shoshonitic/Latitic MIs

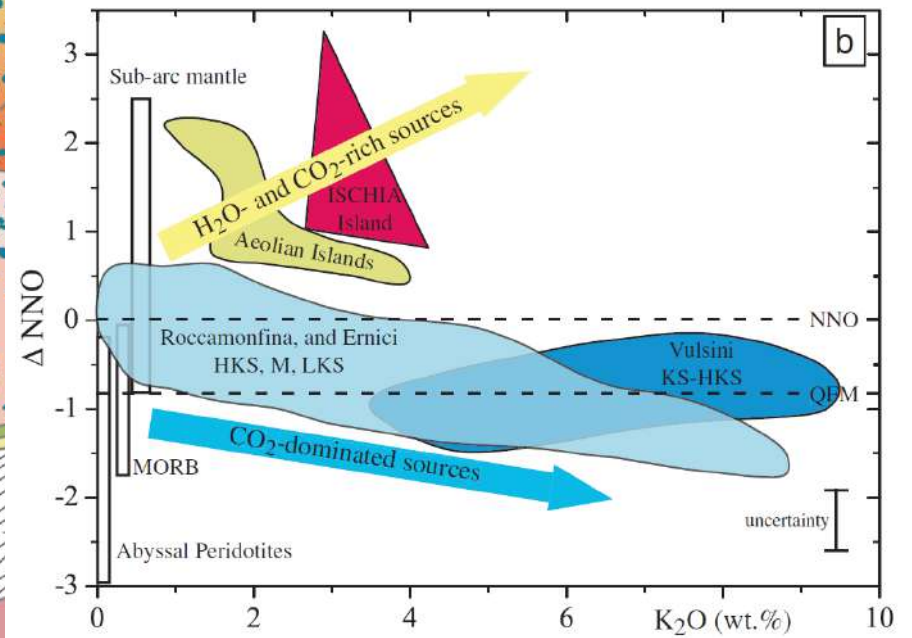








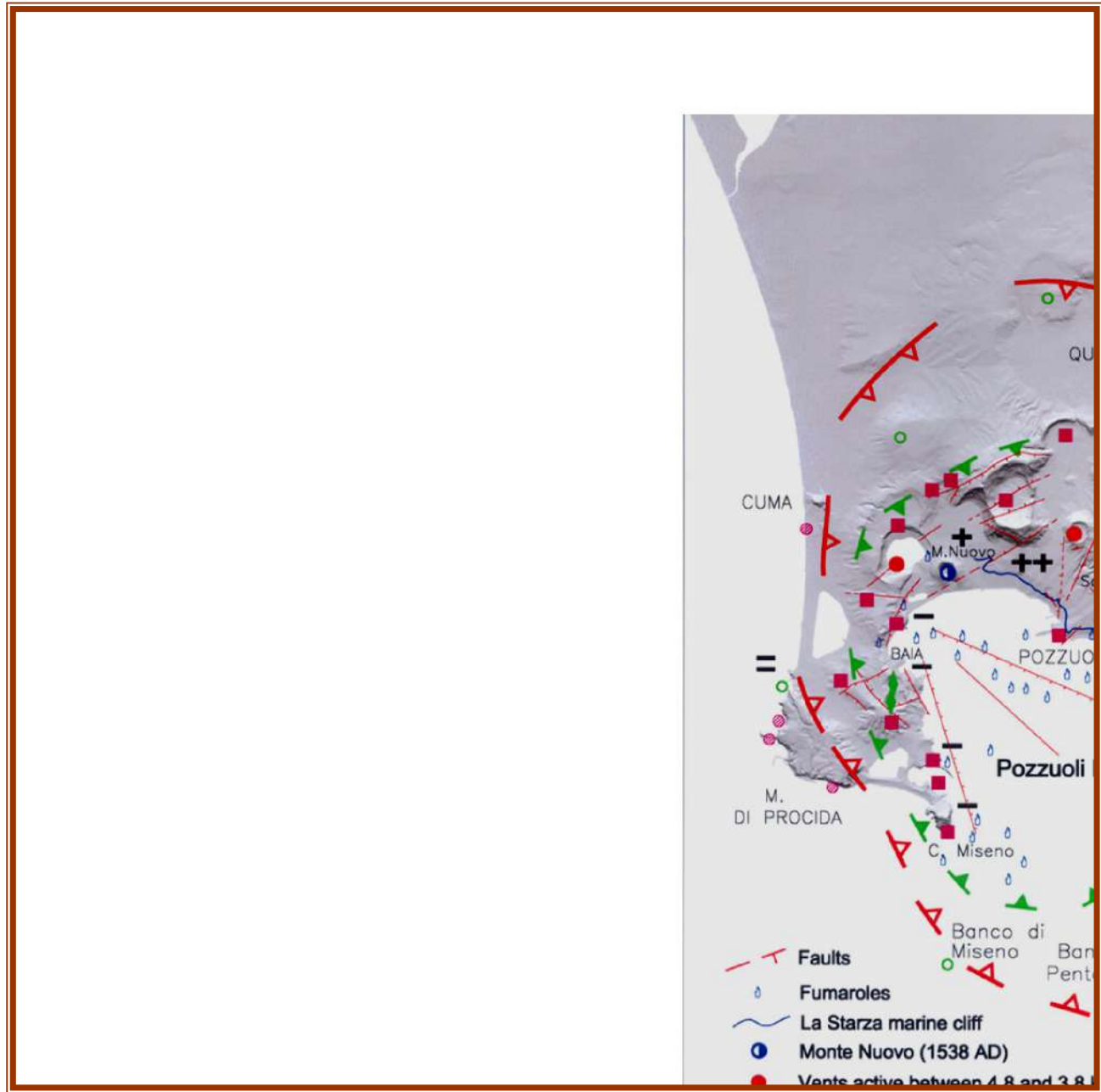
Moretti et al., 2012 (accepted in J.Pet.)



D'Antonio et al., 2012 (under review in Contrib. Min. Pet.)

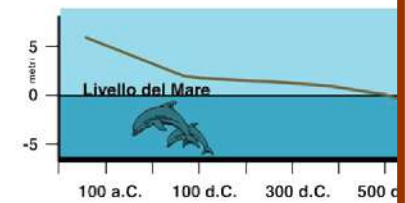
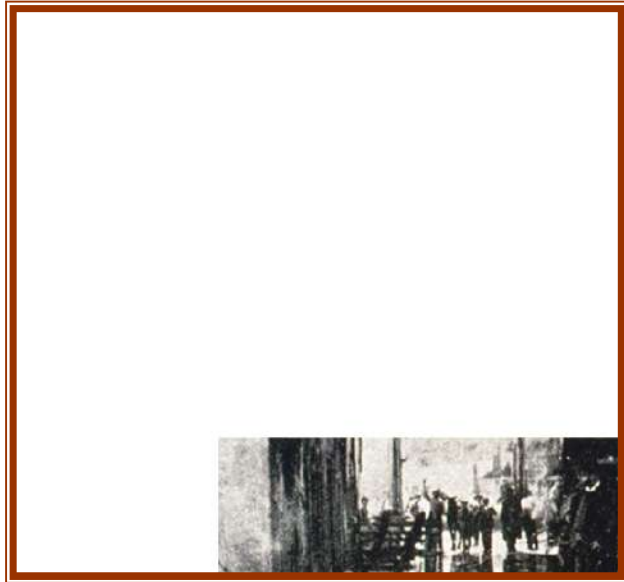
Campi Flegrei caldera

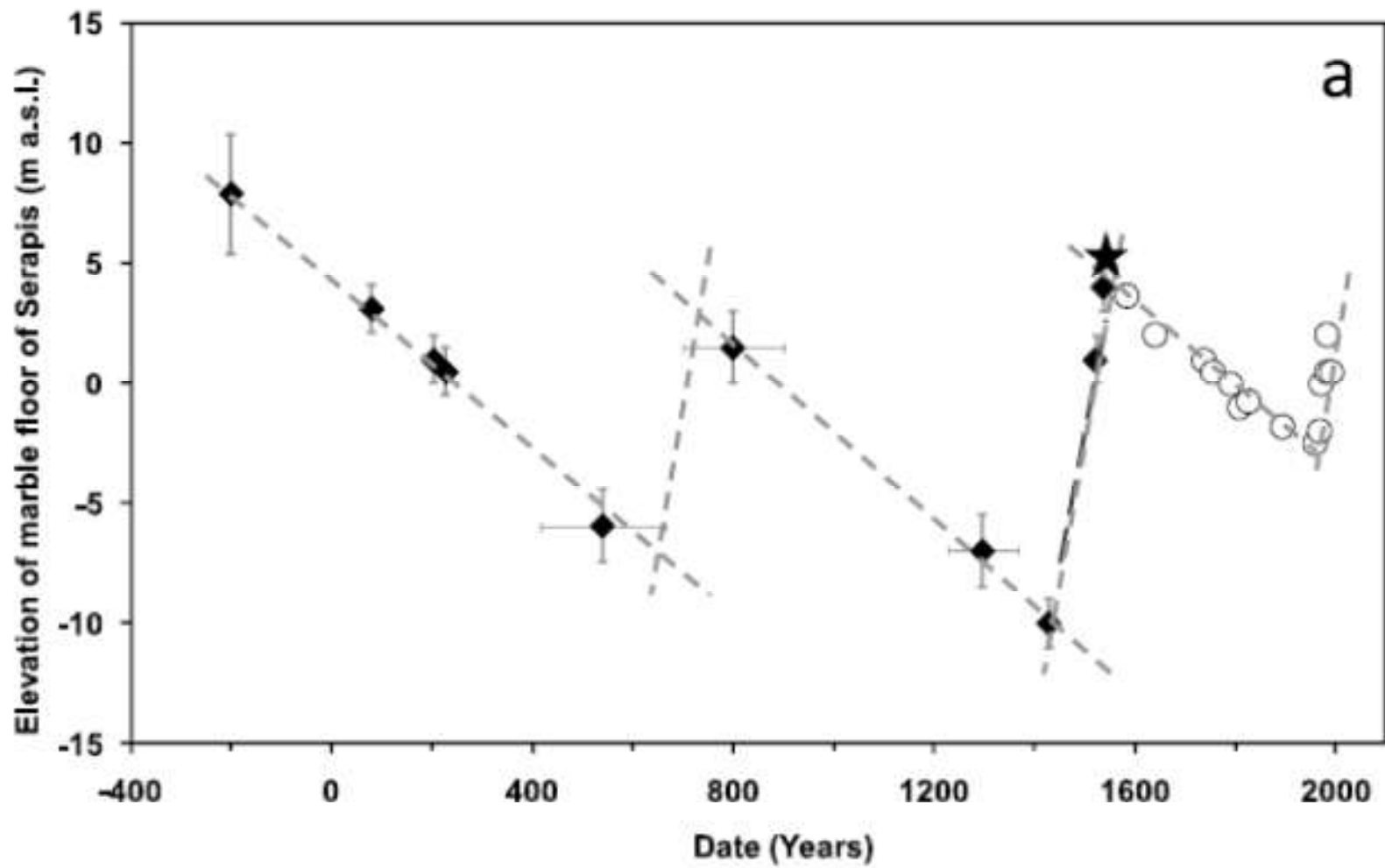
Structural map



Campi Flegrei caldera

Ground movement at
Pozzuoli - Serapeo
over the past 2 ka





ELEVATION OF THE BENCHMARK 25A AND SERAPEO FLOOR FROM 1905 TO 2009

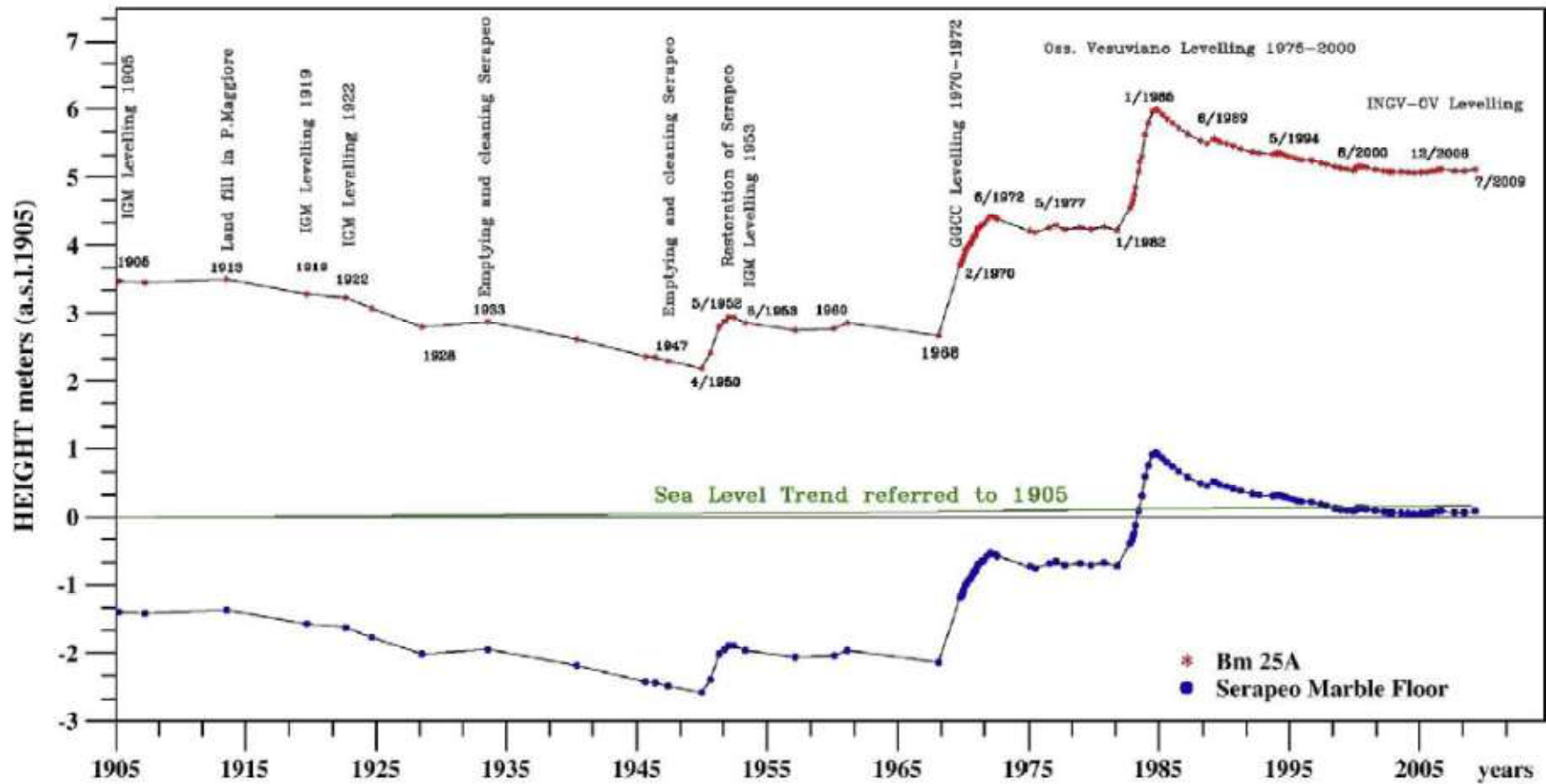


Fig. 7. Elevation changes of the floor of Serapeum and benchmark BM 25A (masl) from 1905 to 2009 referred to the sea level in 1905.

Solfatara



IPF

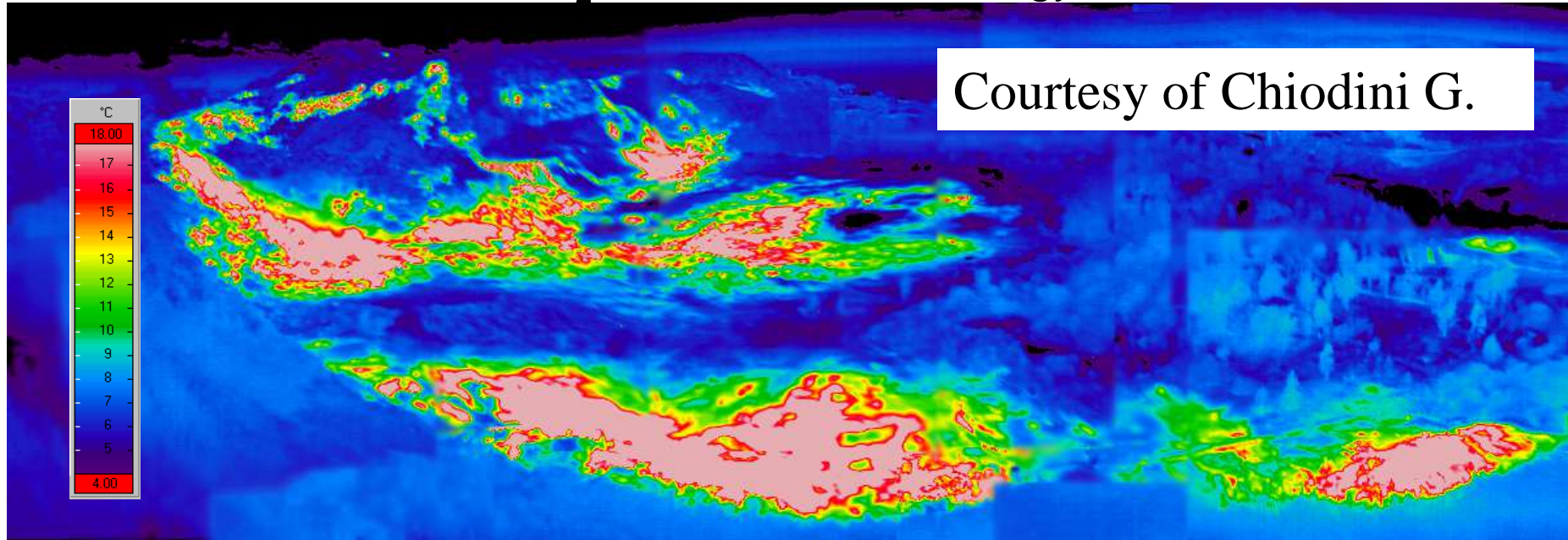


Sulfur Production in Solfatara Volcano (Naples)





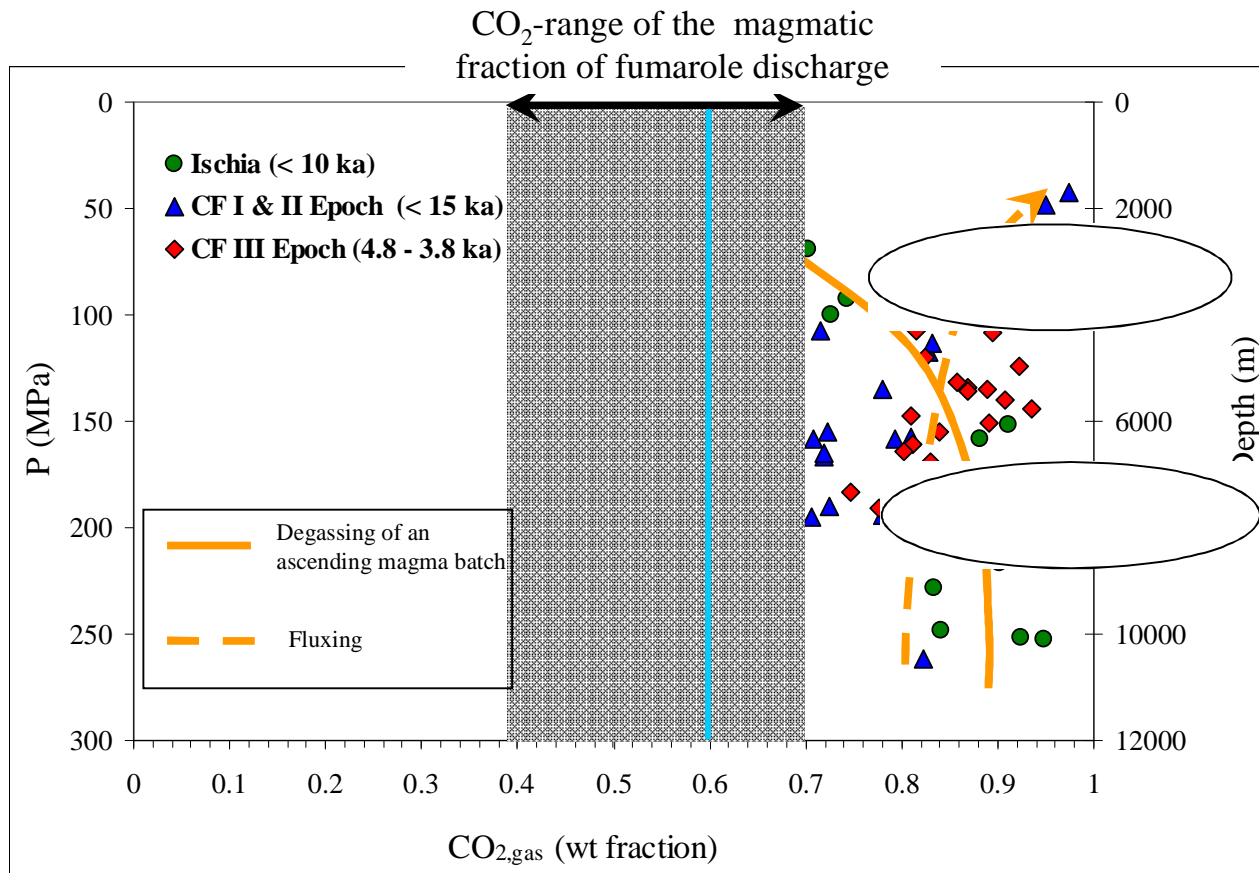
CO₂ flux and thermal energy release



	Solfatara	Nisyros	Vesuvio	Vulcano
CO ₂ t d ⁻¹	1500	100	300	200
H ₂ O/CO ₂ fumaroles	2.2	23.4	3.7	5.3
H ₂ O t d ⁻¹	3300	2340	1100	1060
Condensation J d ⁻¹	7.3x10 ¹²	5.2x10 ¹²	2.4x10 ¹²	2.3x10 ¹²
Cooling of liquid J d ⁻¹	1.1x10 ¹²	7.7x10 ¹¹	3.6x10 ¹¹	3.5x10 ¹¹
Thermal energy J d ⁻¹	8.4x10 ¹²	5.9x10 ¹²	2.8x10 ¹²	2.7x10 ¹²

The energy released by the DDS (mainly through steam condensation) are very large, and cannot be neglected in the thermal balance of a volcanic system.

Unrest: Petrologic & geochemical modelling



Mangiacapra et al., 2008 (GRL)

Click Here for Full Article
 GEOPHYSICAL RESEARCH LETTERS, VOL. 35, L21304, doi:10.1029/2008GL035550, 2008

The deep magmatic system of the Campi Flegrei caldera (Italy)
 A. Mangiacapra,¹ R. Moretti,¹ M. Kihneriora,² L. Civetta,^{2,1} G. Orsi,¹ and P. Papale¹

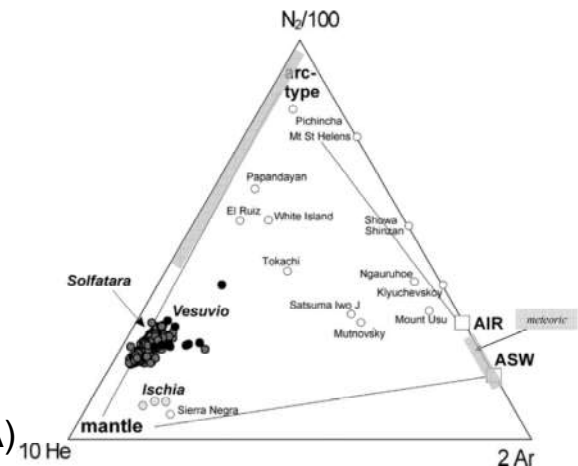


Arienzo et al., 2010 (CHEMGE)

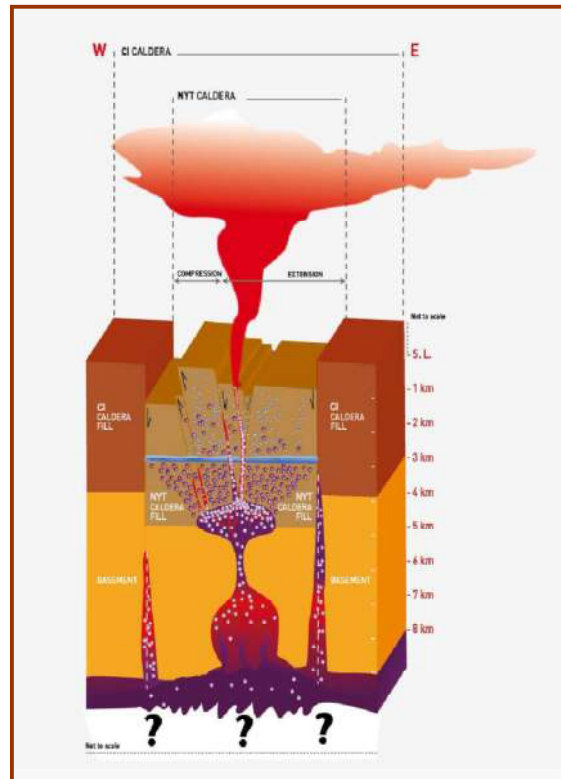
The feeding system of Agnano-Monte Spina eruption (Campi Flegrei, Italy):
 Dragging the past into present activity and future scenarios
 I. Arienzo^{1,2}, R. Moretti¹, L. Civetta^{1,2}, G. Orsi¹, P. Papale¹

Moretti et al. under review in EPSL

Caliro et al., 2007 (GCA)



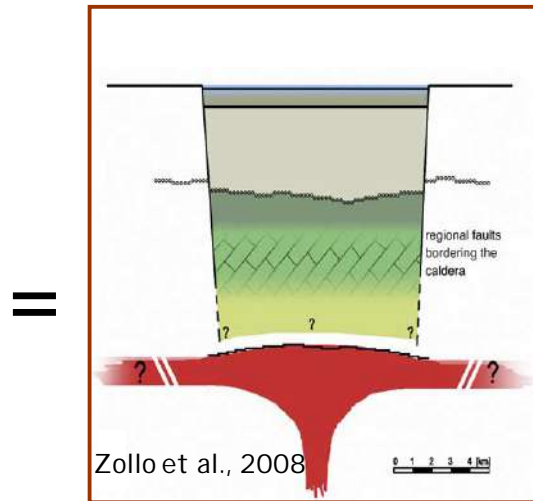
Ubrest: Petrologic & geochemical modelling



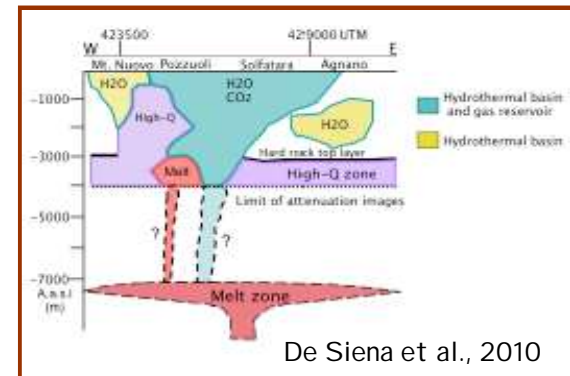
Arienzo et al., 2010; Chem. Geol.

Melt Inclusions

Magma System Architecture



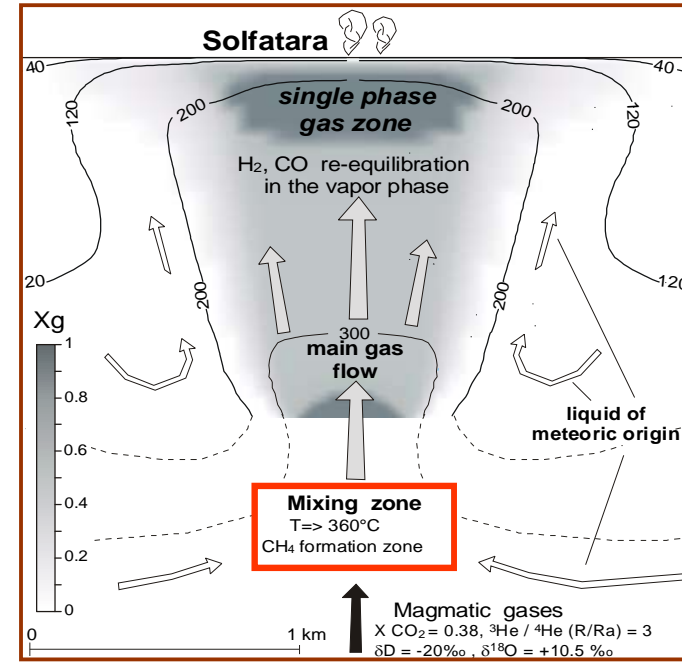
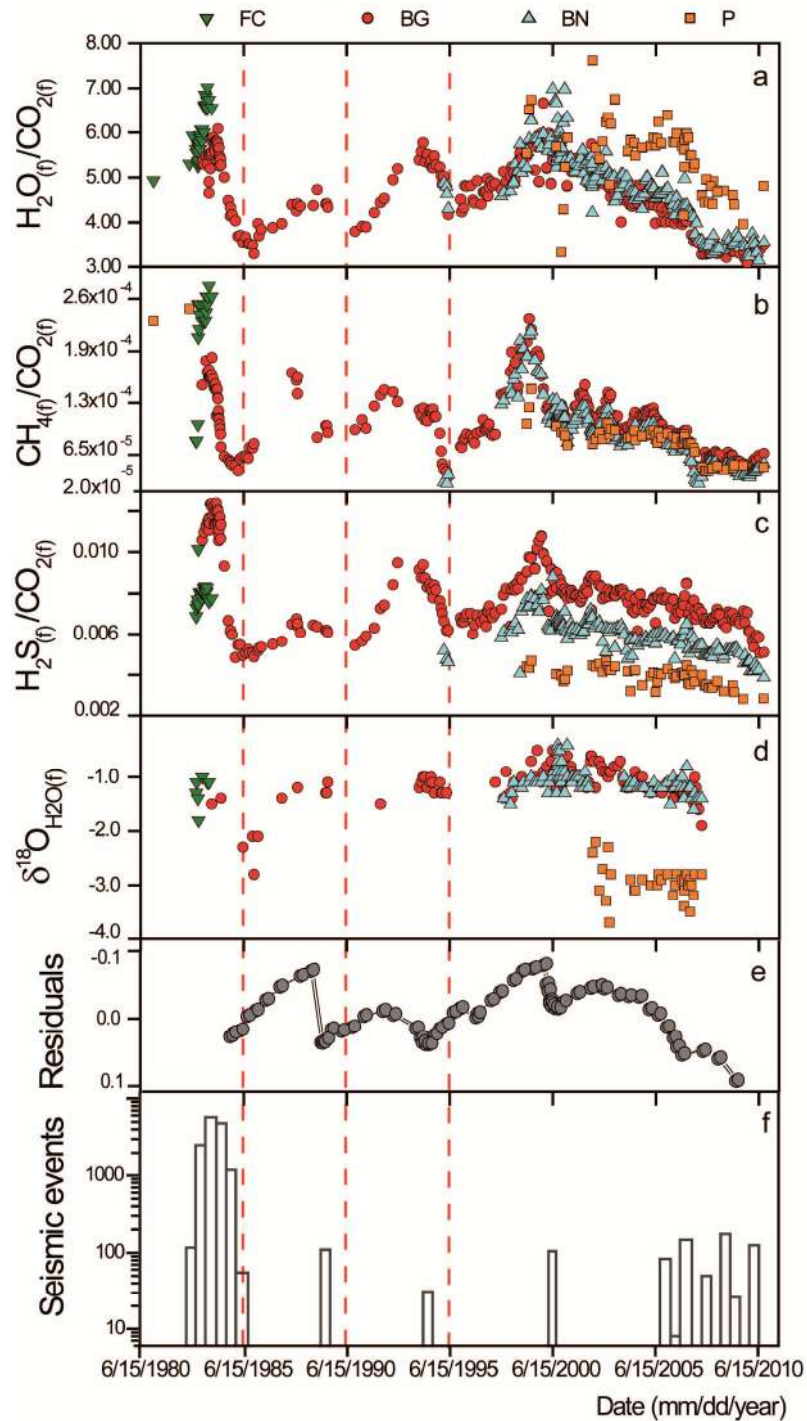
Seismic Tomography



Seismic attenuation

Geo-volcanological picture of the A-MS magmatic feeding system and of the CFc sector involved in the eruption. The A-MS system can represent a useful proxy to sketch present and future scenarios in which magmas and their gases interact with the hydrothermal system.

Unrest: Fluid geochemical modelling



Caliro et al., 2007

Moretti et al., under review in EPSL

Melt composition (#) (wt.%, volatile-free)							
SiO₂	TiO₂	Al₂O₃	FeO_{tot}	MgO	CaO	Na₂O	K₂O
59.04	0.46	17.14	3.83	0.68	2.42	4.22	7.64

Constrained features of the magma body after rise and emplacement at 4 km-depth
P = 100 MPa (&); **T** = 1173 K (§); **logfO₂** = NNO+1.2 (#)
H₂O^{TOT} = 3.5 wt% (£); **CO₂^{TOT}** = 2 wt% (£); **S^{TOT}** = 0.013 wt% (£)

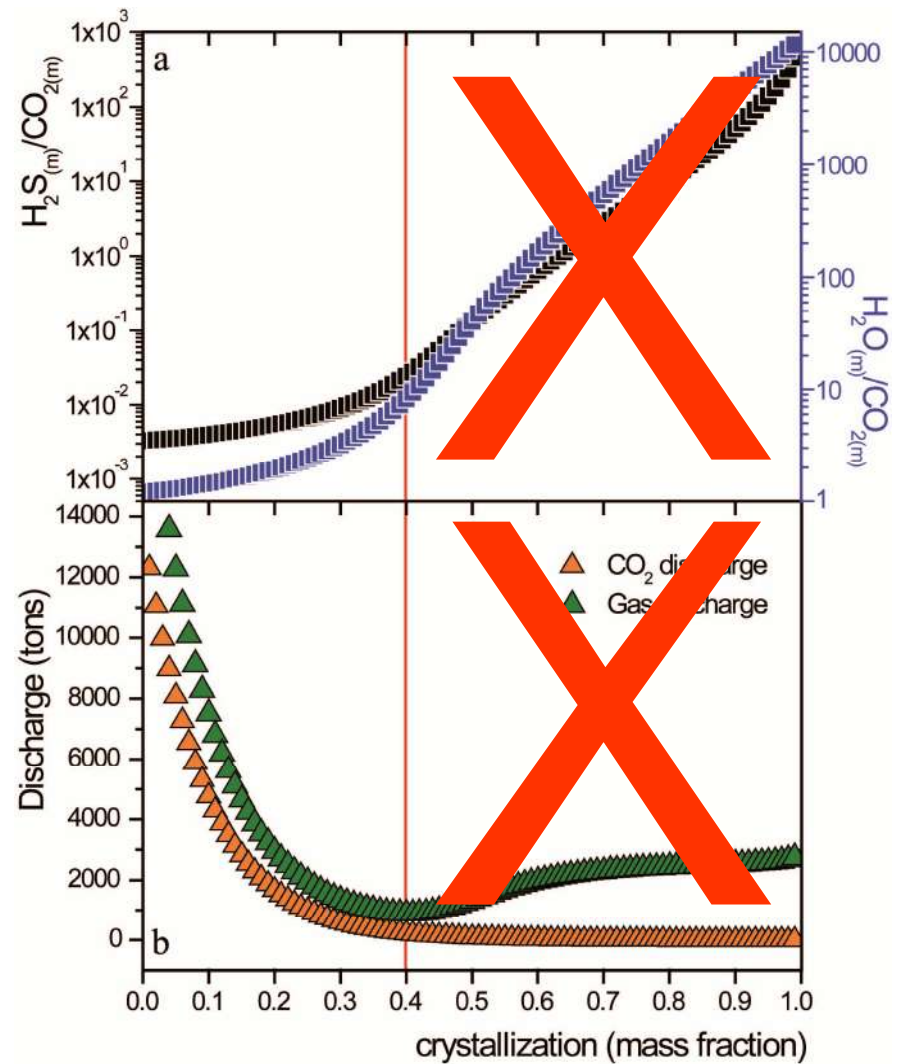
Computed conditions

H₂O^{gas} = 31.61 wt%	H₂O/CO₂ (mol) = 1.14
CO₂^{gas} = 68.01 wt%	H₂S/CO₂ (mol) = 0.004
SO₂^{gas} = 0.16 wt%	SO₂/H₂S (mol) = 0.4
H₂S^{gas} = 0.22 wt%	

$\rho_{\text{melt+gas}}$ = 2008 kg/m ³
ρ_{melt} = 2511 kg/m ³
m^{gas} = 3 wt%
$V^{\text{gas}}/V^{\text{tot}}$ = 0.21

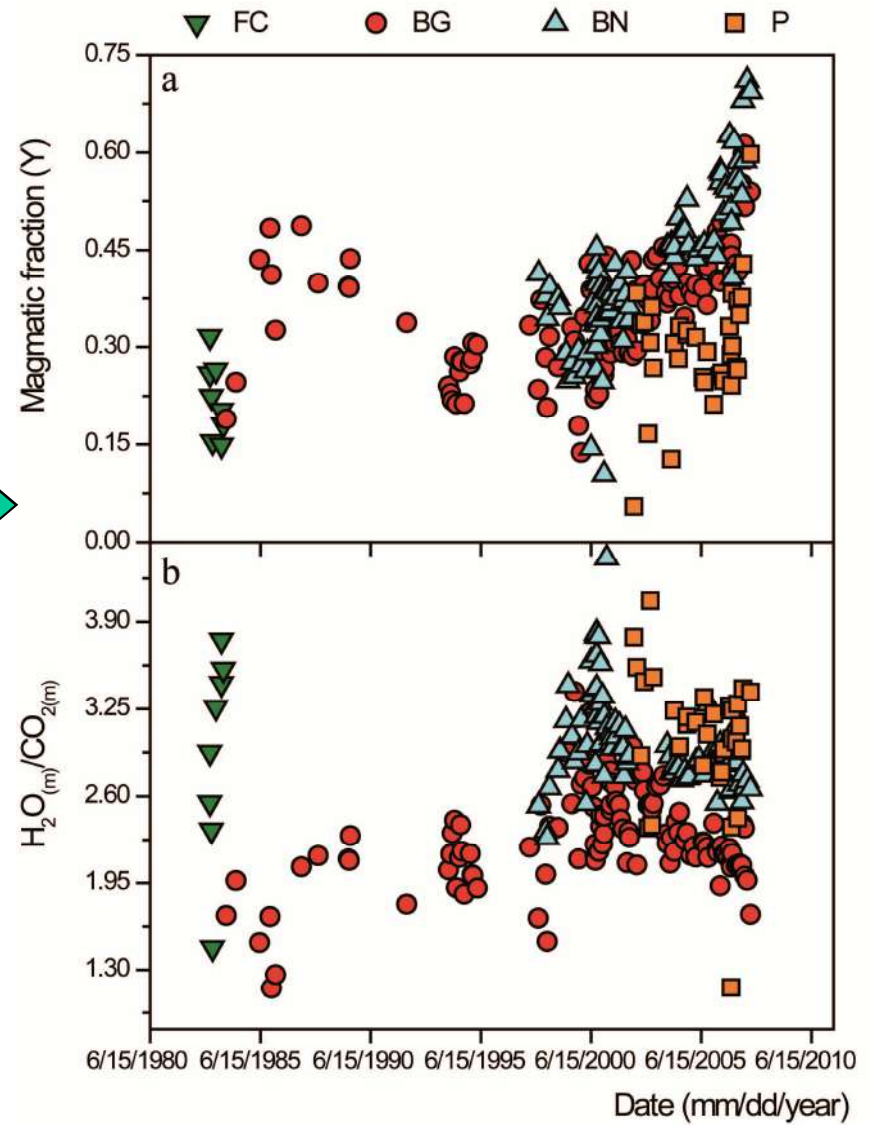
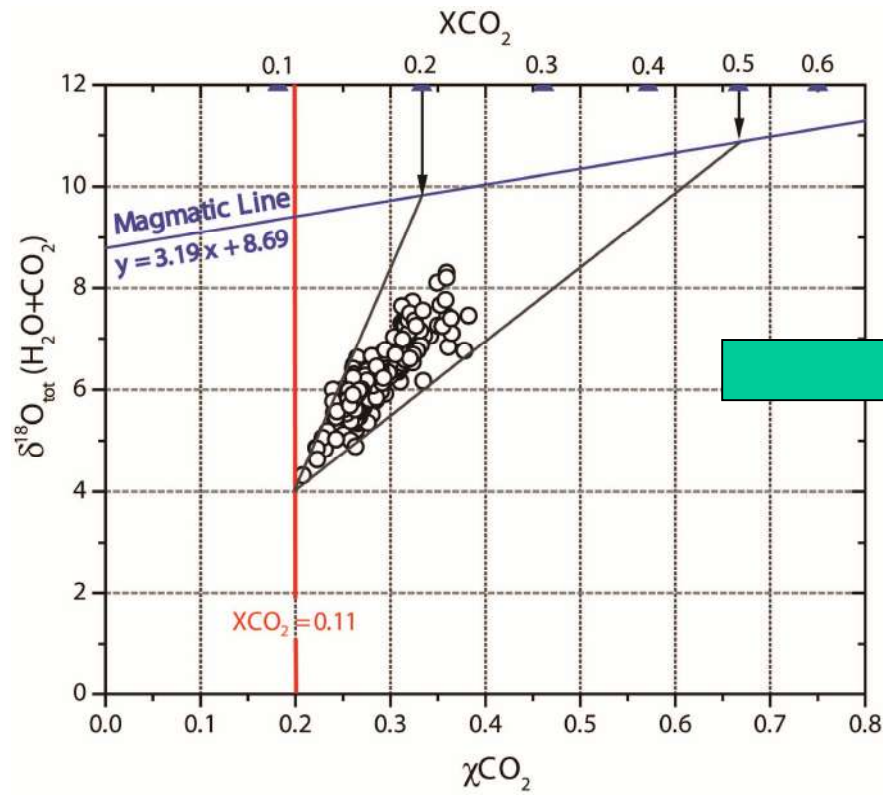
Simulation performed for a magma crystallizing and degassing (open-system) continuously → no volatile rejuvenation

Calculation scaled to 2x10¹¹ kg of magma.



The shallow body crystallizes and cools in 20-30 years !

Unrest: Fluid geochemical modelling



Moretti et al., Under Review in
EPSL

Melt composition (#) (wt.%, volatile-free)

SiO ₂	TiO ₂	Al ₂ O ₃	FeO _{tot}	MgO	CaO	Na ₂ O	K ₂ O
59.04	0.46	17.14	3.83	0.68	2.42	4.22	7.64

Constrained features of the magma body after rise and emplacement at 4 km-depth

P = 100 MPa (&); T = 1173 K (§); logfO₂ = NNO+1.2 (#)

H₂O^{TOT} = 3.5 wt% (£); CO₂^{TOT} = 2 wt% (£); S^{TOT} = 0.013 wt% (£)

Computed conditions

H ₂ O ^{gas} = 31.61 wt%	H ₂ O/CO ₂ (mol) = 1.14
CO ₂ ^{gas} = 68.01 wt%	H ₂ S/CO ₂ (mol) = 0.004
SO ₂ ^{gas} = 0.16 wt%	SO ₂ /H ₂ S (mol) = 0.4
H ₂ S ^{gas} = 0.22 wt%	

ρ_{melt+gas} = 2008 kg/m³

ρ_{melt} = 2511 kg/m³

m^{gas} = 3 wt%

V^{gas}/V^{tot} = 0.21

Composition of the deep gas separating from the trachytic body 8 km deep

P = 200 Mpa (@); T = 1223 K (§); logfO₂ = NNO+1.2 (#)

H ₂ O ^{gas} = 21.21 wt%	H ₂ O/CO ₂ (mol) = 0.66
CO ₂ ^{gas} = 78.59 wt%	H ₂ S/CO ₂ (mol) = 0.00058
SO ₂ ^{gas} = 0.17 wt%	SO ₂ /H ₂ S (mol) = 2.26
H ₂ S ^{gas} = 0.04 wt%	

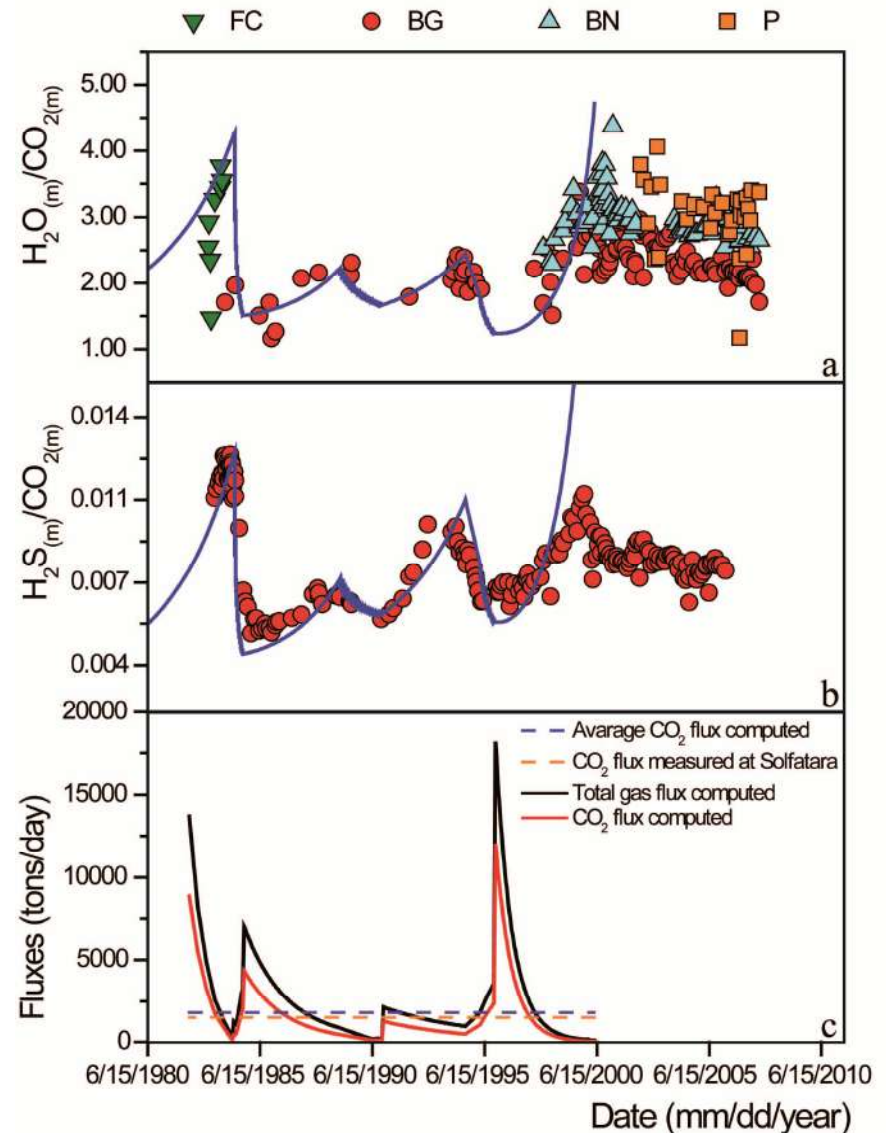
#: from MI studies (Arienzo et al., 2010) and experimental petrology (Roach, 2005);

&: from MI studies (Arienzo et al., 2010; Mangiacapra et al., 2008) and geophysical observations (Berrino, 1994; De Siena et al., 2010; Woo and Kilburn, 2010);

§: from experimental petrology (Roach, 2005);

£: from MI studies (Arienzo et al., 2010);

@: from MI studies (Arienzo et al., 2010; Mangiacapra et al., 2008) and seismic tomography (Zollo et al., 2008).

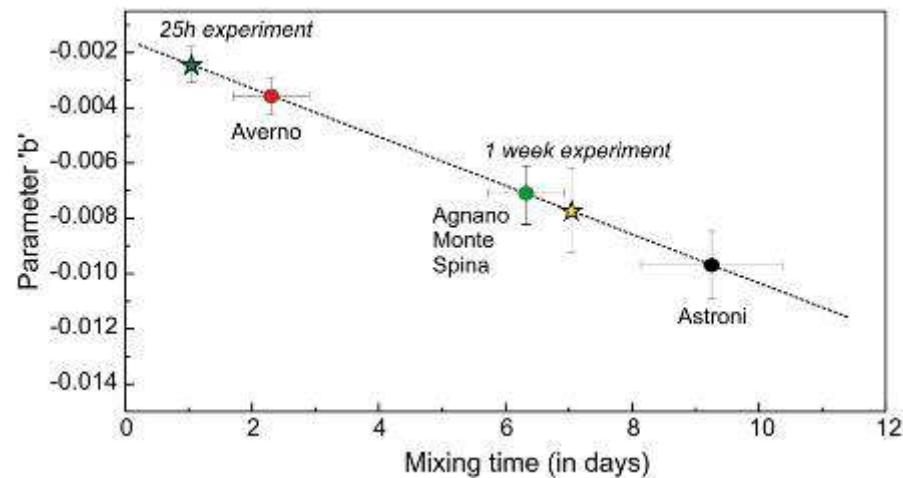


Possible scenarios and future (?) evolutions

3 scenarios can be reasonably hypothesized:

- Only deep gas reaches the surface, fluxing the shallow system
- The 4 km-deep (solidified) magma is experiencing re-melting
- The 8 km deep magma is rising from the large regional reservoir

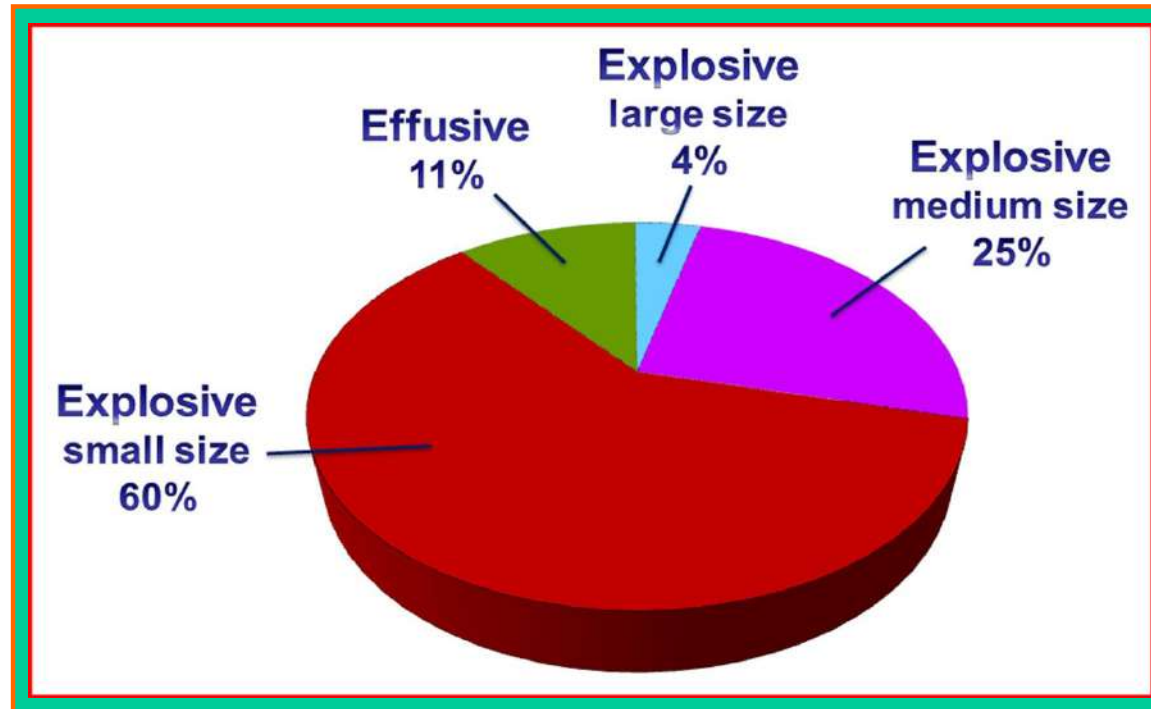
→ Petrologic data show that Phlegrean eruptions regularly follow episodes of new magma arrival and subsequent mixing in the shallow system → Timing is very Fast



Orsi et al. 2004

Possible Eruptive Scenarios

Size and style of a future eruption



Size	A_{1cm} (km^2)	V_{Tephra} (km^3)	V_{DRE} (km^3)	TEM ($kg * 10^{11}$)	Magnitude	Type eruption(s)
Large	> 500	> 0.40	> 0.3	> 5	> 5	Agnano-Monte Spina
Medium	500 - 1000	0.15 - 0.40	0.1 - 0.3	2 - 5	4.3 - 5	Astroni 6
Small	0 - 500	0 - 0.15	0 - 0.1	0 - 2	< 4.3	Monte Nuovo; Averno2

Orsi et al., 2009; E. Planet. Sci. Lett.

Hazard and Risk

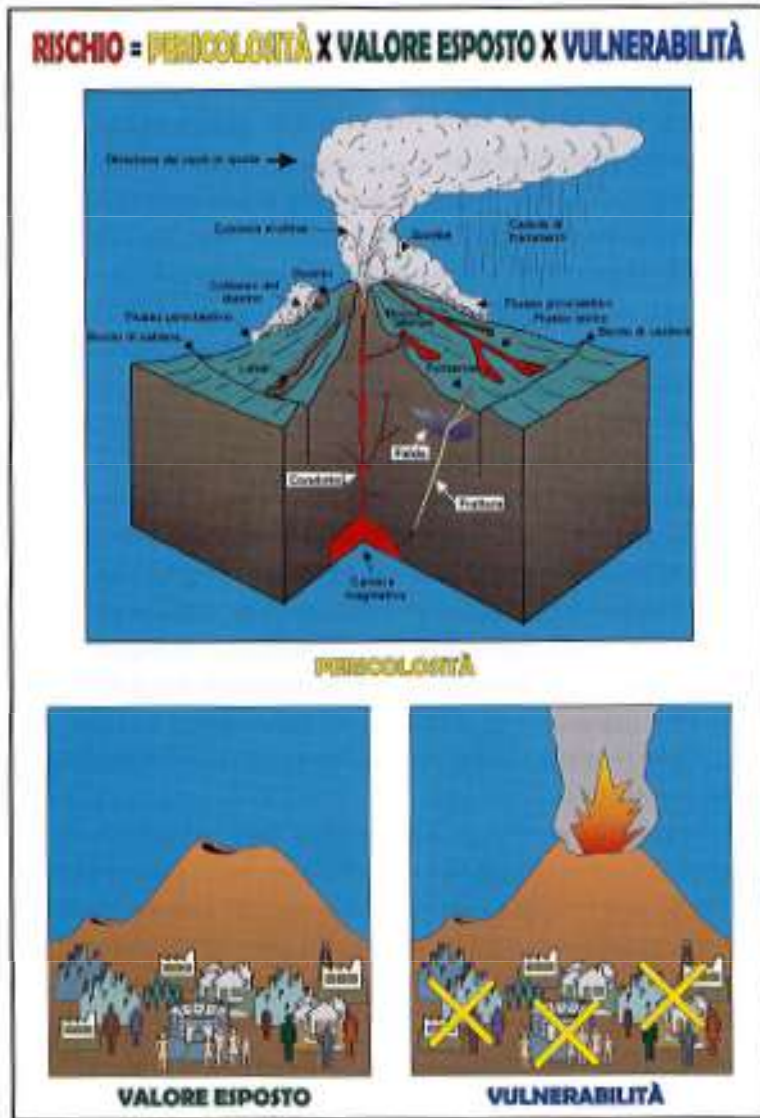
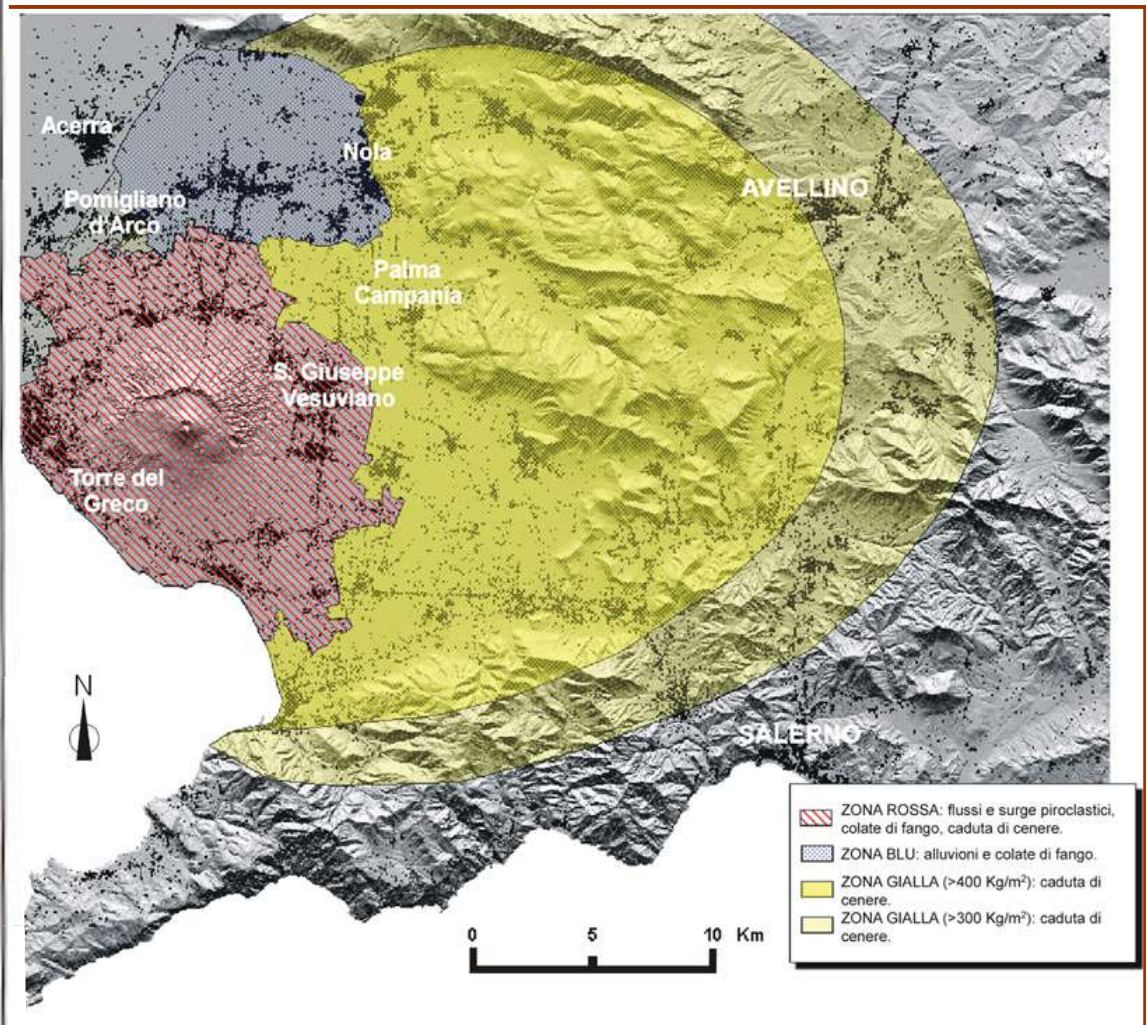


Fig. 1 - Illustrazione delle definizioni di rischio vulcanico.

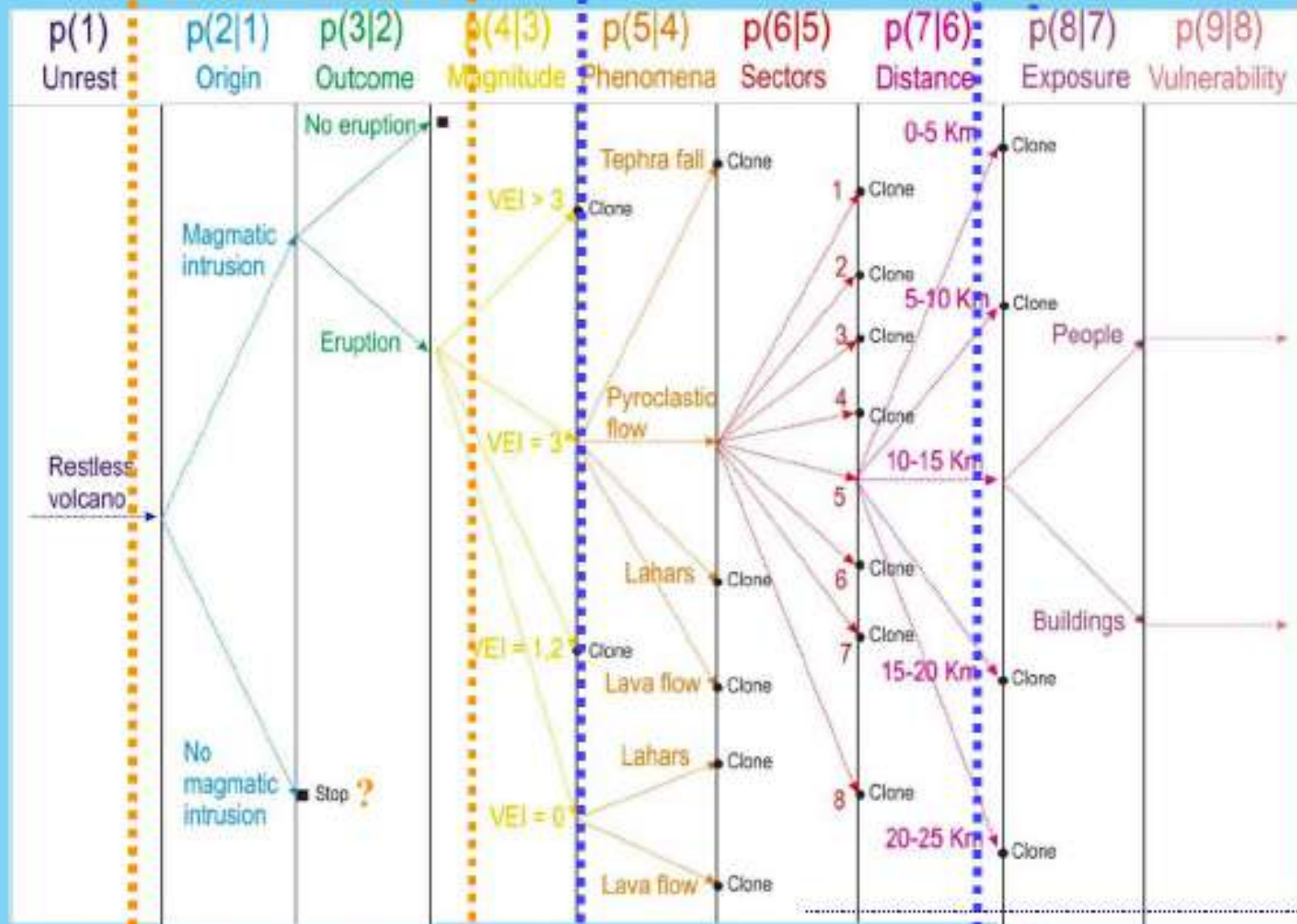


Hazard and Risk

Alert Tresholds and Actions for Risk Mitigation - Vesuvius

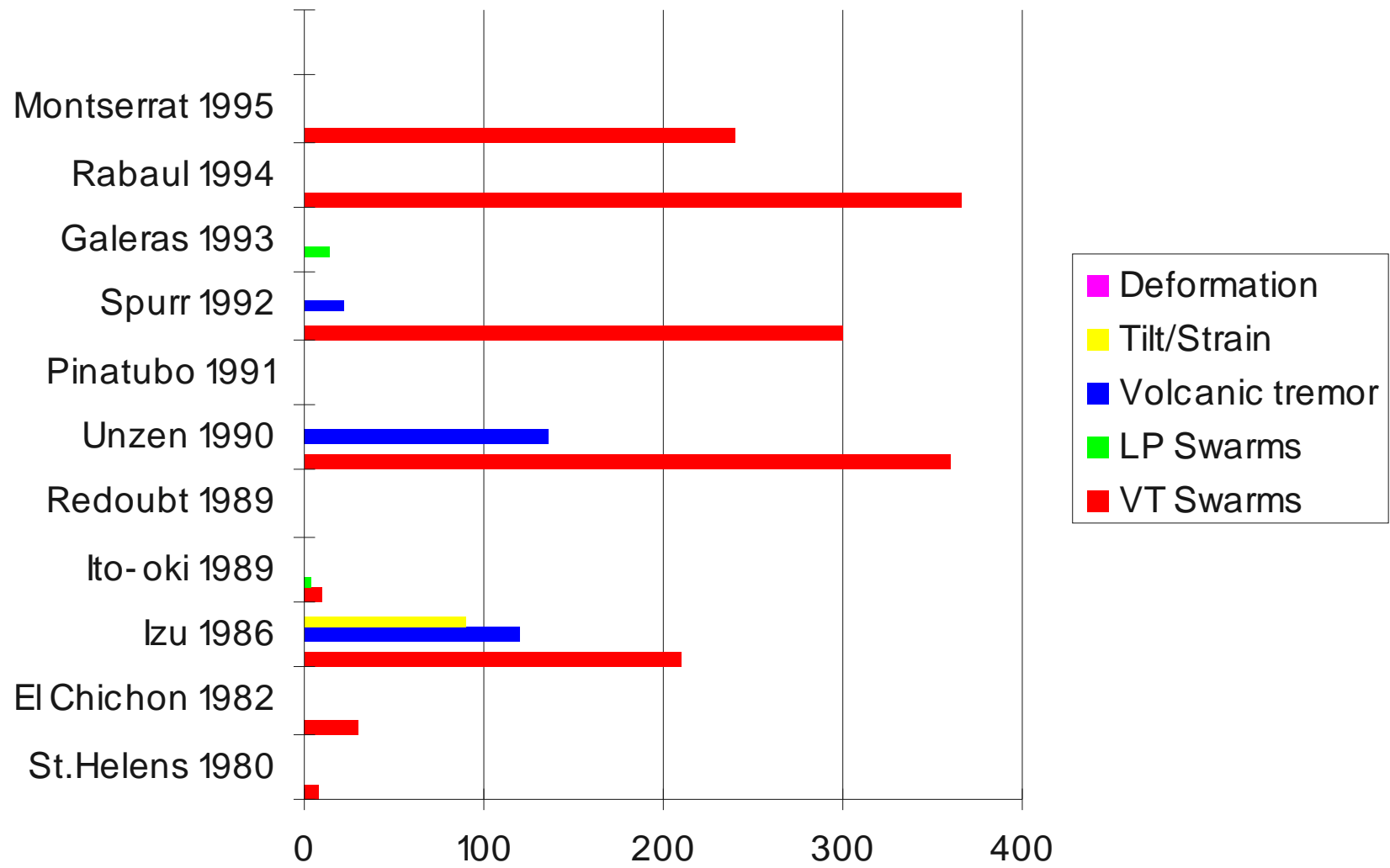
LIVELLI DI ALLERTA	STATO DEL VULCANO	PROBABILITÀ DI ERUZIONE	TEMPO DI ATTESA ERUZIONE	SISTEMA DI PROTEZIONE CIVILE		FASI
				Comunità Scientifica	Risposte Operative	
Base	Nessuna variazione significativa di parametri controllati	Molto bassa	Indefinito, comunque non meno di diversi mesi	Attività di sorveglianza secondo quanto programmato	Commissione Nazionale Attività ordinaria	
Attenzione	Variazione significativa di parametri controllati	Bassa	Indefinito, comunque non meno di alcuni mesi	Stato di allerta tecnico scientifico ed incremento dei sistemi di sorveglianza	Dipartimento della Protezione Civile - Attivazione della fase di attenzione - Comunicazione al Prefetto di Napoli Prefettura di Napoli - Convocazione del C.C.S. - Organizzazione supporto logistico alla Comunità Scientifica - Organizzazione delle prime informazioni alla popolazione unitamente ai Sindaci dei comuni interessati - Comunicazione a: a) Dipartimento della Protezione Civile b) Ministero dell'Interno c) Presidente Giunta Regionale Campania d) Presidente Amministrazione Provinciale di Napoli e) Sindaci	I FASE Attenzione
Preallarme	Ulteriore variazione di parametri controllati	Media	Indefinito, comunque non meno di alcune settimane	Continua l'attività di sorveglianza; simulazione dei possibili fenomeni eruttivi	Dipartimento della Protezione Civile - Attivazione della fase di preallarme - Richiesta dichiarazione Stato d'Emergenza - Convocazione Comitato Operativo di Protezione Civile - Nomina del Commissario Delegato da parte del P.C.M. - Attivazione della Direzione di Comando e Controllo Dipartimento della Protezione Civile (DI.COMA.C.) - Attivazione del C.C.S. nelle Prefetture della Campania e delle regioni ospitanti - Attivazione degli organismi Regionali e Provinciali di P.C. della Campania e di tutte le regioni ospitanti - Posizionamento soccorritori - Allontanamento spontaneo della popolazione	II FASE Preallarme
Allarme	Comparsa di fenomeni e/o andamento di parametri controllati che indicano una dinamica pre-eruttiva	Alta	Da settimane a mesi	Sorveglianza con sistemi remoti	Dipartimento della Protezione Civile (DI.COMA.C.) - Attivazione della fase di allarme - Evacuazione dei 18 comuni vesuviani - Allontanamento capi famiglia con mezzi propri - Attivazione Sala Operativa alternativa - Ripiegamento dei soccorritori - Spostamento Centri Operativi in Zona Gialla - Controllo del territorio evacuato al limite esterno della zona rossa - Allertamento strutture ricettive della Campania	III FASE Allarme
				Sorveglianza con sistemi remoti; definizione cono di interferenza dell'eruzione con la zona gialla	Dipartimento della Protezione Civile (DI.COMA.C.) - Controllo fenomeno per la definizione delle aree della zona gialla da evacuare - Raccolta, elaborazione e catalogazione dati sull'andamento del fenomeno e della operazione - Predisposizione strutture ricettive della Campania ed evacuazione Zona Gialla	IV FASE Evento in corso
				Continua la sorveglianza con sistemi remoti; inizia la ricostruzione dei sistemi di sorveglianza in loco	Dipartimento della Protezione Civile (DI.COMA.C.) - Ricollocazione delle strutture operative sul territorio - Operazioni tecnico-scientifiche di verifica del territorio finalizzate al rientro della popolazione (Regione, Provincia, Comuni, Provv. OO.PP., Gruppi Nazionali, VV.F.) Dipartimento della Protezione Civile - Rientro controllato - Richiesta revoca stato di emergenza	V FASE Dopo l'evento

Long-term forecasting & hazard



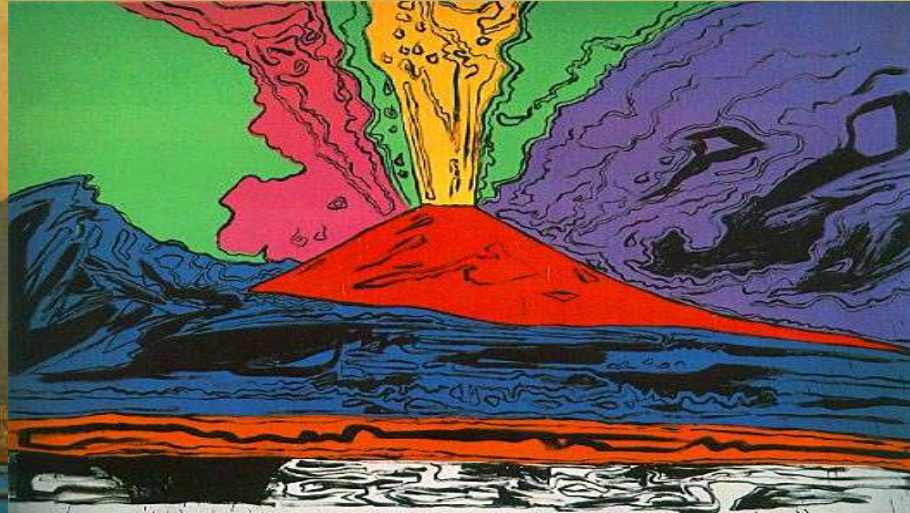
Short-term forecasting

Vulnerability & individual risk



Days before the eruption

Thanks for your attention!



Andy Warhol, 1985

